

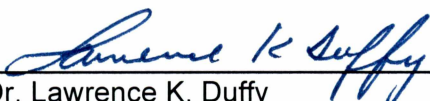
ANALYSIS OF TRINITROPHENYLATED ADENOSINE AND INOSINE USING CAPILLARY  
ELECTROPHORESIS-LASER INDUCED FLUORESCENCE DETECTION AND  
GAMMA-CYCLODEXTRIN

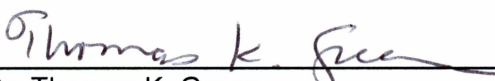
By


Terilyn K. L. Stephen

RECOMMENDED:


  
\_\_\_\_\_  
Dr. Kelly L. Drew

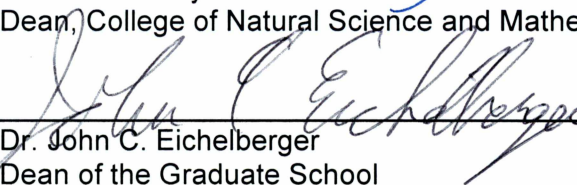
  
\_\_\_\_\_  
Dr. Lawrence K. Duffy

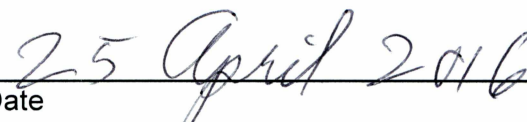
  
\_\_\_\_\_  
Dr. Thomas K. Green  
Advisory Committee Chair

  
\_\_\_\_\_  
Dr. Thomas K. Green  
Chair, Department of Chemistry and Biochemistry

APPROVED:

  
\_\_\_\_\_  
Dr. Paul W. Layer  
Dean, College of Natural Science and Mathematics

  
\_\_\_\_\_  
Dr. John C. Eichelberger  
Dean of the Graduate School

  
\_\_\_\_\_  
Date



ANALYSIS OF TRINITROPHENYLATED ADENOSINE AND INOSINE USING CAPILLARY  
ELECTROPHORESIS-LASER INDUCED FLUORESCENCE DETECTION AND  
GAMMA-CYCLODEXTRIN

A  
THESIS

Presented to the Faculty  
of the University of Alaska Fairbanks

in Partial Fulfillment of the Requirements  
for the Degree of

MASTER OF SCIENCE

By

Terilyn Koehler Lawson Stephen, B.S.

Fairbanks, Alaska

May 2016

## Abstract

Adenosine (Ado) and adenine ribonucleotides are essential in cell metabolism and energy production, cellular signaling, and DNA and RNA synthesis. The biosynthesis of these molecules takes place in both the intracellular and extracellular space via transphosphorylation reactions catalyzed by several distinct kinase enzymes like adenylate kinase. Several analytical detection methodologies have been developed to monitor these molecules in biological tissue, including both liquid chromatography (LC) and capillary electrophoresis (CE) techniques. However, many of these methodologies are limited by separation resolution and sample injection volume requirements. This thesis presents a novel capillary electrophoresis-laser induced fluorescence detection (CE-LIF) method with high separation power to analyze Ado and Inosine (Ino), a metabolite of Ado, by derivatization with 2,4,6-trinitrobenzenesulfonic acid to form fluorescent trinitrophenylated complexes of Ado (TNP-Ado) and Ino (TNP-Ino). The development and validation of the CE-LIF method, optimization of the trinitrophenylation reaction, and fluorescence enhancement of TNP-Ado and TNP-Ino with  $\gamma$ -cyclodextrin will be discussed. Detection limits were 1.6  $\mu\text{M}$  for Ado and 4  $\mu\text{M}$  for Ino in rat brain tissue. Large-volume sample stacking (LVSS) was employed to further enhance the sensitivity of the CE-LIF method, with detection limits of 310 nM and 159 nM for Ado and Ino, respectively. The CE-LIF method offers promise for the analysis of Ado, Ino and potentially other adenine ribonucleotides in small volume generating biological experiments like *in vivo* microdialysis and single cell metabolomics.



## Table of Contents

	Page
Signature Page .....	i
Title Page.....	iii
Abstract.....	v
Table of Contents.....	vii
List of Figures .....	ix
List of Tables .....	xiii
List of Appendices.....	xv
List of Abbreviations.....	xvii
Acknowledgments.....	xxi
Chapter 1 Introduction.....	1
1.1 Biological Significance of Adenosine and Adenine Ribonucleotides.....	1
1.2 Current Methodologies to Detect Adenosine and Adenine Ribonucleotides.....	5
1.3 Summary of Research Aims .....	8
1.4 References .....	11
Chapter 2 Analysis of Trinitrophenylated Adenosine and Inosine using Capillary Electrophoresis-Laser Induced Fluorescence Detection and $\gamma$ -Cyclodextrin .....	15
2.1 Abstract.....	15
2.2 Introduction.....	16
2.3 Methods .....	19
2.3.1 Safety Considerations .....	19
2.3.2 Chemicals and Reagents .....	19
2.3.3 Preparation of TNP-Ado and TNP-Ino Standards.....	20
2.3.4 $^1\text{H}$ , HMQC and ROESY NMR Spectra.....	20
2.3.5 CE-LIF Analysis and LVSS Studies.....	21

2.3.6 Trinitrophenylation Reactions .....	22
2.3.7 Biological Sample Preparation .....	22
2.3.8 Statistical Analysis .....	23
2.4 Results and Discussion .....	23
2.4.1 CE-LIF Optimization.....	23
2.4.2 Determination of $\gamma$ -CD Association Constants.....	25
2.4.3 Structural Determination of TNP-Ado and $\gamma$ -CD Inclusion Complex .....	28
2.4.4 Trinitrophenylation Reaction Kinetics Monitored by CE-LIF.....	31
2.4.5 CE-LIF Method Validation .....	34
2.4.6 Analysis of Adenosine and Inosine in Rat Brain Tissue.....	35
2.4.7 Large-Volume Sample Stacking of TNP-Ado and TNP-Ino.....	36
2.5 Conclusions.....	39
2.6 Acknowledgments .....	39
2.7 References.....	41
Chapter 3 Conclusion.....	45
3.1 Overview .....	45
3.2 Future Directions .....	45
Appendix A Supporting Information for Chapter 2 .....	47
Appendix B Trinitrophenylation and Capillary Electrophoresis Analysis of Adenine Ribonucleotides, N <sup>6</sup> -Cyclohexyladenosine, Guanosine, Cytidine, and Uridine .....	53

## List of Figures

Figure 1.1. Structures of adenosine and adenine ribonucleotides .....	1
Figure 1.2. Primary intracellular <i>de novo</i> biosynthesis pathway for the formation of adenosine and adenine ribonucleotides .....	2
Figure 1.3. Extracellular release of ATP and <i>de novo</i> biosynthesis pathway for the formation of adenosine and adenine ribonucleotides .....	3
Figure 2.1. (A) Chemical structures of Adenosine (Ado) and Inosine (Ino). (B) Trinitrophenylation reaction scheme between 2,4,6-trinitrobenzenesulfonic acid (TNBS) and the ribose group of Ado or Ino to form the TNP complex .....	19
Figure 2.2. Effect of $\gamma$ -CD concentration on the separation and fluorescence of TNP-Ado (10 $\mu$ M), TNP-Ino (10 $\mu$ M), TNBS (~12.5 mM) and fluorescein (internal standard, IS, 0.02 $\mu$ M) dissolved in aCSF and 0.1 M carbonate buffer at pH 10 .....	24
Figure 2.3. Effect of $\gamma$ -CD on the integrated fluorescence of a 10 $\mu$ M standard of TNP-Ado in water.....	25
Figure 2.4. The relationship between the electrophoretic mobility $\mu_i$ ( $\text{cm}^2/\text{V}\cdot\text{s}$ ) of 10 $\mu$ M standards of TNP-Ado and TNP-Ino and concentration of $\gamma$ -CD (M) at 25 $^\circ\text{C}$ .....	27
Figure 2.5. Partial 2D ROESY spectrum of 1:1 mixture of $\gamma$ -CD and TNP-Ado (~5 mM each) in $\text{D}_2\text{O}$ .....	29
Figure 2.6. Proposed inclusion complex of TNP-Ado: $\gamma$ -CD .....	31
Figure 2.7. Rates of the trinitrophenylation of Ado (100 $\mu$ M) at 50 $^\circ\text{C}$ and 37 $^\circ\text{C}$ and Ino (100 $\mu$ M) at 50 $^\circ\text{C}$ .....	33
Figure 2.8. Electropherograms of a 5 $\mu$ L sample of rat forebrain homogenate (A) and an 8 $\mu$ M Ado and Ino standard (B) after 6 hours of reaction time .....	36
Figure 2.9. Large volume sample stacking (LVSS) of TNP-Ado (20 nM) and TNP-Ino (20 nM) standards in water.....	37
Figure 2.10. LVSS electropherogram of a 4 nM standard of TNP-Ino and TNP-Ino in water .....	38
Figure A2.1. $^1\text{H}$ -NMR of synthesized TNP-Adenosine standard in $\text{D}_2\text{O}$ (Varian 300 MHz) .....	47
Figure A2.2. $^1\text{H}$ -NMR of synthesized TNP-Inosine standard in $\text{D}_2\text{O}$ (Bruker 600 MHz) .....	48
Figure A2.3. HMQC of ~5mM $\gamma$ -CD in $\text{D}_2\text{O}$ (Bruker 600 MHz).....	49
Figure A2.4. HMQC of 1:1 mixture of TNP-Ado: $\gamma$ -CD (~5 mM each) in $\text{D}_2\text{O}$ (Bruker 600 MHz) .....	50
Figure A2.5. Effect of 0.1, 0.15 and 0.5 M sodium carbonate buffer at pH 10 on the trinitrophenylation of Ado (100 $\mu$ M) at 37 $^\circ\text{C}$ .....	51



Figure B1.1. Structure of adenosine (Ado) .....	53
Figure B1.2. Steady state fluorescence emission of 10 $\mu$ M TNP-Ado standard in various aqueous and non-aqueous solvents.....	56
Figure B1.3. Comparison of relative fluorescence peak height of 10 $\mu$ M TNP-Ado standard in H <sub>2</sub> O using CE-LIF with various types and concentrations of cyclodextrins in 20 mM sodium borate BGE at pH 9.4.....	57
Figure B1.4. Comparison of Ado concentrations in rat forebrain tissue using different sample extraction techniques .....	59
Figure B2.1. Structures of adenine ribonucleotides .....	60
Figure B2.2. <sup>1</sup> H NMR of TNP-AMP in D <sub>2</sub> O (Bruker 600 MHz).....	62
Figure B2.3. <sup>31</sup> P NMR of TNP-AMP in D <sub>2</sub> O (Bruker 600 MHz).....	63
Figure B2.4. CE-LIF electropherogram of TNP-AMP and TNP-AMP with TNBS spike .....	64
Figure B2.5. <sup>1</sup> H NMR of TNP-ADP in D <sub>2</sub> O (Bruker 600 MHz) .....	65
Figure B2.6. <sup>1</sup> H COSY NMR of TNP-ADP in D <sub>2</sub> O (Bruker 600 MHz) .....	66
Figure B2.7. <sup>31</sup> P NMR of TNP-ADP in D <sub>2</sub> O (Bruker 600 MHz) .....	67
Figure B2.8. <sup>1</sup> H NMR of TNP-ATP in D <sub>2</sub> O (Bruker 600 MHz) .....	68
Figure B2.9. <sup>1</sup> H COSY NMR of TNP-ATP in D <sub>2</sub> O (Bruker 600 MHz) .....	69
Figure B2.10. <sup>31</sup> P NMR of TNP-ATP in D <sub>2</sub> O (Bruker 600 MHz) .....	70
Figure B2.11. <sup>31</sup> P COSY NMR of TNP-ATP in D <sub>2</sub> O (Bruker 600 MHz) .....	71
Figure B2.12. CE-LIF electropherogram of TNP-ATP and TNP-ATP with TNBS spike.....	72
Figure B3.1. Structure of N <sup>6</sup> -cyclohexyladenosine (CHA).....	73
Figure B3.2. <sup>1</sup> H NMR of TNP-CHA in DMSO-d <sub>6</sub> (Bruker 600 MHz).....	76
Figure B3.3. <sup>1</sup> H COSY NMR of TNP-CHA in DMSO-d <sub>6</sub> (Bruker 600 MHz) .....	77
Figure B3.4. CE-LIF electropherogram of TNP-Ado, TNP-CHA, TNBS and IS in aCSF .....	78
Figure B3.5. The relationship between the electrophoretic mobility $\mu_i$ (cm <sup>2</sup> /V•s) of 10 $\mu$ M standard of TNP-CHA and concentration of $\gamma$ -CD (M) at 25 °C .....	89
Figure B3.6. Rate of the trinitrophenylation of CHA (100 $\mu$ M) at 50°C .....	80
Figure B3.7. Comparison of <sup>1</sup> H NMR of 1mM CHA standard in aCSF diluted in D <sub>2</sub> O before and after 24 hr storage at -80°F (Bruker 600 MHz) .....	81

Figure B4.1. Structure of guanosine (Gua), cytidine (Cyt) and uridine (Uri) .....	82
Figure B4.2. <sup>1</sup> H NMR of TNP-Gua in D <sub>2</sub> O (Bruker 600 MHz).....	84
Figure B4.3. <sup>1</sup> H COSY NMR of TNP-Gua in D <sub>2</sub> O (Bruker 600 MHz).....	85
Figure B4.4. <sup>1</sup> H NMR of TNP-Cyt in D <sub>2</sub> O (Bruker 600 MHz) .....	86
Figure B4.5. <sup>1</sup> H COSY NMR of TNP-Cyt in D <sub>2</sub> O (Bruker 600 MHz) .....	87
Figure B4.6. <sup>1</sup> H NMR of TNP-Uri in D <sub>2</sub> O (Bruker 600 MHz).....	88
Figure B4.7. <sup>1</sup> H COSY NMR of TNP-Uri in D <sub>2</sub> O (Bruker 600 MHz).....	89



## List of Tables

Table 2.1 Values for CE-LIF Method .....	34
Table 2.2 LVSS Values for a 20 nM standard of TNP-Ado and TNP-Ino in H <sub>2</sub> O .....	38



## List of Appendices

Appendix A Supporting Information for Chapter 2 .....	47
Appendix B Trinitrophenylation and Capillary Electrophoresis Analysis of Adenine Ribonucleotides, N <sup>6</sup> -Cyclohexyladenosine, Guanosine, Cytidine, and Uridine .....	53
B.1 Additional Analysis on Adenosine.....	53
B.1.1 Introduction.....	53
B.1.2 Methods.....	53
B.1.3 Results and Discussion.....	55
B.1.4 Conclusions.....	59
B.2 Adenine Ribonucleotides.....	60
B.2.1 Introduction.....	60
B.2.2 Methods.....	61
B.2.3 Results and Discussion.....	61
B.2.4 Conclusions.....	72
B.3 N <sup>6</sup> -Cyclohexyladenosine .....	73
B.3.1 Introduction.....	73
B.3.2 Methods.....	74
B.3.3 Results and Discussion.....	75
B.3.4 Conclusions.....	81
B.4 Guanosine, Cytidine and Uridine.....	82
B.4.1 Introduction.....	82
B.4.2 Methods.....	83
B.4.3 Results and Discussion.....	83
B.4.4 Conclusions.....	89
B.5 References.....	91



## List of Abbreviations

Ado	adenosine
ADP	adenosine 5'-diphosphate
cAMP	cyclic adenosine 5'-monophosphate
AMP	adenosine 5'-monophosphate
ATP	adenosine 5'-triphosphate
BGE	background electrolyte
CE	capillary electrophoresis
CE-ESI	capillary electrophoresis-electrospray ionization
CE-FSCV	capillary electrophoresis-fast scan cyclic voltammetry
CE-LIF	capillary electrophoresis-laser induced fluorescence detection
CE-MS	capillary electrophoresis-mass spectrometry
CHA	N <sup>6</sup> -Cyclohexyladenosine
CNS	central nervous system
CNT	concentrative nucleoside transporters
aCSF	artificial cerebral spinal fluid
Cyt	cytidine
DMF	dimethylformamide
EDTA	ethylenediaminetetraacetic acid
ENT	equilibrative nucleoside transporters
EOF	electroosmotic flow
FASS	field-amplified sample stacking
FSCV	fast-scan cyclic voltammetry
γ-CD	γ-cyclodextrin
amino-γ-CD	3A-amino-3A-deoxy-(2AS, 3AS)-γ-cyclodextrin
carboxymethylated-γ-CD	randomly carboxymethylated-γ-cyclodextrin



2-HP- $\gamma$ -CD	(2-hydroxypropyl)- $\gamma$ -cyclodextrin
methyl- $\gamma$ -CD	randomly methylated- $\gamma$ -cyclodextrin
Gua	guanosine
HMQC	heteronuclear multiple quantum coherence
Ino	inosine
IS	internal standard
LC	liquid chromatography
LC/APCI-MS/MS	liquid chromatography/atmospheric pressure chemical ionization-tandem mass spectrometry
LC-MS	liquid chromatography coupled to mass spectrometry
LVSS	large-volume sample stacking
LOD	limit of detection
LOQ	limit of quantification
$u_c$	actual electrophoretic mobility the bound inclusion complex
$\mu_{ep}$	actual electrophoretic mobility of the analyte
$\mu_{eof}$	actual electrophoretic mobility the electroosmotic flow
$\mu_f$	actual electrophoretic mobilities of the free, unbound analyte
$\mu_i$	actual electrophoretic mobilities
$\mu_{obs}$	mobility observed electrophoretic mobility of an analyte
NDPKs	nucleoside-diphosphate kinases
NMF	N, N-dimethylformamide
NMR	nuclear magnetic resonance
5'-ectoNT	ecto-5' nucleotidases
PCA	perchloric acid
ROESY	rotational nuclear Overhauser effect spectroscopy
RSD	relative standard deviation

SAH	S-adenosyl-L-homocysteine
S/N	signal to noise
TNBS	2,4,6-trinitrobenzenesulfonic acid
TNP-Ado	trinitrophenylated-adenosine
TNP-ADP	trinitrophenylated-adenosine 5'-diphosphate
TNP-AMP	trinitrophenylated-adenosine 5'-monophosphate
TNP-ATP	trinitrophenylated-adenosine 5'-triphosphate
TNP-CHA	trinitrophenylated-N <sup>6</sup> -Cyclohexyladenosine
TNP-Cyt	trinitrophenylated-cytidine
TNP-Ino	trinitrophenylated-inosine
TNP-Gua	trinitrophenylated-guanosine
TNP-Uri	trinitrophenylated-uridine
TRIS	tris(hydroxymethyl)aminomethane
Uri	uridine



## Acknowledgments

First and foremost, I would like to express my deepest appreciation and gratitude to my advisor, Dr. Tom Green, for his endless guidance and patience during both my undergraduate and graduate education. Without his enthusiasm and knowledge, my thesis research would not have been successful. His excitement for scientific inquiry and the success of his students is a quality I plan to carry all of my life. So thank you Dr. Green, I truly would not be where I am today without your support.

I would also like to express my deepest gratitude to my committee members, Dr. Kelly Drew and Dr. Larry Duffy. Their insight and advice was invaluable throughout the entirety of my education. Their input has greatly contributed to my understanding of biochemistry and neuroscience.

I would like to thank the Department of Chemistry and Biochemistry and all the members of Dr. Green's and Dr. Drew's research groups for their vital input and comments, especially Kate Guillemette, Saurav Bhowmick and Dr. Carl Murphy for their direct contributions and endless help and advice. I am also thankful for my officemates, Nicole Knight, Canrong "Jackey" Qiu and Kristin Gagne, for their friendship and support.

Finally but not the least, I would like to express my greatest gratitude to my family. I could not imagine completing my thesis without my husband, Michael Stephen. His love, support, and the numerous dinner deliveries and late night well-being phone calls I received while working in the laboratory kept me focused and motivated to finish. I am also grateful for parents, Phyllis and Jim Lawson, for their love and strong work ethic, which I have learned from them over the years. I love and thank the three of you from the bottom of my heart.

This research project was funded by the Alaska Space Grant Program, an Institutional Development Award from the National Institutes of Health and a grant award, R15NS074422, from the National Institute of Neurological Disorders and Stroke of the National Institutes of Health.



# Chapter 1

## Introduction

### 1.1 Biological Significance of Adenosine and Adenine Ribonucleotides

Adenosine and adenine ribonucleotides such as adenosine triphosphate (ATP) play a number of key roles biological and pathological processes. These roles include cellular metabolism,<sup>1,2</sup> cellular signaling,<sup>3,4</sup> and DNA and RNA synthesis.<sup>5,6</sup> Figure 1.1 shows the molecular structures of adenosine (Ado) and several essential adenine ribonucleotides. Both adenosine and adenine ribonucleotides are comprised of a single, adenine nitrogenous base and a 5-carbon ribose sugar ring joined by a  $\beta$ -N<sub>9</sub>-glycosidic bond between the N<sub>9</sub> of the adenine base and 1' carbon of the ribose sugar. Adenine ribonucleotides, however, contain additional phosphate groups attached to the 5' carbon of the ribose sugar.

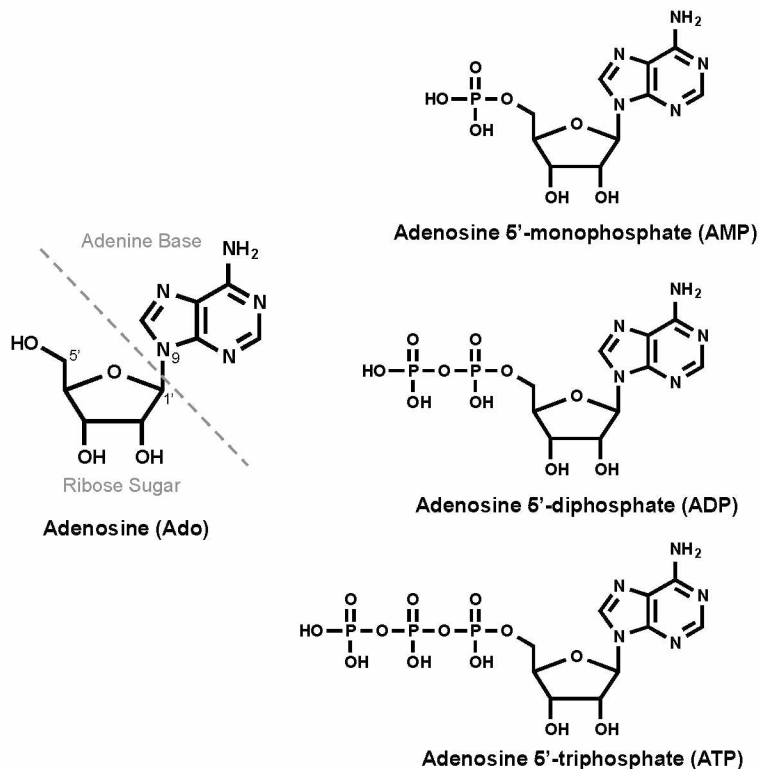
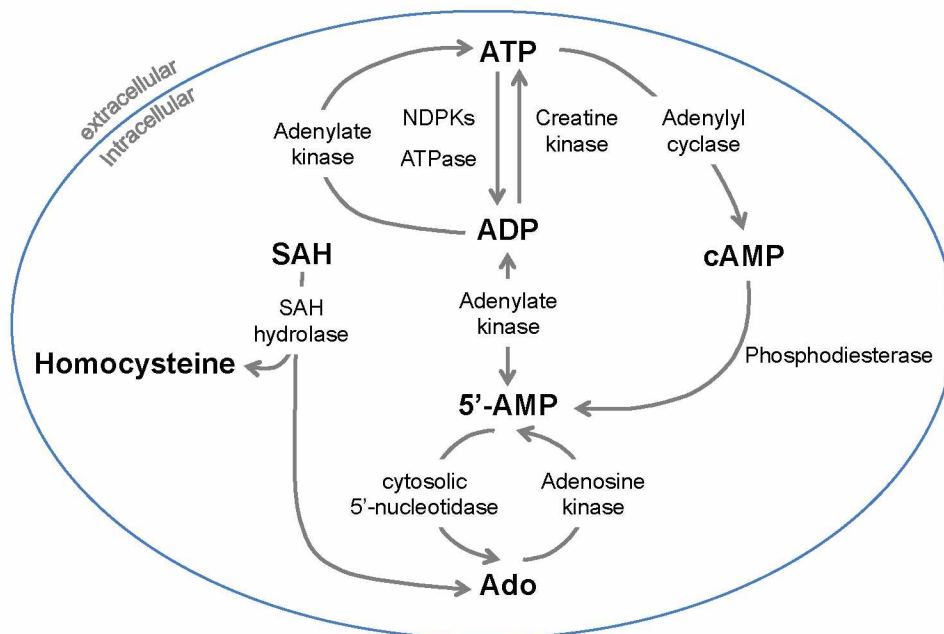


Figure 1.1. Structures of adenosine and adenine ribonucleotides

The *de novo* biosynthesis or metabolic pathways of these molecules takes place in both the intracellular and extracellular space. For example, the primary generation of ATP in aerobic organisms is through cellular respiration, which occurs intracellularly in the cytosol during glycolysis and pyruvate oxidation, and in the mitochondria during the citric acid cycle and oxidative phosphorylation.<sup>1</sup> Additionally, ATP, other adenine ribonucleotides including adenosine 5' phosphate (ADP) and adenosine 5' monophosphate (AMP), and Ado can be synthesized intracellularly via transphosphorylation reactions.<sup>1,7</sup> Figure 1.2 shows the primary intracellular pathways for the formation of these molecules. The start of this pathway is typically described by the conversion of ATP to ADP by nucleoside-diphosphate kinases (NDPKs) and ATPases. After ADP is formed, it can be further converted to 5'-AMP by adenylate kinase and eventually to Ado via cytosolic 5'-nucleotidase. As apparent in Figure 1.2, these transphosphorylation reactions are reversible and alternative intracellular pathways exist.



**Figure 1.2. Primary intracellular *de novo* biosynthesis pathway for the formation of adenosine and adenine ribonucleotides.** Abbreviations: adenosine 5'-triphosphate (ATP), adenosine 5'-diphosphate (ADP), adenosine 5'- monophosphate (AMP), cyclic 5'-adenosine monophosphate (cAMP), adenosine (Ado), S-Adenosyl-L-homocysteine (SAH) and nucleoside-diphosphate kinases (NDPKs). Figure adapted from Dunwiddie and Masino. 2001.<sup>7</sup>

It is also possible that ADP, AMP and Ado can be metabolized extracellularly during certain cell signaling events.<sup>8-10</sup> Figure 1.3 shows the release of ATP into the extracellular space in a cell such as a neuron or epithelial cell. Once ATP is released, it can be metabolized extracellularly to its adenine ribonucleotide precursors by ectoenzymes ecto-ATPase and ecto-5' nucleotidases (5'-ectoNT).<sup>8</sup> These metabolites can then be further utilized in extracellular signaling or transported back into the cell via nucleoside transporters.

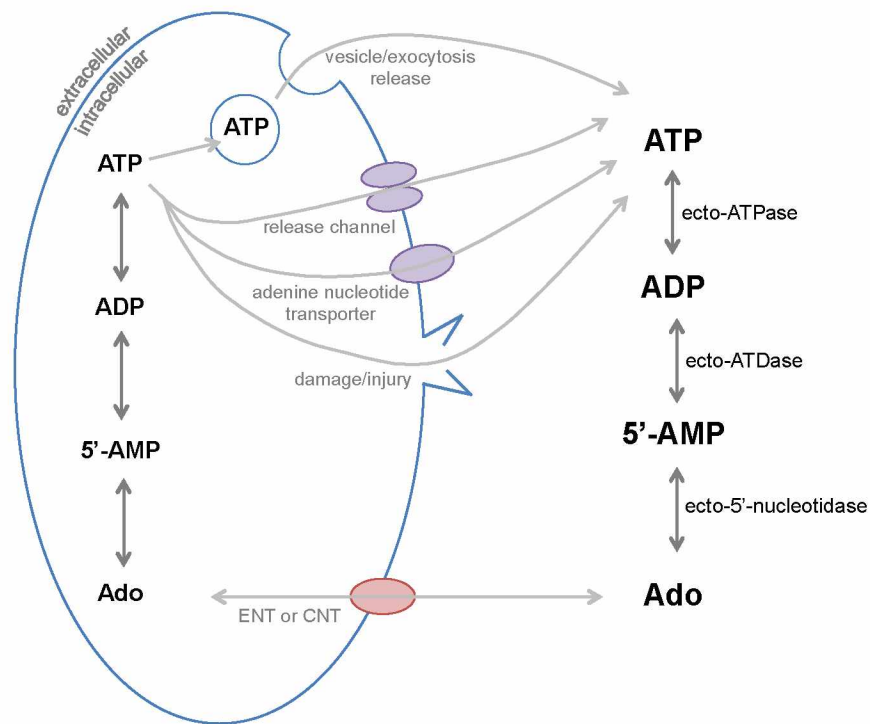


**Figure 1.3. Extracellular release of ATP and *de novo* biosynthesis pathway for the formation of adenosine and adenine ribonucleotides.** Abbreviations: adenosine 5'-triphosphate (ATP), adenosine 5'-diphosphate (ADP), adenosine 5'- monophosphate (AMP), adenosine (Ado), equilibrative or concentrative nucleoside transporters (ENT, CNT).

Nucleotide transporters, more specifically equilibrative and concentrative nucleoside transporters (ENT, CNT) are essential in maintaining extracellular adenosine concentrations. These transporters also play a role in the salvage or recycling of nucleotides when *de novo* biosynthesis of nucleotides is unfavorable.<sup>11</sup> ENTs and CNTs are membrane-associated



proteins that facilitate the bi-directional movement of nucleosides across the cell membrane. ENTs transport purine nucleosides like Ado as well as pyrimidine nucleosides across the cell membrane depending on the nucleotide concentration gradient.<sup>12</sup> CNTs are also bi-directional, but the direction of transport is dependent on the cell's transmembrane sodium gradient regardless of the nucleoside concentration gradient.<sup>13</sup> In the case of Ado, ENTs and CNTs regulate both extracellular and intracellular concentration levels.<sup>8</sup> If intracellular Ado levels are low due to the normal conversion of Ado to AMP or other metabolites like inosine (Ino), an extracellular concentration gradient will form resulting in the influx of Ado through the transporters. If there is a diminishment in extracellular Ado concentrations, typically caused by a mutation or inhibition of enzymes like adenosine deaminase or adenosine kinase, an intracellular Ado accumulation occurs. This reversal of the concentration gradient causes the transporters to also reverse direction resulting in a net efflux of Ado into the extracellular space.

The significance of the enzyme adenosine kinase in maintaining extracellular Ado concentrations should also be noted. As shown in Figure 1.2, adenosine kinase is responsible for the intracellular phosphorylation of Ado to AMP. Adenosine kinase is considered the primary regulator of intracellular Ado levels. However more recently, it has also been shown to regulate extracellular synaptic Ado concentrations in the CNS, especially in astrocytes, during non-pathological conditions.<sup>14</sup> This finding is significant because it identifies an additional mechanism to nucleoside transporters for maintaining extracellular Ado concentrations.

As stated earlier, Ado and adenine ribonucleotides are essential cellular signaling molecules. This type of extracellular signaling is also referred to as purinergic signaling<sup>8,15</sup> and is widely distributed across biological tissue.<sup>7,16,17</sup> There are two distinct families of purinergic receptors, P<sub>1</sub> and P<sub>2</sub>. P<sub>1</sub> receptors, also called adenosine receptors since they are activated endogenously by extracellular Ado,<sup>18</sup> are G-protein-coupled receptors that signal by inhibiting or activating the production of intracellular cyclic AMP. There are 4 subtypes of P<sub>1</sub> receptors, A<sub>1</sub>, A<sub>2A</sub>, A<sub>2B</sub>, and A<sub>3</sub>. P<sub>2</sub> receptors primarily bind ATP, ADP or uracil ribonucleotides and are divided

in to 2 subtypes, P<sub>2X</sub> and P<sub>2Y</sub>.<sup>8,19</sup> P<sub>2X</sub> receptors are G-protein-coupled receptors that also signal by inhibiting or activating production of intercellular cyclic AMP, where as P<sub>2Y</sub> receptors are ligand-gated channels.

The physiological role of Ado and adenine ribonucleotides, especially in cellular signaling, is great. However, the effect and impact of their actions can also vary depending on cell and tissue type. In the nervous system, the role of Ado and ATP in normal physiology includes promoting and maintaining sleep,<sup>20</sup> regulation of glia-neuron communication,<sup>21</sup> and the regulation of cerebral blood flow.<sup>22,23</sup> In the cardiovascular system, Ado and ATP help regulate vascular tone<sup>24</sup> and platelet aggregation,<sup>25</sup> as well as cell migration, proliferation and death in endothelial and skeletal muscle cells.<sup>26</sup> Ado and adenine ribonucleotides also play significant roles in maintaining the normal physiology of many other biological processes, including the immune response and inflammation,<sup>17</sup> bone development and remodeling,<sup>27</sup> and insulin secretion in pancreatic  $\beta$ -cells.<sup>28</sup>

In addition, recent research has highlighted the potential of Ado, adenine ribonucleotides, and purinergic receptors as key targets for therapeutic interventions in a variety of pathological conditions.<sup>16,29</sup> For example, Ado released during cerebral hypoxia and ischemia exhibits acute neuroprotective effects that reduces the severity of damage to local neuronal tissue.<sup>30</sup> Subsequently, Ado agonists and allosteric modulators of P<sub>1</sub> receptors have been investigated as potential therapies for stroke events.<sup>31,32</sup>

## **1.2 Current Methodologies to Detect Adenosine and Adenine Ribonucleotides**

The widespread role of Ado and adenine ribonucleotides in biological function highlights the importance of having analytical methodologies capable of accurately detecting and quantifying these molecules in biological tissue. Several of the current methodologies used to monitor these molecules, along with their limitations, will be discussed.

To date, the most commonly used methodology for monitoring Ado and adenine ribonucleotides is liquid chromatography (LC). LC separates molecules from complex liquid mixtures by passing a solvent, or mobile phase, through a column, or stationary phase, packed with an absorbent, stationary material, or stationary phase.<sup>33</sup> Column length, solvent and analyte polarity as well as analyte size affects the separation resolution and efficiency of LC.<sup>33</sup> For the analysis of Ado and adenine ribonucleotides, LC is typically coupled to UV-Vis absorbance detection.<sup>34,35</sup> However, recent studies have established efficient LC methods coupled to mass spectrometry,<sup>36-38</sup> fluorescence,<sup>39</sup> and electrochemical<sup>40</sup> detection. Aside from its commonality and convenience, if LC instrumentation is available for use, some limitations with the methodology do exist. If large sample injection volumes are required for quantification, temporal and spatial sensitivity problems can arise. In addition, large amounts of solvent waste can be generated by LC methodologies and can lead to high user costs if high priced solvents are required for separation. Despite these pitfalls, recent advancements in LC methodologies have been developed to enhance method sensitivity and increase run time efficiency.

One example is a robust liquid chromatography/atmospheric pressure chemical ionization-tandem mass spectrometry (LC/APCI-MS/MS) approach developed by Van Dycke et al. for the quantification of Ado in cell culture medium.<sup>37</sup> Samples were analyzed without the need for extraction on a reverse phase LC column. An injection volume of 5  $\mu$ L was used with a total run time of 4.5 min. Quantification of Ado was carried out by MS/MS with a broad concentration range from 15.6 ng/ml to 2000 ng/ml. Another robust and sensitive approach using liquid chromatography coupled to mass spectrometry (LC-MS) was developed by Song et al. for the quantification of Ado (and other neurochemicals) during *in vivo* brain studies.<sup>38</sup> This method relies on the derivatization reaction between benzoyl chloride and the ribose-hydroxy group of Ado (or primary and secondary amines and phenols groups of other neurochemicals like amino acids and dopamine). 5  $\mu$ L samples of *in vivo* brain microdialysis were reacted with 2.5  $\mu$ L of benzoyl chloride in 2.5  $\mu$ L of borate buffer prior to analysis on a reverse phase C18 LC column.

An injection volume of 9  $\mu\text{L}$  was used with a total run time of 8 min. Quantification of Ado was carried out by MS with a reported limit of detection of 25 nM for Ado.

Another methodology used for monitoring Ado and adenine ribonucleotides in biological matrices is capillary electrophoresis (CE). Samples are separated electrokinetically by passing an applied voltage across a background electrolyte.<sup>41</sup> The separation efficiency can be manipulated by a variety of variables including the pH of the background electrolyte and the additions of background electrolyte modifiers such as cyclodextrin molecules.<sup>41</sup> Several CE methods have been reported for the analysis of Ado and adenine ribonucleotides, including detection by UV-Vis absorbance detection,<sup>42</sup> laser induced fluorescence,<sup>43</sup> mass spectrometry,<sup>44</sup> and electrochemical<sup>45</sup> detection. CE typically has higher separation efficiency than LC and requires microliter or less sample injection volumes. A disadvantage of CE can arise if samples need to be derivatized or reacted prior to analysis. This not only causes an extra step in analysis, but also may lead to sample degradation, matrix interference and an increase in cost.

A recent method that demonstrates the robust separation power of CE is a CE-mass spectrometry (CE-MS) approach developed by Liu and colleagues for analysis of nucleotides in a single cell.<sup>44</sup> The method is able to successfully separate and quantify 16 anionic nucleotides (including AMP, ADP and ATP) from a single neuron using a custom-built CE-electrospray ionization (CE-ESI) system coupled to a micro-time-of-flight mass spectrometer. Large-volume sample stacking was used to concentrate samples during analysis and typically resulted in 103 nL injection volumes and 40 min run times. Reported limits of detection were 2.2 nM for AMP, 8.9 nM for ADP, and 6.9 nM for ATP.

Bioluminescence methodologies have also reported for the detect adenine ribonucleotides, specifically ATP, in cells.<sup>46</sup> The luciferase-luciferin bioluminescence assay relies on requirement of ATP for the oxidation of the protein luciferin to oxyluciferin by the firefly enzyme luciferase.<sup>47</sup> The reaction emits light, which can be then detected by spectroscopy techniques. This

methodology can allow for ATP to be detected *in vivo* by optic microscopy, however, great care has to be made to reduce biomass or other ATP contamination.

Recently, research has focused on developing methodologies that can monitor Ado and adenine ribonucleotides in real-time. These methods rely on fast-scan cyclic voltammetry (FSCV) probes<sup>48</sup> and enzyme-based biosensor technology,<sup>49</sup> which can both monitor Ado and ATP on a sub-second time scale. Analysis occurs by placing a carbon electrode or nanoparticle aptamer-based biosensor into living cells or tissue and rapidly changing its voltage. This causes the molecule of interest to either undergo oxidization and reduction rapidly in FSCV or to hybridize with the sensor in enzyme-based biosensor technology, thus allowing for appropriate detection. Although both of these systems are robust, limitations can arise from signal interference by other biological compounds with similar oxidation potential and/or from temperature fluctuations since both methods are temperature dependent.

### **1.3 Summary of Research Aims**

It is apparent that almost all current Ado and adenine ribonucleotides detection methods have some type of limitation. The primary aim of this thesis was to develop a novel Ado detection methodology using capillary electrophoresis-laser induced fluorescence detection (CE-LIF) to provide researchers with an alternative, and in some instances a more robust, approach for the quantification of Ado in biological samples. This research was based on previous work done by Green et al.<sup>50</sup> showing the ability of Ado to undergo a trinitrophenylation reaction with 2,4,6-trinitrobenzenesulfonic acid (TNBS) to form a stable trinitrophenylated derivative that exhibits enhanced fluorescence emission when in the presence of  $\gamma$ -cyclodextrin ( $\gamma$ -CD). The trinitrophenylated derivative of Ado (TNP-ADO), unlike Ado or adenine ribonucleotides alone, has two absorbance maxima of ~410 nm and ~476 nm and a detectable single fluorescence emission between 530-560 nm. From this previous work, it was hypothesized that TNP-Ado would be detectable by CE-LIF and thus, leading to a novel and

sensitive method that is capable of monitoring Ado in minute concentrations and sample volumes. This research is discussed in Chapter 2 and shows the development, optimization and biological application of the CE-LIF method for the analysis of Ado and Inosine, a metabolite of Ado.

A secondary aim of this thesis was to expand the CE-LIF method shown in Chapter 2 for the analysis of adenine ribonucleotides and structurally similar analogs in biological samples. Unfortunately, several complications arose with the CE-LIF analysis of these molecules so more research is needed to fully expand the CE-LIF for accurate analysis. Results from this aim will be discussed in Appendix B.



## 1.4 References

- (1) Nelson, D. L.; Lehninger, A. L.; Cox, M. M. *Lehninger principles of biochemistry*; Macmillan, 2008.
- (2) Koupenova, M.; Ravid, K. *Journal of cellular physiology* **2013**.
- (3) Fields, R. D.; Burnstock, G. *Nature Reviews Neuroscience* **2006**, 7, 423-436.
- (4) Bours, M.; Swennen, E.; Di Virgilio, F.; Cronstein, B.; Dagnelie, P. *Pharmacology & therapeutics* **2006**, 112, 358-404.
- (5) Pisetsky, D.; Berkower, I.; Wickner, R.; Hurwitz, J. *Journal of molecular biology* **1972**, 71, 557-571.
- (6) Conaway, R.; Conaway, J. *Journal of Biological Chemistry* **1988**, 263, 2962-2968.
- (7) Dunwiddie, T. V.; Masino, S. A. *Annual review of neuroscience* **2001**, 24, 31-55.
- (8) Brady, S. T.; Siegel, G. J.; Albers, R. W.; Price, D. L. *Basic neurochemistry*, 8th ed., 2012.
- (9) Zimmermann, H.; Braun, N. *Journal of autonomic pharmacology* **1996**, 16, 397-400.
- (10) Schwiebert, E. M.; Zsembery, A. *Biochimica et Biophysica Acta (BBA)-Biomembranes* **2003**, 1615, 7-32.
- (11) Hyde, R. J.; Cass, C. E.; Young, J. D.; Stephen A. Baldwin, J. D. *Molecular membrane biology* **2001**, 18, 53-63.
- (12) Baldwin, S. A.; Beal, P. R.; Yao, S. Y.; King, A. E.; Cass, C. E.; Young, J. D. *Pflügers Archiv* **2004**, 447, 735-743.
- (13) Gray, J. H.; Owen, R. P.; Giacomini, K. M. *Pflügers Archiv* **2004**, 447, 728-734.
- (14) Etherington, L.-A. V.; Patterson, G. E.; Meechan, L.; Boison, D.; Irving, A. J.; Dale, N.; Frenguelli, B. G. *Neuropharmacology* **2009**, 56, 429-437.
- (15) Abbracchio, M. P.; Burnstock, G. *The Japanese Journal of Pharmacology* **1998**, 78, 113-145.
- (16) Burnstock, G. *Pharmacological reviews* **2006**, 58, 58-86.
- (17) Eltzschig, H. K.; Sitkovsky, M. V.; Robson, S. C. *New England Journal of Medicine* **2012**, 367, 2322-2333.
- (18) Olah, M. E.; Stiles, G. L. *Annual review of pharmacology and toxicology* **1995**, 35, 581-606.
- (19) Burnstock, G. *Cellular and Molecular Life Sciences* **2007**, 64, 1471-1483.
- (20) Porkka-Heiskanen, T.; Kalinchuk, A. V. *Sleep and Biological Rhythms* **2011**, 9, 18-23.



- (21) Daré, E.; Schulte, G.; Karovic, O.; Hammarberg, C.; Fredholm, B. B. *Physiology & behavior* **2007**, *92*, 15-20.
- (22) Blood, A. B.; Hunter, C. J.; Power, G. G. *The Journal of physiology* **2003**, *553*, 935-945.
- (23) Phillis, J. W. *Critical Reviews™ in Neurobiology* **2004**, *16*.
- (24) Rubino, A.; Ralevic, V.; Burnstock, G. *British journal of pharmacology* **1995**, *115*, 648-652.
- (25) Jin, J.; Kunapuli, S. P. *Proceedings of the National Academy of Sciences* **1998**, *95*, 8070-8074.
- (26) Burnstock, G. *Arteriosclerosis, thrombosis, and vascular biology* **2002**, *22*, 364-373.
- (27) Mediero, A.; Cronstein, B. N. *Trends in Endocrinology & Metabolism* **2013**, *24*, 290-300.
- (28) Nichols, C.; Shyng, S.-L.; Nestorowicz, A.; Glaser, B.; Clement, J. t.; Gonzalez, G.; Aguilar-Bryan, L.; Permutt, M.; Bryan, J. *Science* **1996**, *272*, 1785-1787.
- (29) Jacobson, K. A.; Gao, Z.-G. *Nature Reviews Drug Discovery* **2006**, *5*, 247-264.
- (30) Cunha, R. A. *Purinergic signalling* **2005**, *1*, 111-134.
- (31) Bona, E.; Ådén, U.; Gilland, E.; Fredholm, B.; Hagberg, H. *Neuropharmacology* **1997**, *36*, 1327-1338.
- (32) Phillis, J. *Brain research* **1995**, *705*, 79-84.
- (33) Harris, D. C. *Quantitative chemical analysis*; Macmillan, 2010.
- (34) Wojcik, W.; Neff, N. *Journal of neurochemistry* **1982**, *39*, 280-282.
- (35) Coolen, E. J.; Arts, I. C.; Swennen, E. L.; Bast, A.; Stuart, M. A. C.; Dagnelie, P. C. *Journal of Chromatography B* **2008**, *864*, 43-51.
- (36) Qian, T.; Cai, Z.; Yang, M. *Analytical biochemistry* **2004**, *325*, 77-84.
- (37) Van Dycke, A.; Verstraete, A.; Pil, K.; Raedt, R.; Vonck, K.; Boison, D.; Boon, P. *Journal of chromatography. B, Analytical technologies in the biomedical and life sciences* **2010**, *878*, 1493-1498.
- (38) Song, P.; Mabrouk, O. S.; Hershey, N. D.; Kennedy, R. T. *Analytical chemistry* **2011**, *84*, 412-419.
- (39) Haink, G.; Deussen, A. *Journal of Chromatography B* **2003**, *784*, 189-193.
- (40) Pani, A. K.; Jiao, Y.; Sample, K. J.; Smeyne, R. J. *PloS one* **2014**, *9*, e92422.
- (41) Weinberger, R. *Practical capillary electrophoresis*, 2nd ed.; Academic Press: San Diego, California, 2000.

- (42) Özer, N.; Aksoy, Y.; Ögüs, I. H. *Journal of biochemical and biophysical methods* **2000**, *45*, 141-146.
- (43) Tseng, H. C.; Dadoo, R.; Zare, R. N. *Analytical biochemistry* **1994**, *222*, 55-58.
- (44) Liu, J.-X.; Aerts, J. T.; Rubakhin, S. S.; Zhang, X.-X.; Sweedler, J. V. *Analyst* **2014**, *139*, 5835-5842.
- (45) Fang, H.; Pajski, M. L.; Ross, A. E.; Venton, B. J. *Analytical Methods* **2013**, *5*, 2704-2711.
- (46) Hammerstedt, R. H. *Analytical biochemistry* **1973**, *52*, 449-455.
- (47) DeLuca, M.; McElroy, W. D. *Biochemistry* **1974**, *13*, 921-925.
- (48) Ross, A. E.; Venton, B. J. *Analytical chemistry* **2014**.
- (49) Frenguelli, B.; Llaudet, E.; Dale, N. *Journal of neurochemistry* **2003**, *86*, 1506-1515.
- (50) Green, T. K.; Denoroy, L.; Parrot, S. *The Journal of Organic Chemistry* **2010**, *75*, 4048-4055.



## Chapter 2

### Analysis of Trinitrophenylated Adenosine and Inosine using Capillary Electrophoresis-Laser Induced Fluorescence Detection and $\gamma$ -Cyclodextrin<sup>1</sup>

#### 2.1 Abstract

Monitoring molecules such as adenosine (Ado) and inosine (Ino) in the central nervous system has enabled the field of neuroscience to correlate molecular concentration dynamics to neurological function, behavior and disease. *In vivo* sampling techniques are commonly used to monitor these dynamics, however, many techniques are limited by the sensitivity and sample volume requirements of currently available detection methods. Here, we present a novel capillary electrophoresis-laser induced fluorescence detection (CE-LIF) method that analyzes Ado and Ino by derivatization with 2,4,6-trinitrobenzenesulfonic acid to form fluorescent trinitrophenylated complexes of Ado (TNP-Ado) and Ino (TNP-Ino). These complexes exhibit ~25 fold fluorescence enhancement upon the formation of inclusion complexes with  $\gamma$ -cyclodextrin ( $\gamma$ -CD). Association constants were determined as 4600 M<sup>-1</sup> for Ado and 1000 M<sup>-1</sup> for Ino by CE-LIF and the structure of the TNP-Ado:  $\gamma$ -CD association complex was determined by 2D nuclear magnetic resonance (NMR) spectroscopy. Optimal trinitrophenylation reaction conditions and CE-LIF parameters were determined and resulted in the limit of detection to be 1.6  $\mu$ M for Ado and 4  $\mu$ M for Ino. Ado and Ino were simultaneously quantified in homogenized rat forebrain samples to illustrate application of the technique. Large-volume sample stacking (LVSS) was studied on a dilute TNP-Ado and TNP-Ino solution in water and resulted in a ~10-fold enhancement in the method sensitivity.

---

<sup>1</sup> Terilyn K.L. Stephen, Katherine L. Guillemette, and Thomas K. Green. Submitted to *Analytical Chemistry*

## 2.2 Introduction

The ability to monitor endogenous and biologically active molecules in the central nervous system (CNS) has provided neuroscientists a significant tool in understanding the mechanisms behind neurological function, behavior and disease. Much effort has been made in developing highly sensitive and fast detection systems that can be used during *in vivo* and *in vitro* experiments to correlate neurotransmitters and neuromodulators (e.g. glutamate, serotonin and dopamine) concentrations to brain function.<sup>1-3</sup> More importantly, the recognition for a new generation of smaller, low volume sampling probes has also increased the demand for novel detection methods that are capable of analyzing molecules in high sensitivity and spatial resolution.<sup>4-6</sup>

One important signaling molecule that has contributed to this demand is adenosine (Ado, Figure 2.1A). Ado is a purine ribonucleoside that has both excitatory and inhibitory function in neurotransmission<sup>7-9</sup> through the activation of 4 receptor subtypes (A<sub>1</sub>, A<sub>2A</sub>, A<sub>2B</sub> and A<sub>3</sub>). It is reported that activation of Ado receptors in the CNS exhibits neuroprotective properties during ischemic,<sup>10,11</sup> hypoxic,<sup>12,13</sup> and epileptic induced injury.<sup>14,15</sup> Ado is also vital in energy homeostasis<sup>16,17</sup> and thermoregulation<sup>18,19</sup> since it is a precursor for adenosine 5'-monophosphate (AMP), 3'-5'-cyclic adenosine monophosphate (cAMP) and adenosine 5'-triphosphate (ATP).

Common means to monitoring Ado dynamics in the brain is by *in vivo* sampling<sup>2,20,21</sup> and tissue extraction.<sup>22,23</sup> Separation and detection of Ado is typically accomplished with liquid chromatography (LC) and UV-absorbance<sup>24,25</sup> but fluorescence,<sup>26</sup> mass spectrometry,<sup>2,27</sup> and electrochemical<sup>23</sup> detection have also been reported. One disadvantage of the LC methods are the requirement of microliter sample volumes that can seriously limit temporal resolution during *in vivo* experiments.<sup>2,20</sup> More recently, studies have focused on developing enzymatic<sup>13,28</sup> and fast scan cyclic voltammetry<sup>22,29</sup> probes in hopes of eliminating temporal resolution problems by measuring Ado on a sub-second time scale during *in vivo* experiments. Unfortunately,

compounds with similar oxidation potentials such as hydrogen peroxide and ATP can create signal interference and add additional resolution issues.<sup>29</sup>

Another separation technique with high separation efficiency and a low sample volume requirement is capillary electrophoresis (CE). CE has high mass sensitivity and separations are not dependent on column length, like LC. Analytes are electrokinetically separated from complex matrixes by passing an applied voltage through a background electrolyte (BGE) and several detection techniques can be coupled to CE including UV-absorbance,<sup>30</sup> laser-induced fluorescence,<sup>31</sup> and mass spectrometry.<sup>32</sup> Online or in-capillary sample preconcentration techniques can also be used with CE to enhance the sensitivity and resolution. These techniques rely on reducing the band width of the analyte while in the capillary and injection of large amounts of the analyte/sample.<sup>33</sup> Large-volume sample stacking (LVSS), field-amplified sample stacking (FASS) and pH-mediated sample stacking are just several of the reported stacking techniques used to improve the limitations of CE.<sup>34,35</sup>

CE coupled with laser-induced fluorescence detection<sup>31</sup> (CE-LIF) and fast scan cyclic voltammetry (CE-FSCV)<sup>22</sup> has also been recently used to monitor Ado in brain tissue extractions. However, both methodologies have limitations. The CE-LIF method developed by Tseng et al.<sup>31</sup> requires Ado to be reacted with chloroacetaldehyde under extreme temperatures (95-100°C) to exhibit fluorescence properties. The high heat required for this method can be disadvantageous if samples are temperature sensitive and may result in sample degradation and/or increased signal interference. The CE-FSCV method by Fang et al.<sup>22</sup> uses instrumentation that was built in-house, consequently minimizing the accessibility of the method to other research groups. Despite these previous efforts, the warrant for a highly sensitive and accessible method capable of monitoring Ado in small sample volumes is still unmet, therefore, delaying the ability of neuroscientists to further investigate the role of Ado in biological function.

Here, we report a novel CE-LIF method for monitoring Ado (Figure 2.1A) that uses a less invasive fluorescence labeling procedure, commercially available instrumentation and the

potential to use sample-stacking techniques to improve analyte sensitivity when needed. The method requires small sample volumes (5  $\mu$ L) and provides biologically relevant sensitivity as well as the ability to quantify inosine (Ino, Figure 2.1A), another biologically significant nucleoside. A key step in developing the method was to find a fluorescence labeling procedure that was able to react with Ado and be detectable by a CE-LIF system. Earlier studies<sup>36-38</sup> had shown that Ado could be reacted with 2,4,6-trinitrobenzenesulfonic acid (TNBS) to form a stable trinitrophenylated derivative (TNP-Ado, Figure 2.1B) that has two absorbance maxima at  $\sim$ 410 nm and  $\sim$ 476 nm and single fluorescence emission between 530-560 nm. We previously investigated the reaction kinetics and steady-state fluorescence of TNP-Ado and discovered that the steady state fluorescence of TNP-Ado was enhanced  $\sim$ 100-fold by the addition of  $\gamma$ -cyclodextrin ( $\gamma$ -CD)<sup>39</sup>. Cyclodextrins (CDs) contain a hydrophobic cavity that can enhance the fluorescence emission of smaller molecules by forming inclusion complexes.<sup>40</sup> This phenomenon was easily translated to the CE-LIF method by the addition of CDs to the BGE. We also determined the structure of the TNP-Ado:  $\gamma$ -CD using 2D nuclear magnetic resonance (NMR) spectroscopy. The trinitrophenylation reaction of Ado and Ino with TNBS was successful at submicromolar concentrations in small volumes and resulted in a separation time under 6 minutes using commercial available CE-LIF instrumentation. Therefore, other research groups monitoring these molecules during small volume generating experiments can easily adapt our method.

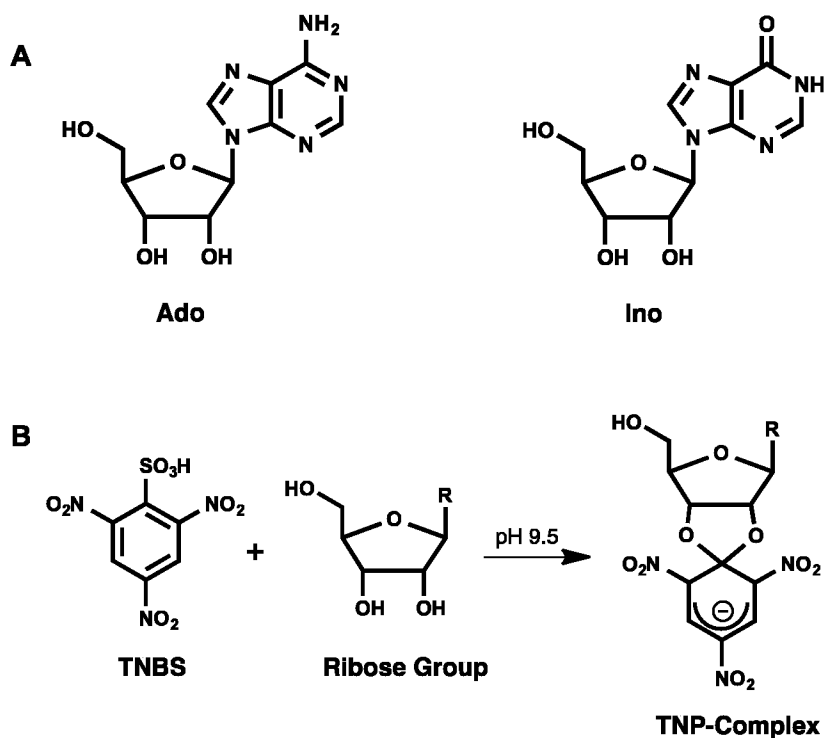


Figure 2.1. (A) Chemical structures of Adenosine (Ado) and Inosine (Ino). (B) Trinitrophenylation reaction scheme between 2,4,6-trinitrobenzenesulfonic acid (TNBS) and the ribose group of Ado or Ino to form the TNP complex.

## 2.3 Methods

### 2.3.1 Safety Considerations

2,4,6-trinitrobenzenesulfonic acid (TNBS, picrylsulfonic acid, ~1M in H<sub>2</sub>O) should be handled with gloves and precaution. It should not be allowed to dry out, as it is potentially explosive when dry. A minor byproduct of the trinitrophenylation reaction between adenosine (Ado) or inosine (Ino) and TNBS is picric acid. Picric acid is also potentially explosive when dry.

### 2.3.2 Chemicals and Reagents

All chemicals were analytical grade and purchased from VWR (Randor, PA) unless otherwise noted. Water was purified from a Thermo Scientific GenPure ultrapure water system with an 18.2 MΩ•cm resistivity. Ino, TNBS, fluorescein and 2-hydroxypropyl-γ-cyclodextrin were



purchased from Sigma Aldrich (St. Louis, MO). Randomly methylated- $\gamma$ -cyclodextrin and randomly carboxymethylated- $\gamma$ -cyclodextrin were purchased from CTD, Inc. (Alachua, FL). A fresh standard of artificial cerebral spinal fluid (aCSF) solution was prepared as needed and contained 120 mM NaCl, 45.7 mM NaHCO<sub>3</sub>, 3.3 mM KCl, 1.2 mM NaH<sub>2</sub>PO<sub>4</sub>, 240 mM MgSO<sub>4</sub>, 50 mM CaCl<sub>2</sub>, and 100 mM glucose. For the 0.1 M sodium carbonate buffer at pH 10, equal volumes of a 0.2 M sodium bicarbonate and 0.2 M sodium carbonate solution were mixed. The background electrolyte (BGE) was 20 mM sodium borate with 2 mM  $\gamma$ -cyclodextrin at pH 9.4 unless otherwise noted. The BGE was filtered through a 0.2  $\mu$ m PTFE syringe filter (VWR, Randor, PA) prior to use.

### 2.3.3 Preparation of TNP-Ado and TNP-Ino Standards

A similar procedure to Green et al.<sup>39</sup> and Hiratsuka et al.<sup>38</sup> was followed. For the TNP standards, 60 mg of either Ado or Ino was dissolved in 2 mL of Milli-Q H<sub>2</sub>O and 0.88 mL of TNBS (~1M in H<sub>2</sub>O) was added. The pH was continuously monitored for 3 hours, adding 1 M NaOH until the pH was stabilized at 10. The reaction was left overnight and purified the next morning on a Sephadex LH-20 column (Sigma Aldrich, St. Louis, MO). The purified standard was retained at the top of the column after eluting impurities with water and appeared as a bright reddish-orange band. The standard was eluted from the column with methanol, dried by rotary evaporation and analyzed by <sup>1</sup>H NMR spectroscopy in D<sub>2</sub>O to confirm purity (Figure A2.1 and A2.2 in Appendix A).

### 2.3.4 <sup>1</sup>H, HMQC and ROESY NMR Spectra

All NMR spectra were obtained at 600 MHz (Bruker Ascend). Temperature-dependent <sup>1</sup>H NMR spectra were referenced to D<sub>2</sub>O according to its known variation of chemical shift with temperature. Two-dimensional heteronuclear multiple quantum coherence (HMQC) and rotational nuclear Overhauser effect spectroscopy (ROESY) spectra were recorded on 1:1

mixtures of TNP-Ado and cyclodextrin (~5 mM each). HMQC spectra were acquired using the standard pulse sequence provided by Bruker. The standard ROESY pulse sequence and the method of phase cycling described by States et al.<sup>41</sup> was used. The spectra were collected into 1024 data points in each block with quadrature detection by using a spectral width of 3000 Hz and mixing time of 200 ms. Typically 256 t1 experiments were collected with 32 scans signal averaged for each t1 value. The recycle time was 1.5 s. The data were zero-filled in both dimensions to give 2048 x 2048 real data points. Gaussian apodization was imposed in each dimension prior to Fourier transformation.

### **2.3.5 CE-LIF Analysis and LVSS Studies**

An Agilent Technologies 7100 automated CE system (Santa Clara, CA) coupled to a Picometrics Zetalif laser-induced fluorescence detector (France) was used for analysis. A 405 nm Oxiuux Laser Diode (France) with the power adjusted to 25 mW was used for an excitation wavelength and separations were performed, unless otherwise stated, on a 75  $\mu$ m ID, 360  $\mu$ m OD fused silica capillary (Polymicro Technologies, Phoenix, AZ). Capillary were cut to a total length of 48 cm and an effective length of 20 cm (28 cm to the detection window). New capillaries were conditioned for a total of 45 min: 15 min 1 M NaOH, 15 min Milli-Q H<sub>2</sub>O and 15 min BGE. All non-sample-stacking separation experiments were performed at 25°C with normal polarity at +10 kV (anode at inlet) and hydrodynamic injections were typically 50 mbar for 1 s. For LVSS studies, samples were injected hydrodynamically at 50 mbar ranging from 60 to 240 s. Voltage was applied in reversed polarity at -10 kV (cathode at inlet) until the electric current reached 70-95% of the value when filled with BGE. Once reached, the voltage was switched to normal polarity at +10 kV and separations proceeded normally. Before each individual run, the capillary was preconditioned for 2 min with 0.1 M NaOH followed by 2 min with BGE and post-conditioned for 2 min with Milli-Q H<sub>2</sub>O.

### 2.3.6 Trinitrophenylation Reactions

Stock solutions, 1 mM of Ado and Ino, were diluted to 0.1 mM in aCSF. Reactions were performed in triplicates and 20  $\mu\text{L}$  of 0.1 mM of the standard solution in aCSF was reacted with 10  $\mu\text{L}$  of TNBS ( $\sim 1\text{ M}$  in  $\text{H}_2\text{O}$ ), 10  $\mu\text{L}$  of 1 M NaOH and 120  $\mu\text{L}$  of 0.1 M carbonate buffer at pH 10. The reactions were vortexed and then placed in a heat block set at either 37  $^\circ\text{C}$  or 50  $^\circ\text{C}$ . To determine the percentage of product conversion by CE-LIF analysis, 10  $\mu\text{L}$  of the reaction mixture was diluted by 10x in Milli-Q  $\text{H}_2\text{O}$  containing 0.02  $\mu\text{M}$  of sodium fluorescein (internal standard, IS) and monitored every 2 hours for 10 hr, then at 20 and 24 hrs. Calibration curves were made using standards of 8, 40, 80, 400 and 800  $\mu\text{M}$  TNP-Ado and TNP-Ino containing the same ratios volumes of TNBS, NaOH and carbonate buffer as the trinitrophenylation reactions (1  $\mu\text{L}$  sample to 0.5  $\mu\text{L}$   $\sim 1\text{M}$  TNBS, 0.5  $\mu\text{L}$  1M NaOH and 6  $\mu\text{L}$  0.1M carbonate buffer). These calibration standards were diluted by 10x prior to CE-LIF analysis in Milli-Q  $\text{H}_2\text{O}$  containing 0.02  $\mu\text{M}$  of internal standard.

### 2.3.7 Biological Sample Preparation

Tissue samples were prepared from donated adult Sprague-Dawley rat whole brain tissue and procedures were followed from previous literature.<sup>30</sup> Brain tissue was kept frozen at -80  $^\circ\text{C}$  and forebrain tissue ranging from 50 to 100 mg was removed for analysis. 5  $\mu\text{L}$  of Milli-Q water (95-100  $^\circ\text{C}$ ) was added for every 1 mg of tissue and samples were boiled at 95-100  $^\circ\text{C}$  for 5 min. Tissue was homogenized using a VWR disposable pellet mixer (Randor, PA) and centrifuged at 13000 rmps at 4  $^\circ\text{C}$  for 5 mins. Tissue supernatant was then transferred to a 0.22  $\mu\text{m}$  nylon centrifuge tube filter (Spin-X, Corning, Inc., Corning, NY), centrifuged at 1300 rmps at 4  $^\circ\text{C}$  for 5 mins, and frozen at -80  $^\circ\text{C}$  until reacted for analysis. For the reaction, 2.5  $\mu\text{L}$  of TNBS ( $\sim 1\text{M}$  in  $\text{H}_2\text{O}$ ), 2.5  $\mu\text{L}$  of 1M NaOH and 30  $\mu\text{L}$  of 0.1 M carbonate buffer (pH 10) was added to 5  $\mu\text{L}$  of tissue supernatant. Samples were vortexed, placed in a heat block at 50  $^\circ\text{C}$  for 6 hr and diluted by 10x prior to CE-LIF analysis in Milli-Q  $\text{H}_2\text{O}$  containing 0.02  $\mu\text{M}$  of internal standard.

### 2.3.8 Statistical Analysis

Analyte peaks were manually integrated using ChemStation software (Agilent Technologies, Santa Clara, CA). All values reported are the mean  $\pm$  standard deviation. Calibration curves were constructed using the peak area of the analyte divided by the peak area of the internal standard ratio versus concentration of the analyte. For the association (binding) constant determination, data was fitted by 2-parameter nonlinear curve fitting<sup>42</sup> in GraphPad Prism (La Jolla, CA).

## 2.4 Results and Discussion

### 2.4.1 CE-LIF Optimization

The CE-LIF parameters were optimized for detection of TNP-Ado and TNP-Ino in biologically relevant sample concentrations and volumes using pure TNP standards synthesized as previously stated in the methods section. A background electrolyte (BGE) of 20 mM sodium borate at pH 9.4 was chosen for the separation of TNP-Ado and TNP-Ino. A basic BGE is needed because TNP complexes can ring open at low pH therefore resulting in a loss of stability and fluorescence.<sup>43,44</sup> The integrated fluorescence intensities of TNP-Ado and TNP-Ino were significantly enhanced upon the addition of  $\gamma$ -CD in the BGE (Figure 2.2 and 2.3). Other modified cyclodextrins were investigated for fluorescence enhancement, including 2-hydroxypropyl- $\gamma$ -cyclodextrin, randomly methylated- $\gamma$ -cyclodextrin, and randomly carboxymethylated- $\gamma$ -cyclodextrin, but none provided enhancement above that of  $\gamma$ -CD, and all were more expensive. The addition of 2 mM  $\gamma$ -CD in the BGE (Figure 2.2A) showed approximately a 30-fold and 17-fold fluorescence enhancement for TNP-Ado (10  $\mu$ M) and TNP-Ino (10  $\mu$ M), respectively. These results are in general agreement with the Green et al.<sup>39</sup> study that reported an  $\sim$ 100-fold enhancement in the integrated steady-state fluorescence intensity of TNP-Ado (4  $\mu$ M) with 10 mM  $\gamma$ -CD compared to water alone. The addition of 2 mM  $\gamma$ -CD in the

BGE delivered stable baselines and reproducible separations and its addition was further confirmed by calculation of association constants, later discussed.

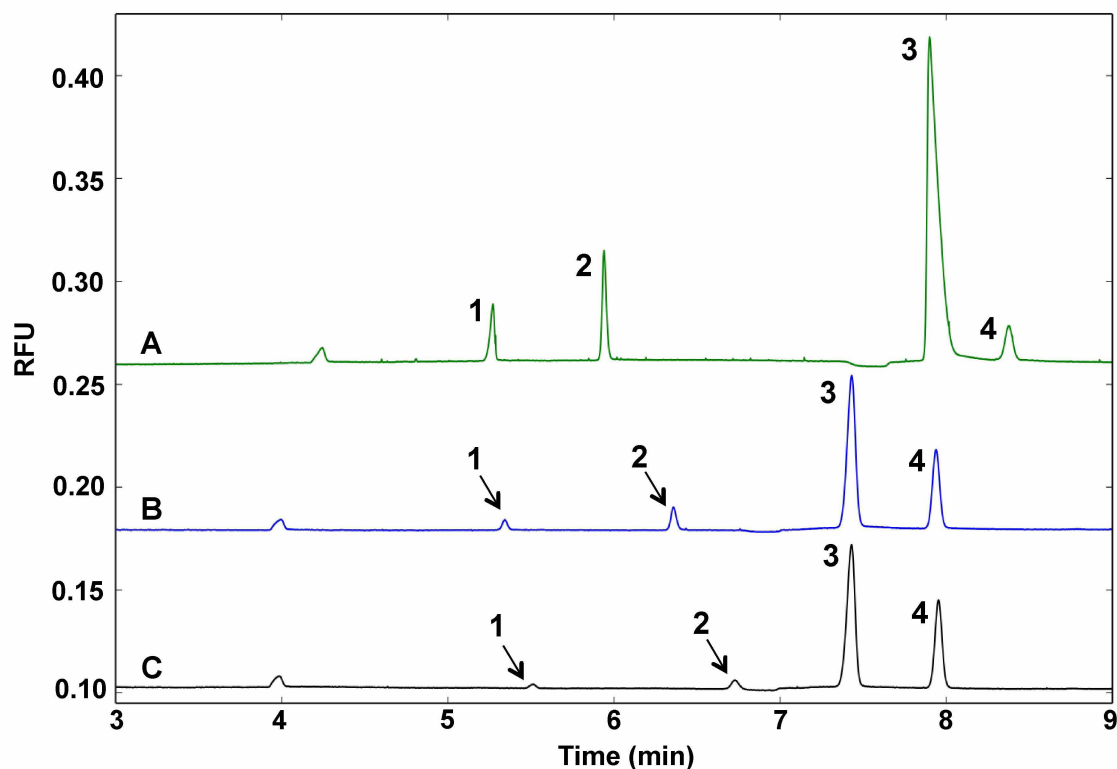


**Figure 2.2. Effect of  $\gamma$ -CD concentration on the separation and fluorescence of TNP-Ado (10  $\mu$ M), TNP-Iso (10  $\mu$ M), TNBS (~12.5 mM) and fluorescein (internal standard, IS, 0.02  $\mu$ M) dissolved in aCSF and 0.1 M carbonate buffer at pH 10. (A) 2 mM  $\gamma$ -CD; (B) 0.2 mM  $\gamma$ -CD, (C) 0 mM  $\gamma$ -CD. Peak identification: 1 TNP-Ado, 2 TNP-Iso, 3 TNBS, 4 IS. CE Parameters: Inner capillary diameter 75  $\mu$ m; total length 40 cm; effective length 28 cm; injection pressure 50 mbar; injection time 1 s; applied voltage 10 kV; laser power 25 mW; 25°C; BGE 20 mM sodium borate with various  $\gamma$ -CD concentrations at pH 9.4.**

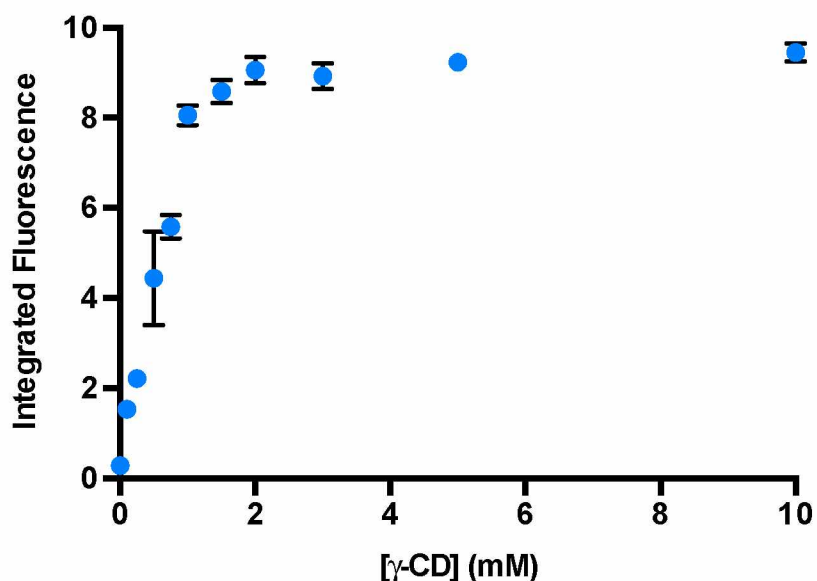
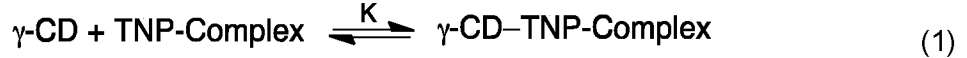


**Figure 2.3. Effect of  $\gamma$ -CD on the integrated fluorescence of a 10  $\mu$ M standard of TNP-Ado in water.** CE-LIF parameters: Inner capillary diameter 50  $\mu$ m; effective length 28 cm; injection pressure 50 mbar; injection time 1 s; applied voltage 20 kV; laser power 25 mW; BGE 20 mM sodium borate with various  $\gamma$ -CD concentrations at pH 9.4.

#### 2.4.2 Determination of $\gamma$ -CD Association Constants

The ability of  $\gamma$ -CD to enhance the fluorescence and shorten the migration time of the TNP-complexes is based on the CDs ability to form inclusion complexes with small molecules.<sup>40</sup> Because CDs contain a hydrophobic cavity, small molecules with nonpolar regions can associate with the cavity in equilibrium. As shown in Figure 2.2, an increase in  $\gamma$ -CD concentration alters the migration (mobility) time of TNP-Ado and TNP-Ino. This relationship can be used to characterize the association or binding interactions between the  $\gamma$ -CD and the TNP-complexes.

Green et al.<sup>39</sup> determined that TNP-Ado forms a 1:1 complex with  $\gamma$ -CD. Assuming 1:1 stoichiometry, the equilibrium between  $\gamma$ -CD, the TNP-Complex and inclusion complex can be modeled by a simple reversible complexation (Equation 1 and 2).



$$K = \frac{[\gamma\text{-CD-TNP-Complex}]}{[\gamma\text{-CD}][\text{TNP-Complex}]} \quad (2)$$

The association (binding) constant,  $K$ , measures the affinity of the TNP-Complex to bind with  $\gamma$ -CD and can be experimentally determined by CE methods.<sup>45</sup> In CE, the separation of analytes in a complex mixture is dependent on the actual electrophoretic mobility of the analyte ( $\mu_{ep}$ ) and the electroosmotic flow (EOF) mobility ( $\mu_{eof}$ ), the pumping mechanism resulting from the movement of charges through the capillary when current is applied.<sup>46</sup> The strength and direction of the  $\mu_{ep}$  and  $\mu_{eof}$  are largely dependent on the pH and concentration of the BGE<sup>46</sup> and as a result, the observed electrophoretic mobility of an analyte ( $\mu_{obs}$ ) is the sum of the  $\mu_{ep}$  and  $\mu_{eof}$  vectors (Equation 3).

$$\mu_{obs} = \mu_{ep} \pm \mu_{eof} \quad (3)$$

The association constant,  $K$ , can be expressed as a function of CD concentration and the actual electrophoretic mobilities of the free, unbound analyte ( $\mu_f$ ) and the bound inclusion complex ( $\mu_c$ ). Rundlett and Armstrong<sup>42,45</sup> derived an equation that can be experimentally solved for  $K$  by 2 parameter nonlinear curve fitting (Equation 4)

$$\mu_i = \frac{\mu_f + \mu_c K[\text{CD}]}{1 + K[\text{CD}]} \quad (4)$$

where  $\mu_i$  is the experimentally measured electrophoretic mobility of the inclusion complex,  $\gamma$ -CD-TNP-complex,  $\mu_f$  is the electrophoretic mobility of the free, unbound TNP-Complex,  $\mu_c$  is an

estimation of the electrophoretic mobility of the bound inclusion complex at the maximum CD concentration and CD is the concentration of  $\gamma$ -CD.

The actual electrophoretic mobilities ( $\mu_i$ ) of a 10  $\mu$ M standard of TNP-Ado and TNP-Ino were plotted as a function of  $\gamma$ -CD concentration (Figure 2.4). The concentration of  $\gamma$ -CD that was added to the BGE ranged from 0 to 0.010 M (10mM). It is expected that the addition of  $\gamma$ -CD to the BGE would change the BGE viscosity and thus, alter the mobility of the inclusion complexes. However the measured change in BGE viscosity upon the addition of  $\gamma$ -CD was negligible. These results allowed us to calculate the electrophoretic mobilities ( $\mu_i$ ) without correcting for a change in BGE viscosity. Based on Figure 2.4, it was also determined that the addition of 2 mM  $\gamma$ -CD to the BGE provided a maximum decrease in the electrophoretic mobilities ( $\mu_i$ ) of TNP-Ado and TNP-Ino.

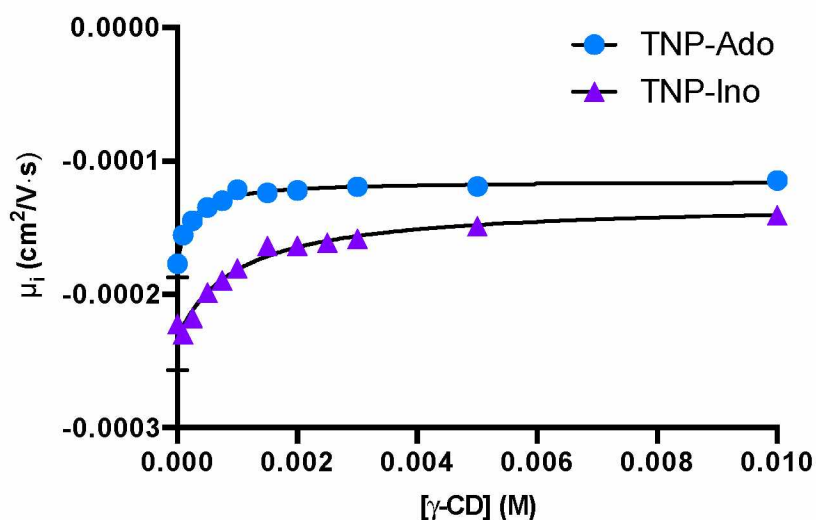


Figure 2.4. The relationship between the electrophoretic mobility  $\mu_i$  (cm<sup>2</sup>/V·s) of 10  $\mu$ M standards of TNP-Ado and TNP-Ino and concentration of  $\gamma$ -CD (M) at 25 °C. See Figure 2.3 for CE-LIF parameters.



As also shown in Figure 2.4, plots were fitted with Equation 4<sup>42,45</sup> by 2-parameter non-linear curve fitting,  $K$  and  $\mu_c$  as variables. The association constants for TNP-Ado and TNP-Ino were calculated to be  $4600 \pm 460 \text{ M}^{-1}$  with a  $R^2$  of 0.9779 and  $1000 \pm 190 \text{ M}^{-1}$  with a  $R^2$  of 0.9348, respectively (Table 2.1). Based on the similarities in chemical structure, it was predicted that the association constants of TNP-Ado and TNP-Ino would yield similar values. This prediction was based on the assumption that the trinitrophenyl group of the complex associates with  $\gamma$ -CD, not the nucleotide base.<sup>39</sup> Our results, however, show that TNP-Ino has a lower affinity for  $\gamma$ -CD compared to TNP-Ado. The lower association constant can be explained by the fact that TNP-Ino possesses an acidic amido hydrogen located on the nucleotide base with a  $pK_a$  of 8.8.<sup>47</sup> Since the pH of the BGE is 9.4, the dianionic form of TNP-Ino predominates in solution and results in an increase in water solubility. We suggest that this increase in solubility causes the TNP-Ino molecule to reduce its affinity for forming an inclusion complex with  $\gamma$ -CD and thus, results in a lower association constant compared to TNP-Ado.

### 2.4.3 Structural Determination of TNP-Ado and $\gamma$ -CD Inclusion Complex

To further investigate the strong association between TNP-Ado with  $\gamma$ -CD, we used 2D NMR to determine the structure of the TNP-Ado:  $\gamma$ -CD inclusion complex. Green et al.<sup>39</sup> have conducted NMR studies on the TNP-Ado:  $\gamma$ -CD inclusion complex using ROESY experiments. However, a definitive interpretation of their results was not provided.

Hydrogen assignments for both TNP-Ado and  $\gamma$ -CD were determined using the Green et al.<sup>39</sup> study and further confirmed using HMQC experiments on  $\sim 5 \text{ mM}$  solutions of  $\gamma$ -CD (no TNP-Ado) and a 1:1 mixture of TNP-Ado:  $\gamma$ -CD in  $D_2O$  (see Figure A2.3 and A2.4 in Appendix A). In the presence of  $\gamma$ -CD, the aromatic H-2 and H-8 of the adenine base of TNP-Ado appear as singlets at  $\sim 8.25$  and  $\sim 8.15$  ppm, respectively (see top of spectra in Figure 2.5 and structure in Figure 2.6). The two  $H_{\text{TNP}}$  resonances of the TNP moiety are assigned to 7.90 and 8.43 ppm and are anisochronous hydrogens (Figure 2.5 and 2.6). The broadening of all 4 hydrogen

resonances in the presence of  $\gamma$ -CD is indicative of the strong association between TNP-Ado with  $\gamma$ -CD.<sup>39</sup>

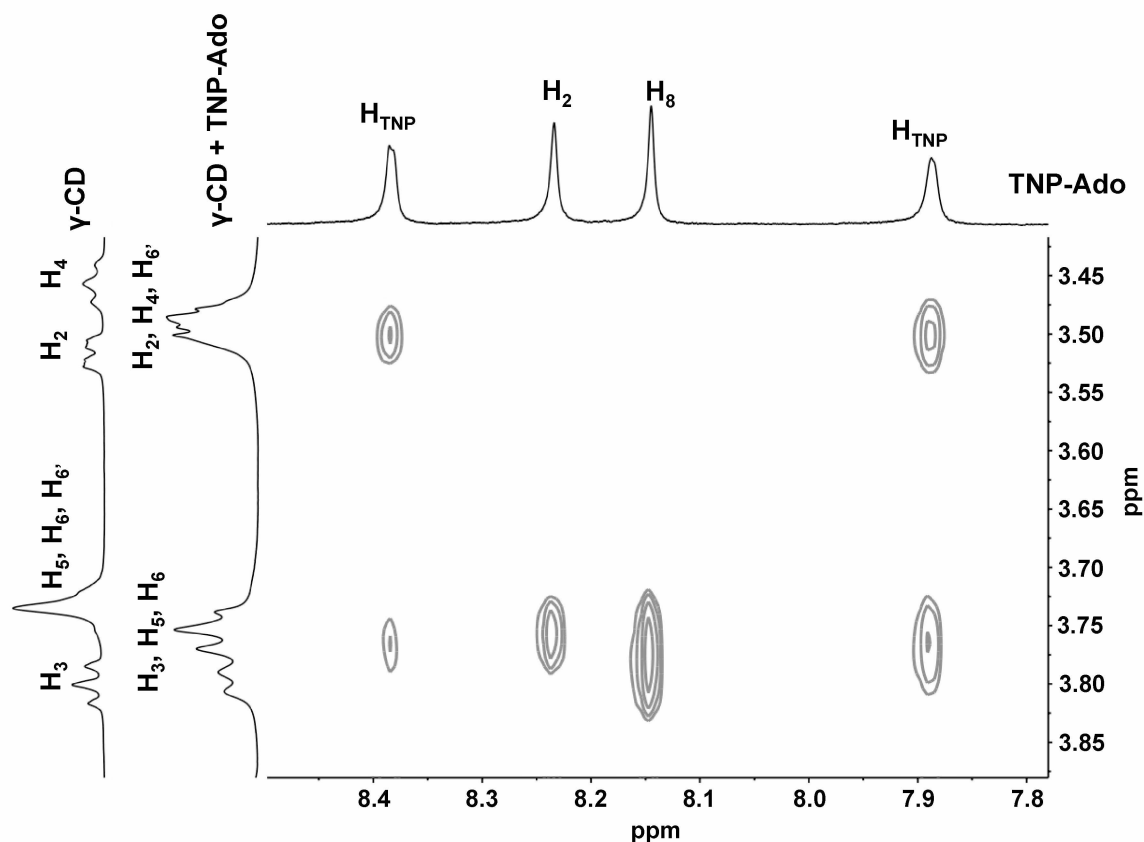


**Figure 2.5. Partial 2D ROESY spectrum of 1:1 mixture of  $\gamma$ -CD and TNP-Ado (~5mM each) in  $D_2O$ . Mixing time 200ms.**

In order to understand the resonance assignments and the structural interaction between TNP-Ado and  $\gamma$ -CD, the structure of  $\gamma$ -CD should be noted. The H-3 and H-5 of the D-glucose units of  $\gamma$ -CD are directed internally towards the hydrophobic cavity, whereas H-2 and H-4 are directed externally.<sup>39,48</sup> The two H-6 hydrogens are positioned on the primary rim of the CD, which are nonequivalent and diastereotopic.<sup>39,48</sup> The H-3 and H-5 resonances of  $\gamma$ -CD are assigned to the triplet at 3.8 ppm and a multiplet at 3.74 ppm, respectively (Figure A2.3 in Appendix A). The H-2, H-4 and 2 H-6 designated as H-6 and H-6' resonances are assigned to 3.52, 3.46 and 3.74 ppm, respectively (Figure A2.3 in Appendix A). The  $^1H$  NMR spectra of  $\gamma$ -CD

in the absence and presence of TNP-Ado are shown on the side in Figure 2.5. This illustrates the upfield shift of H-6' resonance on the primary rim of  $\gamma$ -CD when in the presence of TNP-Ado. This is indicative of a strong association with TNP-Ado and may be a result of ring current effects of the TNP moiety but further investigation is needed to support this hypothesis.

To provide a more definitive interruption of the TNP-Ado:  $\gamma$ -CD inclusion complex structure, 2D ROESY NMR was acquired for a 1:1 TNP-Ado:  $\gamma$ -CD mixture in D<sub>2</sub>O (Figure 2.5). Intense through-space correlations are seen with H-2 and H-8 hydrogens on the adenine base and the downfield region (3.7-3.85 ppm) of the  $\gamma$ -CD. This region contains the internally directed H-3 and H-5 resonances and a single H-6 resonance of  $\gamma$ -CD. Because H-2 and H-8 of TNP-Ado show no correlations to the upfield region (3.45-3.55 ppm) containing the external H-2, H-4 and H-6' resonances of  $\gamma$ -CD, it can be concluded that adenine base of the TNP-Ado molecule is only interacting with the H-3 and H-5 hydrogens of  $\gamma$ -CD. Strong through-space correlations between the two H<sub>TNP</sub> resonances of the TNP-Ado molecule and both the upfield and downfield regions of  $\gamma$ -CD are also seen in Figure 2.5. Due to the correlation with both regions, it can be presumed that the H<sub>TNP</sub> resonances are interacting with the primary H-6 hydrogens of  $\gamma$ -CD.

Figure 2.6 illustrates the proposed structural determination of the TNP-Ado:  $\gamma$ -CD inclusion complex. These results conflict with the findings presented in the Green et al.<sup>39</sup> study. Green originally hypothesized that the TNP moiety of the TNP-Ado complex inserts itself in the hydrophobic cavity containing H-3 and H-5 of  $\gamma$ -CD. This was primarily based on a good size-shape match of  $\gamma$ -CD and TNP-Ado since their NMR studies could not provide a definitive structure. Our results, however, provide strong evidence that the adenine base of the TNP-Ado molecule inserts itself into the primary rim of  $\gamma$ -CD. This model also accounts for the reduced affinity of the dianionic TNP-Ino molecule forming an inclusion complex with  $\gamma$ -CD since the nucleotide base is inserting in the cavity of  $\gamma$ -CD.

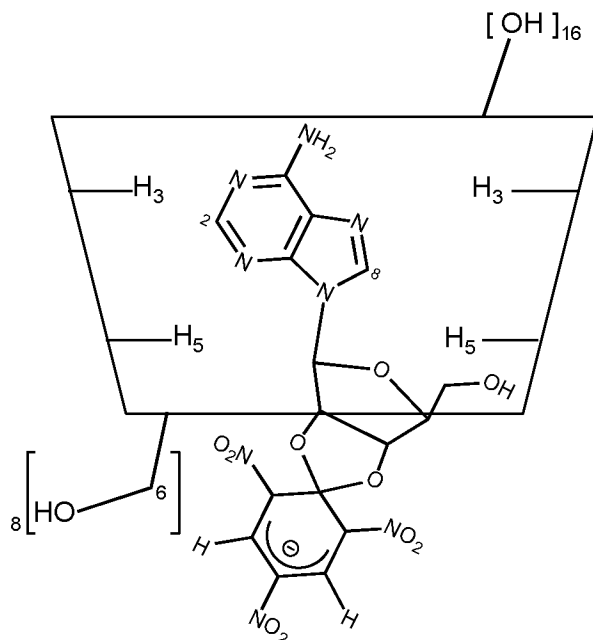


Figure 2.6. Proposed inclusion complex of TNP-Ado:  $\gamma$ -CD.

#### 2.4.4 Trinitrophenylation Reaction Kinetics Monitored by CE-LIF

In order to ensure the trinitrophenylation of Ado and Ino would be successful at biologically relevant concentrations and in small volumes, the reaction kinetics were monitored by CE-LIF. The reaction kinetics of Ado and Ino were monitored with the goal of 90-100% analyte conversion to its corresponding TNP-Complex in a reasonable timeframe and by using a reaction procedure that could be easily translated to the detection of Ado and Ino in various biological matrices (e.g. tissue, plasma, brain microdialysate).

Trinitrophenylation reactions were optimized for time, temperature, reagent concentrations and solvent conditions. The trinitrophenylation of Ado and other nucleic acids have been studied in large volumes (2-5 mL) and at millimolar concentration by UV-Vis absorption.<sup>36,37,44</sup> The rate of Ado conversion is also highly dependent on the pH and composition of the buffer system used.<sup>37,44</sup> Azegami and Iwai<sup>37</sup> reported that a 0.5 M sodium carbonate buffer system at pH 10.0 resulted in a 50% reaction time of 21 min for the conversion of Ado (10 mM) to TNP-Ado at

37°C. The trinitrophenylation of Ado (100 µM) in 3 concentrations of sodium carbonate buffers at pH 10 (0.1 M, 0.15 M and 0.5 M) was monitored at 37°C for 20 hr (See Figure A2.5 in Appendix A). Interestingly, the 100 µM Ado reaction in a 0.5 M sodium carbonate buffer at pH 10 resulted in a lower Ado conversion rate compared to the 0.1 M and 0.15 M sodium carbonate reactions. The maximum percent conversion was less than 60% after 20 hr at all sodium carbonate concentrations.

Because of the low conversion rates of Ado at 37°C, the trinitrophenylation reaction was monitored at a reaction temperature of 50°C. We predicted that at a higher temperature, the reaction rates of Ado and Ino with TNBS would increase and thus, result in a conversion rate close to 100% while yielding a shorter reaction time. A 100 µM standard of Ado and Ino in aCSF was then reacted with TNBS (0.06 M) in a 0.1 M sodium carbonate buffer at pH 10 at 50°C and analyte conversion rates were monitored over 24 hr.

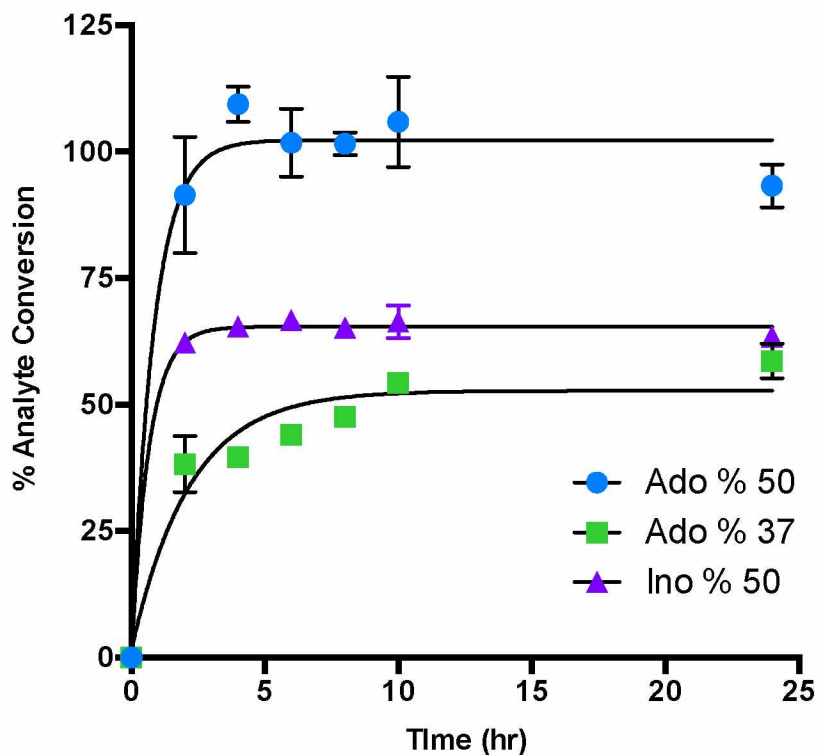


**Figure 2.7. Rates of the trinitrophenylation of Ado (100  $\mu\text{M}$ ) at 50°C and 37°C and Ino (100  $\mu\text{M}$ ) at 50°C.** Reaction monitored as the % conversion of Ado and Ino to the trinitrophenylation products of TNP-Ado and TNP-Ino, respectively. See Figure 2 for CE-LIF parameters not stated; BGE 2 mM  $\gamma$ -CD in 20 mM sodium borate at pH 9.4.

Figure 2.7 shows a comparison of the percent conversion of Ado and Ino to its corresponding TNP-Complex as a function of reaction time and temperature (37°C and 50°C). The trinitrophenylation of Ado at 50°C resulted in ~100% ( $101 \pm 6$ ) conversion to TNP-Ado after 6 hr where as at 37°C, the maximum Ado conversion was ~60% ( $59 \pm 3$ ) after 24 hours. There were no signs of TNP-Ado degradation at 50°C since the Ado conversion rate was stable at 100% after 24 hr. The conversion of Ino to TNP-Ino at 50°C was lower at ~67% ( $67 \pm 2$ ) but also showed no degradation of the TNP-Ino complex after formation. These reactions were also conducted using 20  $\mu\text{L}$  sample volumes and optimized reagent quantities. It was determined that for every 1  $\mu\text{L}$  of sample: 0.5  $\mu\text{L}$  of TNBS (~1M in  $\text{H}_2\text{O}$ ), 0.5  $\mu\text{L}$  of 1M NaOH and 6  $\mu\text{L}$  of 0.1M carbonate buffer at pH 10 were needed to have successful trinitrophenylation of Ado

(~100% conversion after 6 hr) and Ino (~67 % after 6 hr). The addition of 1 M NaOH is required to ensure the pH of the reaction mixture is sustained above 9.5 since reactions performed at neutral and acidic pH values show a lower TNP-complex yield.<sup>43,44</sup> These results confirmed that the trinitrophenylation of Ado and Ino is possible at a biological relevant concentration and volumes and, after formation, the TNP-complexes are stable for analysis by the CE-LIF method.

#### 2.4.5 CE-LIF Method Validation

The repeatability, sensitivity and linear response of the CE-LIF method were tested (Table 2.1). The repeatability of both the analytical method and the trinitrophenylation reaction was determined by the average relative standard deviation (RSD) of 3 individual trinitrophenylated reactions of an 80  $\mu$ M Ado and Ino solution in aCSF. 5  $\mu$ L volumes of the Ado/Ino solutions were reacted with 2.5  $\mu$ L of 1 M TNBS, 2.5  $\mu$ L of 1 M NaOH, 30  $\mu$ L of 0.1 M carbonate buffer at 50°C. The limit of detection (LOD) and limit of quantification (LOQ) were calculated from the same samples based on a signal to noise (S/N) ratio of 3 for LOD and of 10 for LOQ. The LOD and LOQ values reported in Table 2.1 are corrected for the 80x dilution factor required for analysis, 8x due to the trinitrophenylation reaction and 10x in H<sub>2</sub>O for CE-LIF analysis.

**Table 2.1. Values for CE-LIF Method<sup>a</sup>**

Analyte	Association Constant <sup>b</sup> , K (M <sup>-1</sup> )	% Conversion after 6 hr at 50°C <sup>c</sup>	%RSD <sup>c</sup> (n=3)	LOD <sup>c</sup> (S/N=3)	LOQ <sup>c</sup> (S/N=10)	y=mx+b <sup>d</sup>	R <sup>2</sup>	Forebrain Tissue Concentration <sup>e</sup> (n=3)
Ado	4600 ± 460	101 ± 6	9.0	1.6 $\mu$ M	5.3 $\mu$ M	y=2.012x-0.8304	0.9980	14.2 ± 1.7 nmol/mg
Ino	1000 ± 190	67 ± 2	5.4	4 $\mu$ M	13.3 $\mu$ M	y=2.225x -0.9561	0.9923	6.4 ± 0.8 nmol/mg

<sup>a</sup>Table represents analytical validity of the CE-LIF method for Ado and Ino detection. <sup>b</sup>Association constants were calculated by 2-parameter nonlinear curve fitting for a 10  $\mu$ M trinitrophenylated Ado (TNP-Ado) and Ino (TNP-Ino) standard over a range of  $\gamma$ -Cyclodextrin ( $\gamma$ -CD) concentrations (0-10mM). <sup>c</sup>% conversion, % RSDs, % conversion, LOD and LOQ were calculated by comparing the analyte peak area to IS peak area of 3 individual trinitrophenylated standards with a concentration of 80  $\mu$ M and in 5  $\mu$ L volumes after 6 hours of reaction. <sup>d</sup>The method linearity was tested over a pre-reaction range of 8-800  $\mu$ M. <sup>e</sup>Rat forebrain tissue concentrations were determined in triplicate from 5  $\mu$ L of homogenated tissue supernatant and after 6 hours of the trinitrophenylation reaction.

#### 2.4.6 Analysis of Adenosine and Inosine in Rat Brain Tissue

To demonstrate the application of the method, whole tissue homogenates from rat forebrain were analyzed. Forebrain tissue samples were removed from frozen whole rat brain samples, homogenized and extracted according to previous literature.<sup>30</sup> 5  $\mu$ L samples of extracted tissue supernatant were then reacted in triplicate using the optimized reagent ratio of 1  $\mu$ L sample volume to 0.5  $\mu$ L of TNBS (~1M in H<sub>2</sub>O), 0.5  $\mu$ L of 1M NaOH and 6  $\mu$ L of 0.1M carbonate buffer at pH 10. Samples were kept at 50°C for 6 hr and then diluted 10x in H<sub>2</sub>O prior to analysis.

Figure 2.8 shows the electropherograms of the trinitrophenylated forebrain tissue sample and a 5  $\mu$ L standard of 8  $\mu$ M Ado and Ino reacted under the same conditions after 6 hr. Ado and Ino concentrations in the forebrain are reported in Table 2.1 and are within the range of previous reports of Ado analyzed in brain tissue by enzymatic<sup>49</sup> and HPLC<sup>24</sup> methods. It should be noted that Ado concentrations cannot be directly compared to previous studies because there are apparent differences in Ado concentrations due to variations in animal sacrifice methods, brain regions analyzed, and tissue homogenization procedures. Nonetheless, the results shown in Figure 2.8 validate the capability of the method to detect and quantify Ado and Ino in biological samples with a high separation efficiency. The success of the trinitrophenylation reaction in 5  $\mu$ L of biological sample establishes a reaction procedure that could be used during *in vivo* studies like microdialysis, which generate small volumes and require good temporal and spatial resolution. Overall, the CE-LIF method provides a sensitive and novel technique for the analysis of Ado and Ino in brain tissue.



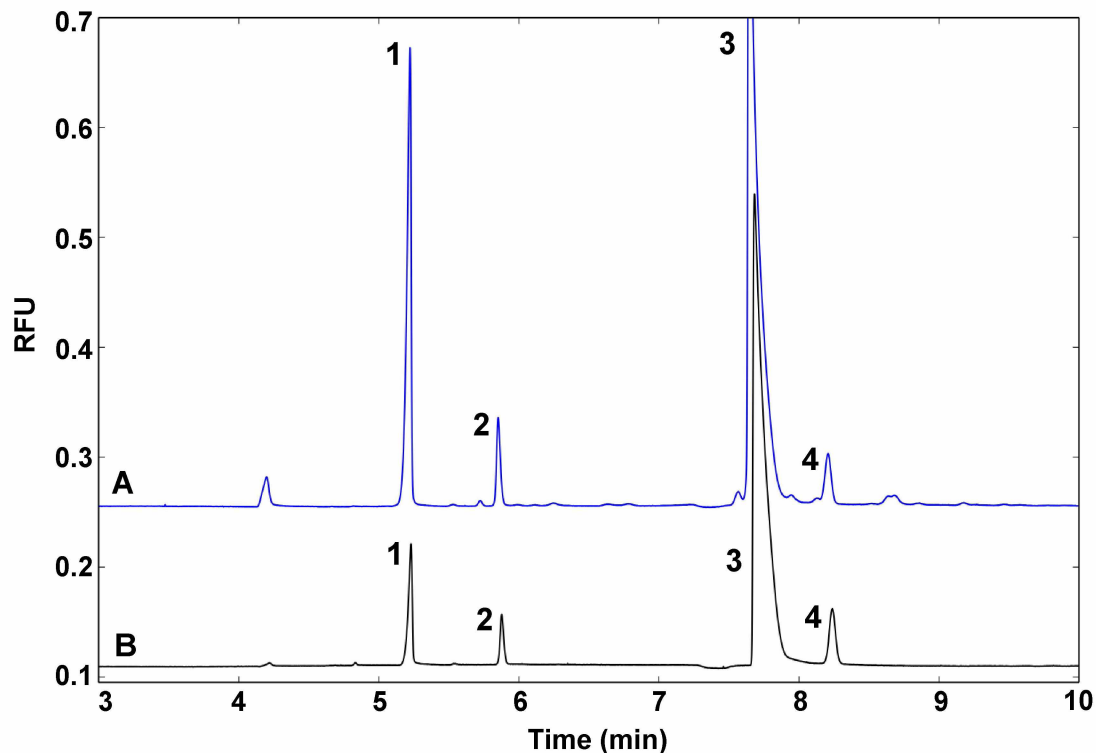


**Figure 2.8. Electropherograms of a 5  $\mu$ L sample of rat forebrain homogenate (A) and an 80  $\mu$ M Ado and Ino standard (B) after 6 hours of reaction time.** Peak identification: 1 TNP-Ado, 2 TNP-Ino, 3 TNBS, 4 IS. See Figure 2 for CE-LIF parameters not stated; BGE 2 mM  $\gamma$ -CD in 20 mM sodium borate at pH 9.4.

#### 2.4.7 Large-Volume Sample Stacking of TNP-Ado and TNP-Ino

Trinitrophenylation of the Ado and Ino required an 8x dilution. The derivatized sample is then further diluted with water prior to CE analysis to enhance peak shape, resulting in an overall dilution of 80x. The LODs and LOQs reported in Table 2.1 take into account this dilution, and are thus in the micromolar range. In an effort to lower the detection limits, LVSS was employed for both TNP-Ado and TNP-Ino.

In Figure 2.9, a 20 nM standard of TNP-Ado and TNP-Ino in water was stacked by 50 mbar hydrodynamic injections ranging from 5 to 240 s. Reverse polarity (negative voltage) was applied for each sample run except for the 5 s run until the electric current reached between 85 to 95% of the normal polarity value when the capillary was filled with BGE. We observed a  $\sim$ 10-

fold enhancement in the LODs for 60 to 240-s injections of TNP-Ado and TNP-Ino compared to the 5-s non-LVSS injection (Table 2.2). With LVSS, the estimated LOD without accounting for the 80x dilution factor is ~4 nM for TNP-Ado and ~2.5 nM for TNP-Ino. Figure 2.10 shows an electropherogram of 180-s injection for a 4 nM standard of TNP-Ino and TNP-Ino in water. The ability to successfully detect TNP-Ado and TNP-Ino at the LOD concentration of 4 nM (320 nM accounting for the 80x dilution factor) concentration highlights the promise in our method to detect nanomolar or lower sample concentrations.

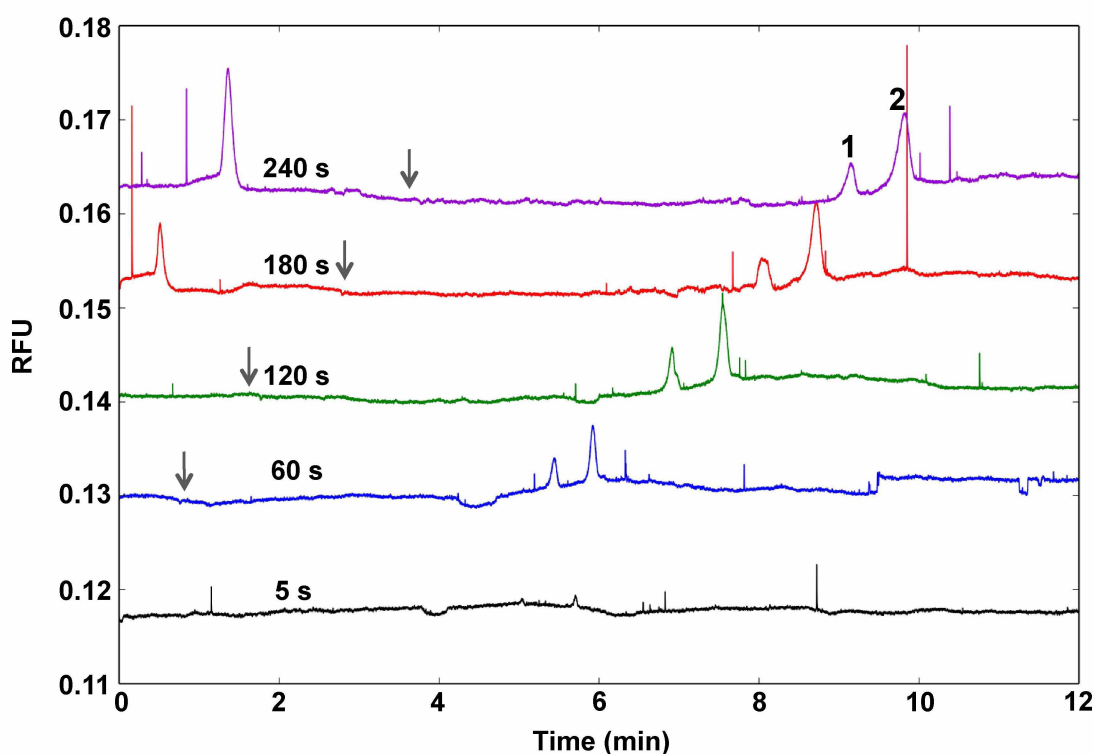


**Figure 2.9. Large-volume sample stacking (LVSS) of TNP-Ado (20 nM) and TNP-Ino (20 nM) standards in water.** Arrows indicate time of polarity switch. Peak identification: 1 TNP-Ado, 2 TNP-Ino. See Figure 2 for CE-LIF parameters not stated; injection pressure 50 mbar; injection time 5-240 s; BGE 2 mM  $\gamma$ -CD in 20 mM sodium borate at pH 9.4.

**Table 2.2. LVSS Values for a 20 nM standard of TNP-Ado and TNP-Ino in H<sub>2</sub>O.**

Injection time (s) <sup>a</sup>	% Capillary Filled	Polarity Switch (min)	LOD (S/N=3) <sup>b</sup>	
			Ado	Ino
5	2	-	3.33 μM	1.53 μM
60	28	0.7	310 nM	159 nM
120	56	1.7	431 nM	240 nM
180	83	2.7	472 nM	234 nM
240	111	3.7	369 nM	195 nM

<sup>a</sup>Corresponding electropherograms shown in Figure 9. Non-LVSS sample is represented by 5 s injection. <sup>b</sup>LOD values are corrected for the 80x dilution factor required by CE-LIF method.

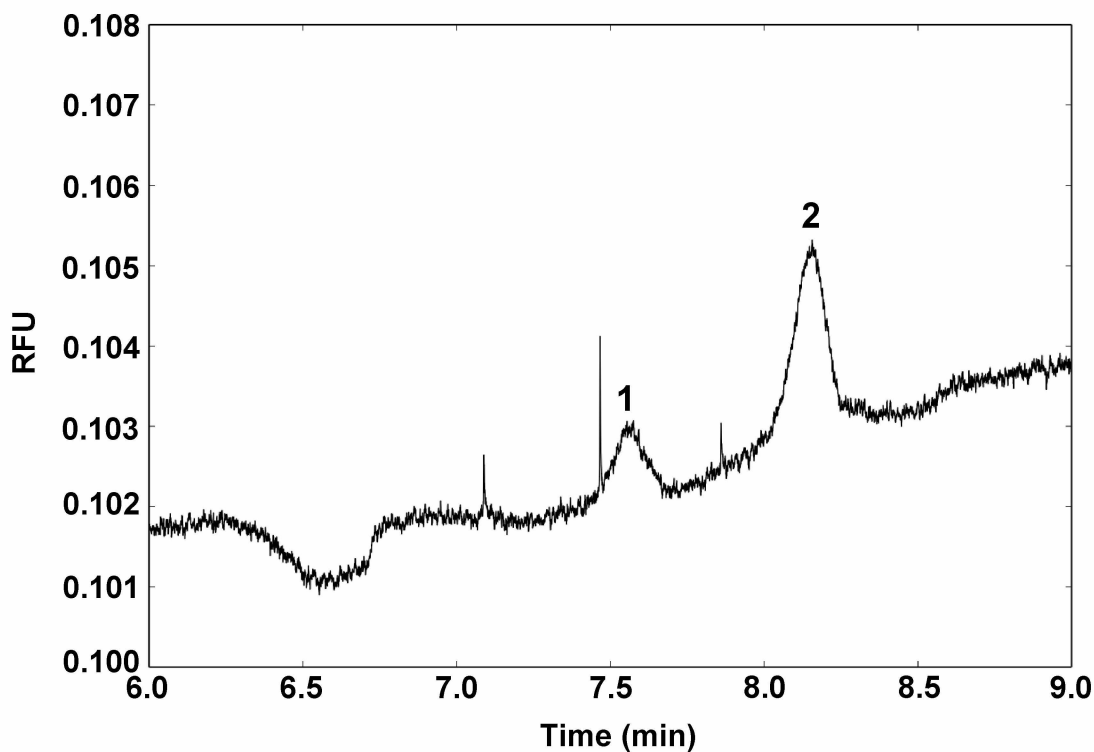


**Figure 2.10. LVSS electropherogram of a 4 nM standard of TNP-Ino and TNP-Ado in water.** Peak identification: 1 TNP-Ado, 2 TNP-Ino. See Figure 2 for CE-LIF parameters not stated; injection pressure 50 mbar; injection time 180 s; 2 mM  $\gamma$ -CD in 20 mM sodium borate BGE at pH 9.4.

## **2.5 Conclusions**

The ability of the CE-LIF method to utilize the fluorescence enhancement properties of  $\gamma$ -CD to measure TNP-Ado and TNP-Ino with submicromolar sensitivity and in small sample volumes has been demonstrated. The method allows for a robust detection system that uses a less invasive fluorescence labeling procedure than previously reported and one that has the ability to be used for the analysis of other biologically significant nucleosides. Although future studies are needed to optimize the use of sample-stacking techniques to improve analyte sensitivity when needed, the high separation resolution and use of commercially available reagents and instrumentation makes this method valuable and applicable to other research groups studying the role of Ado in biological disease, disorders and therapeutic development.

## **2.6 Acknowledgments**

We thank Dr. Kelly Drew and lab members for tissue samples and discussions, Dr. Carl Murphy for NMR discussions, Dr. Canrong Qiu for help with graphics and Dr. Robert Kennedy and Dr. Mohamed Dawod for sample stacking advice. Research reported in this publication was supported in part by the Alaska Space Grant Program, National Institute of Neurological Disorders and Stroke of the National Institutes of Health under grant number R15NS074422, and an Institutional Development Award (IDeA) from the National Institute of General Medical Sciences of the National Institutes of Health under grant number P20GM103395. The content is solely the responsibility of the authors and does not necessarily reflect the official views of the NIH.



## 2.7 References

- (1) Fillenz, M. *Neuroscience & Biobehavioral Reviews* **2005**, *29*, 949-962.
- (2) Song, P.; Mabrouk, O. S.; Hershey, N. D.; Kennedy, R. T. *Analytical chemistry* **2011**, *84*, 412-419.
- (3) Parrot, S.; Sauvinet, V.; Riban, V.; Depaulis, A.; Renaud, B.; Denoroy, L. *Journal of neuroscience methods* **2004**, *140*, 29-38.
- (4) Chen, C.-f.; Drew, K. L. *Journal of Chromatography A* **2008**, *1209*, 29-36.
- (5) Slaney, T. R.; Nie, J.; Hershey, N. D.; Thwar, P. K.; Linderman, J.; Burns, M. A.; Kennedy, R. T. *Analytical chemistry* **2011**, *83*, 5207-5213.
- (6) Hogerton, A. L.; Bowser, M. T. *Analytical chemistry* **2013**, *85*, 9070-9077.
- (7) Xia, J.; Xiong, J.; Wang, H.; Duan, S.; Ye, J.; Hu, Z. *Neuroscience* **2012**, *201*, 46-56.
- (8) Borycz, J.; Pereira, M. F.; Melani, A.; Rodrigues, R. J.; Köfalvi, A.; Panlilio, L.; Pedata, F.; Goldberg, S. R.; Cunha, R. A.; Ferré, S. *Journal of neurochemistry* **2007**, *101*, 355-363.
- (9) Zhang, P.; Bannon, N. M.; Ilin, V.; Volgushev, M.; Chistiakova, M. *The Journal of physiology* **2015**.
- (10) Williams-Karnesky, R. L.; Stenzel-Poore, M. P. *Current neuropharmacology* **2009**, *7*, 217.
- (11) Horiguchi, T.; Shimizu, K.; Ogino, M.; Yamaguchi, N.; Suga, S.; Inamasu, J.; Kawase, T. *Brain research* **2002**, *952*, 222-231.
- (12) Cui, M.; Bai, X.; Li, T.; Chen, F.; Dong, Q.; Zhao, Y.; Liu, X. *PloS one* **2013**, *8*, e57065.
- (13) Frenguelli, B.; Llaudet, E.; Dale, N. *Journal of neurochemistry* **2003**, *86*, 1506-1515.
- (14) Fedele, D. E.; Li, T.; Lan, J. Q.; Fredholm, B. B.; Boison, D. *Experimental neurology* **2006**, *200*, 184-190.
- (15) Gouder, N.; Fritschy, J. M.; Boison, D. *Epilepsia* **2003**, *44*, 877-885.
- (16) Porkka-Heiskanen, T.; Kalinchuk, A. V. *Sleep medicine reviews* **2011**, *15*, 123-135.
- (17) Koupenova, M.; Ravid, K. *Journal of cellular physiology* **2013**.
- (18) Jinka, T. R.; Carlson, Z. A.; Moore, J. T.; Drew, K. L. *Psychopharmacology* **2010**, *209*, 217-224.
- (19) Ticho, S. R.; Radulovacki, M. *Pharmacology Biochemistry and Behavior* **1991**, *40*, 33-40.
- (20) Chen, L.-S.; Fujitaki, J.; Dixon, R. *Journal of Liquid Chromatography & Related Technologies* **1993**, *16*, 2791-2796.

- (21) Porkka-Heiskanen, T.; Strecker, R.; McCarley, R. *Neuroscience* **2000**, *99*, 507-517.
- (22) Fang, H.; Pajski, M. L.; Ross, A. E.; Venton, B. J. *Analytical Methods* **2013**, *5*, 2704-2711.
- (23) Pani, A. K.; Jiao, Y.; Sample, K. J.; Smeyne, R. J. *PloS one* **2014**, *9*, e92422.
- (24) Wojcik, W.; Neff, N. *Journal of neurochemistry* **1982**, *39*, 280-282.
- (25) Coolen, E. J.; Arts, I. C.; Swennen, E. L.; Bast, A.; Stuart, M. A. C.; Dagnelie, P. C. *Journal of Chromatography B* **2008**, *864*, 43-51.
- (26) Haink, G.; Deussen, A. *Journal of Chromatography B* **2003**, *784*, 189-193.
- (27) Van Dycke, A.; Verstraete, A.; Pil, K.; Raedt, R.; Vonck, K.; Boison, D.; Boon, P. *Journal of chromatography. B, Analytical technologies in the biomedical and life sciences* **2010**, *878*, 1493-1498.
- (28) Dale, N.; Gourine, A. V.; Llaudet, E.; Bulmer, D.; Thomas, T.; Spyer, K. M. *The Journal of physiology* **2002**, *544*, 149-160.
- (29) Ross, A. E.; Venton, B. J. *Analytical chemistry* **2014**.
- (30) Özer, N.; Aksoy, Y.; Ögüs, I. H. *Journal of biochemical and biophysical methods* **2000**, *45*, 141-146.
- (31) Tseng, H. C.; Dadoo, R.; Zare, R. N. *Analytical biochemistry* **1994**, *222*, 55-58.
- (32) Phan, N. T.; Hanrieder, J. r.; Berglund, E. C.; Ewing, A. G. *Analytical chemistry* **2013**, *85*, 8448-8454.
- (33) Lian, D.-S.; Zhao, S.-J.; Li, J.; Li, B.-L. *Analytical and bioanalytical chemistry* **2014**, 1-22.
- (34) Lee, S. Y.; Müller, C. E. *Electrophoresis* **2014**, *35*, 855-863.
- (35) Kirschner, D. L.; Jaramillo, M.; Green, T. K. *Analytical chemistry* **2007**, *79*, 736-743.
- (36) Azegami, M.; Iwai, K. *Journal of biochemistry* **1964**, *55*, 346-348.
- (37) Azegami, M.; Iwai, K. *Journal of biochemistry* **1975**, *78*, 409-420.
- (38) Hiratsuka, T.; Sakata, I.; Uchida, K. *Journal of biochemistry* **1973**, *74*, 649-659.
- (39) Green, T. K.; Denoroy, L.; Parrot, S. *The Journal of Organic Chemistry* **2010**, *75*, 4048-4055.
- (40) Hoshino, M.; Imamura, M.; Ikehara, K.; Hama, Y. *The Journal of Physical Chemistry* **1981**, *85*, 1820-1823.
- (41) States, D.; Haberkorn, R.; Ruben, D. *Journal of Magnetic Resonance (1969)* **1982**, *48*, 286-292.

- (42) Rundlett, K. L.; Armstrong, D. W. *Journal of Chromatography A* **1996**, *721*, 173-186.
- (43) Ye, J. Y.; Yamauchi, M.; Yogi, O.; Ishikawa, M. *The Journal of Physical Chemistry B* **1999**, *103*, 2812-2817.
- (44) Ah-kow, G.; Terrier, F.; Pouet, M.-J.; Simonnin, M.-P. *The Journal of Organic Chemistry* **1980**, *45*, 4399-4404.
- (45) Rundlett, K. L.; Armstrong, D. W. *Electrophoresis* **2001**, *22*, 1419-1427.
- (46) Weinberger, R. *Practical capillary electrophoresis*, 2nd ed.; Academic Press: San Diego, California, 2000.
- (47) Psoda, A.; Shugar, D. *Biochimica et Biophysica Acta (BBA)-Nucleic Acids and Protein Synthesis* **1971**, *247*, 507-513.
- (48) Schneider, H.-J.; Hacket, F.; Rüdiger, V.; Ikeda, H. *Chemical reviews* **1998**, *98*, 1755-1786.
- (49) Winn, H.; Rubio, R.; Berne, R. *American Journal of Physiology-Heart and Circulatory Physiology* **1981**, *241*, H235-H242.





## Chapter 3

### Conclusion

#### 3.1 Overview

The primary focus of this thesis was to develop a novel analytical methodology using 2,4,6-trinitrobenzenesulfonic acid (TNBS) derivatization and capillary electrophoresis-laser induced fluorescence detection (CE-LIF) to detect and quantify adenosine (Ado) in biological systems. Our work includes the development of a CE-LIF method, optimization of the trinitrophenylation reaction used to create the detectable form of Ado (TNP-Ado), fluorescence enhancement of TNP-Ado with  $\gamma$ -cyclodextrin, and biological validation of the CE-LIF method in rat brain tissue. We also were able to successfully detect and quantify the molecule inosine, a metabolite of Ado, in rat brain tissue using the CE-LIF method. The limits of detection were 1.6  $\mu\text{M}$  for Ado and 4  $\mu\text{M}$  for Ino. Large-volume sample stacking (LVSS) of Ado and Ino was employed to further enhance the sensitivity of the CE-LIF method, with detection limits of 310 nM and 159 nM for Ado and Ino, respectively.

#### 3.2 Future Directions

The work described in this thesis provides a novel methodology for the analysis of both Ado and Ino in biological tissue. The advantages of using a CE-LIF detection method would potentially allow researchers to quantify these molecules in small volume and low concentration generating experiments like *in vivo* microdialysis. Future studies should focus on optimizing CE-LIF sample stacking techniques like LVSS and field-amplified sample stacking (FASI) in order to enhance the sensitivity and robustness of the CE-LIF method. In addition, future research should include the expansion of the CE-LIF method to selectively detect and quantify adenine ribonucleotides like ATP and AMP. Results from this research would potentially provided

biomedical researchers with the appropriate analytical tool to further understand the role of Ado and adenine ribonucleotides in normal physiology, pathological conditions and therapeutic intervention.

## Appendix A

### Supporting Information for Chapter 2

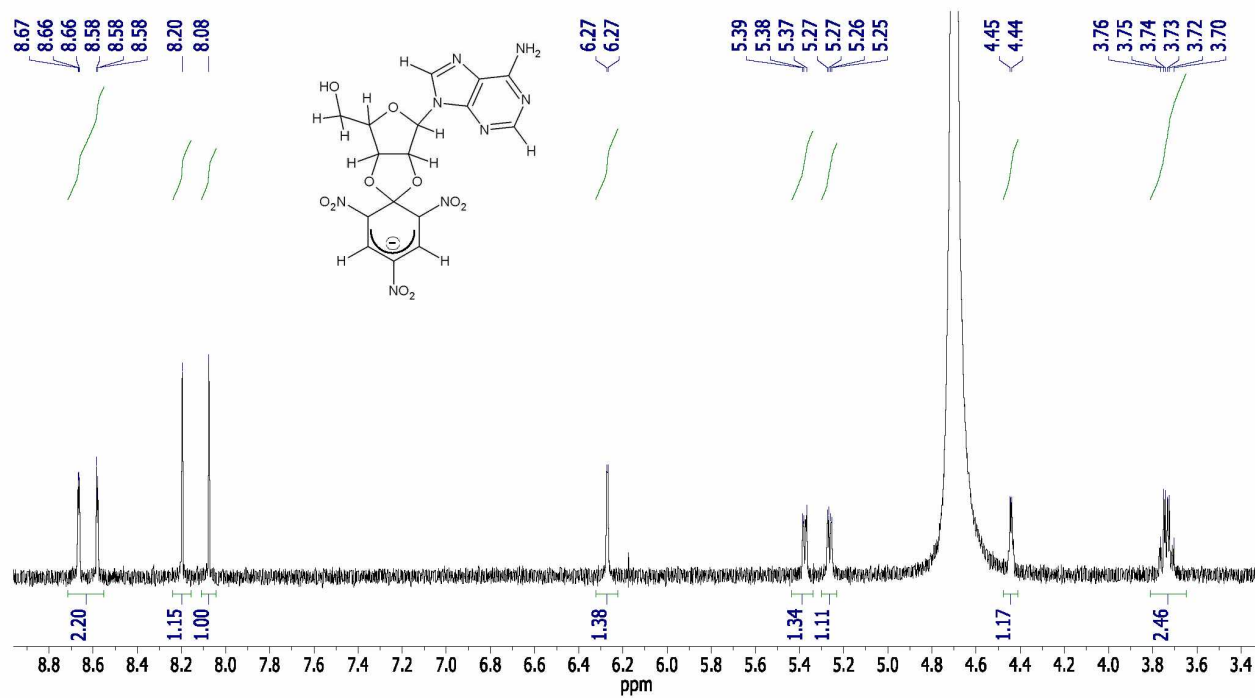


Figure A2.1.  $^1\text{H-NMR}$  of synthesized TNP-Adenosine standard in  $\text{D}_2\text{O}$ . (Varian 300 MHz).

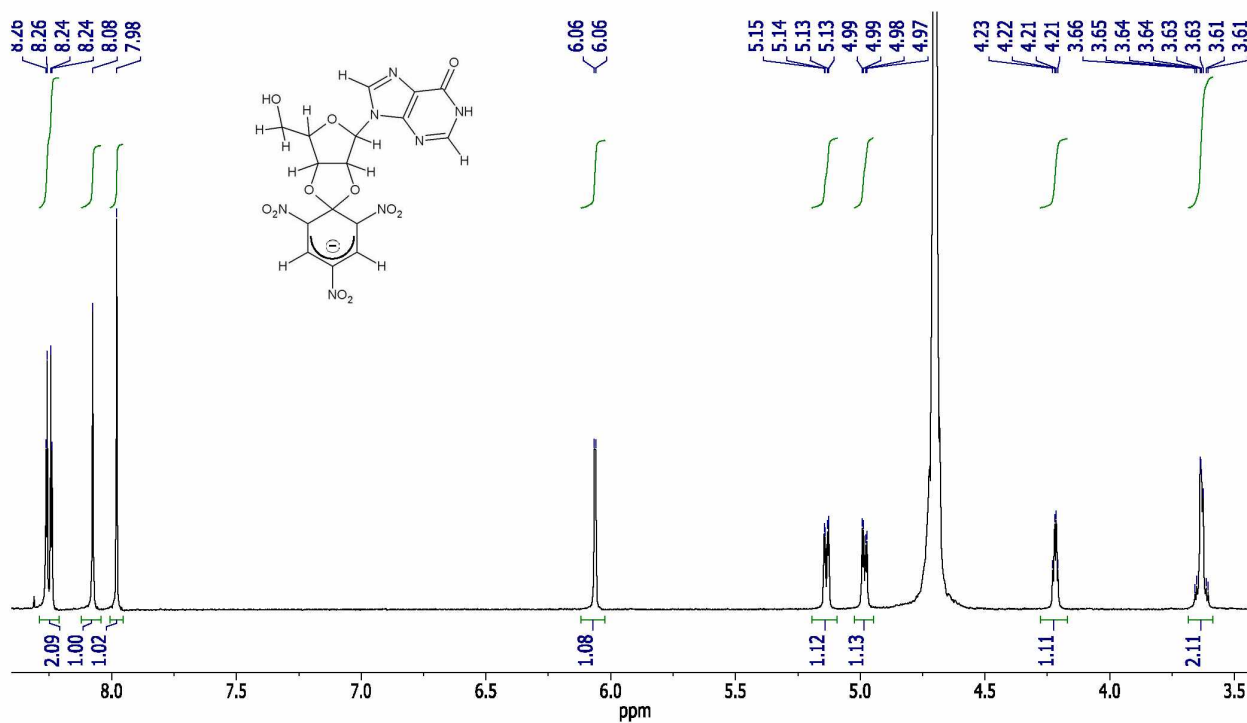


Figure A2.2. <sup>1</sup>H-NMR of synthesized TNP-Inosine standard in D<sub>2</sub>O. (Bruker 600 MHz).

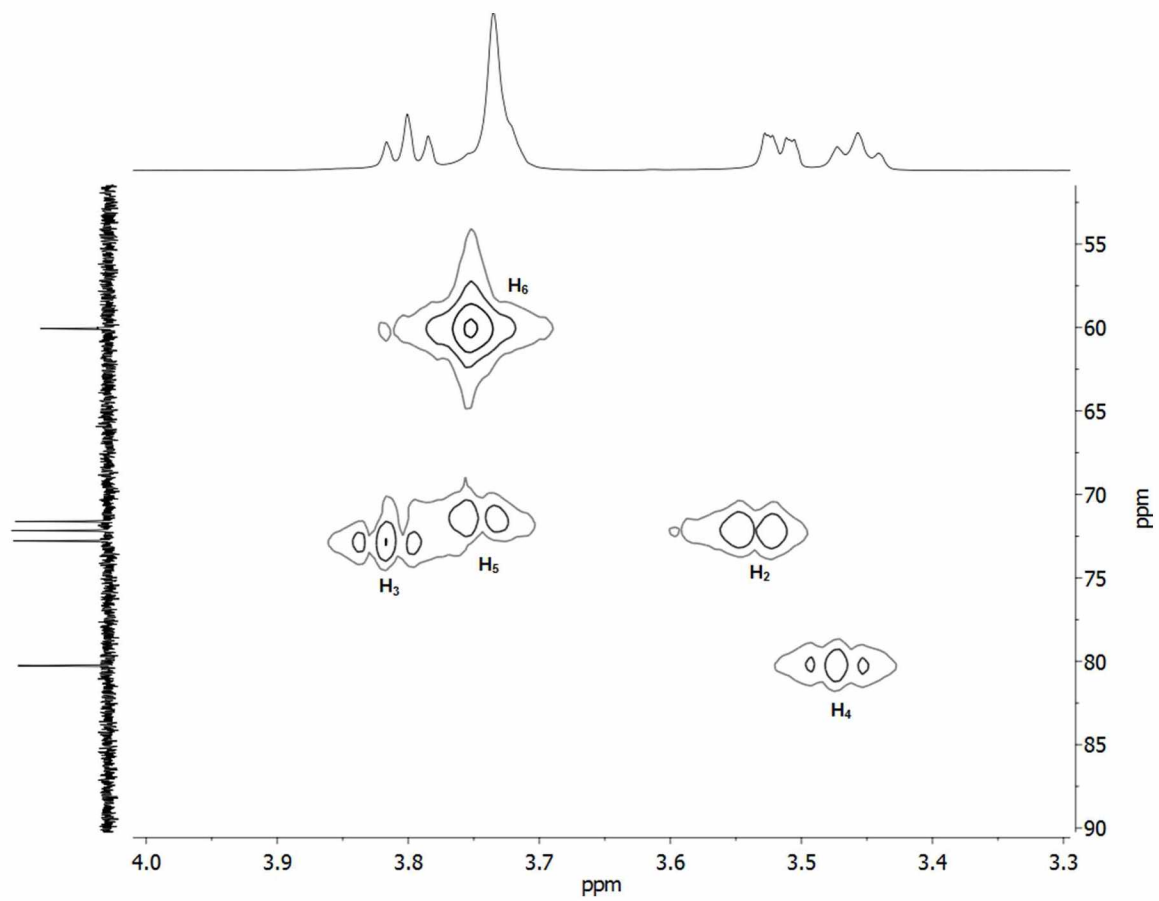


Figure A2.3. HMPC of  $\sim 5$  mM  $\gamma$ -CD in  $D_2O$ . (Bruker 600 MHz).

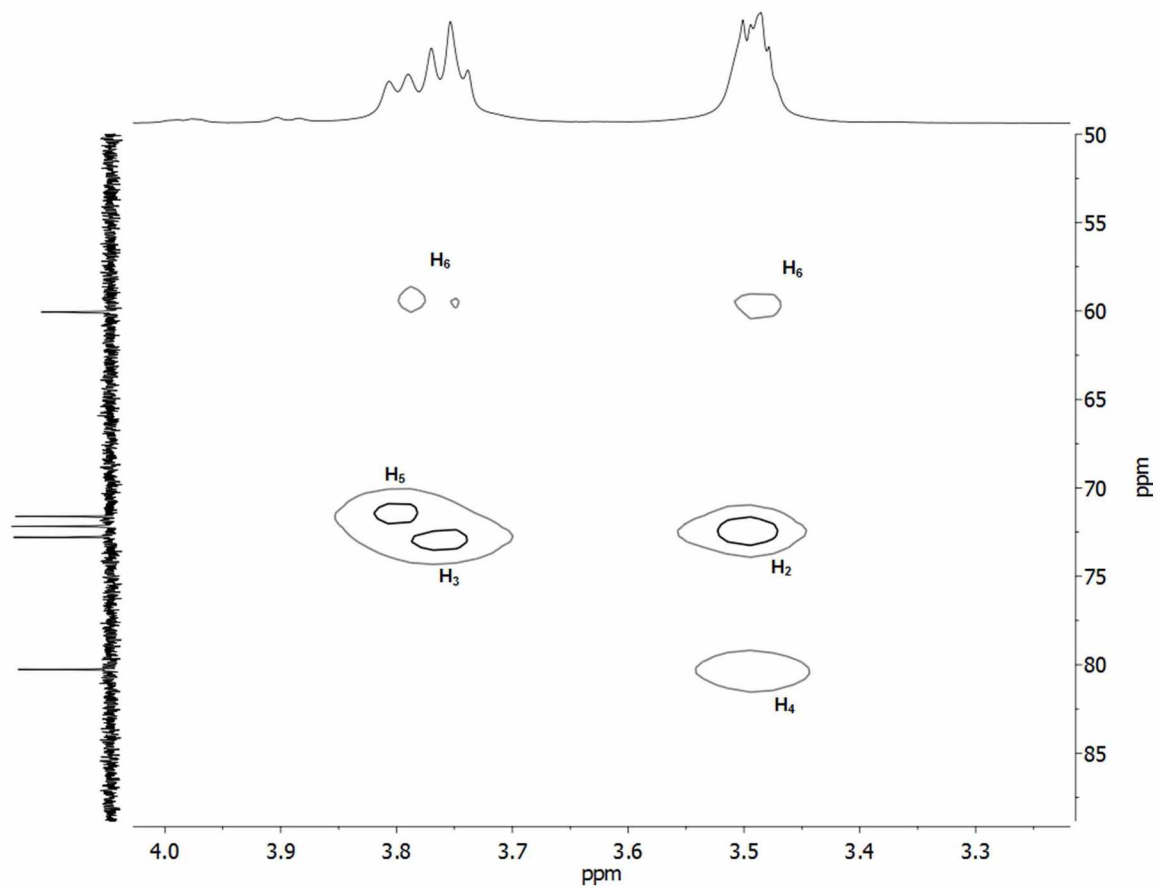


Figure A2.4. HMQC of 1:1 mixture of TNP-Ado:  $\gamma$ -CD (~5mM each) in D<sub>2</sub>O. (Bruker 600 MHz).

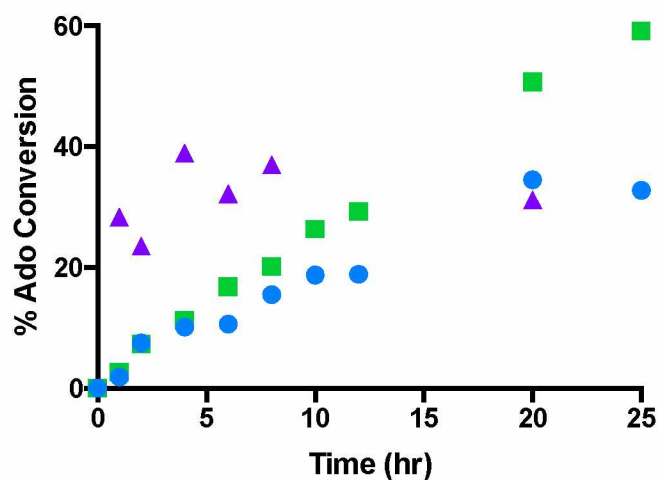


Figure A2.5. Effect of 0.1, 0.15 and 0.5 M sodium carbonate buffer at pH 10 on the trinitrophenylation of Ado (100  $\mu$ M) at 37°C. 0.15 M sodium carbonate (blue circles), 0.15 M sodium carbonate (green squares) and 0.5 M Sodium Carbonate (purple triangles). CE-LIF CE-LIF parameters: Inner capillary diameter 50  $\mu$ m; effective length 28 cm; injection pressure 50 mbar; injection time 1 s; applied voltage 20 kV; laser power 25 mW; 2 mM  $\gamma$ -CD in 20 mM sodium borate BGE at pH 9.4.





## Appendix B

### Trinitrophenylation and Capillary Electrophoresis Analysis of Adenine Ribonucleotides, N<sup>6</sup>-Cyclohexyladenosine, Guanosine, Cytidine, and Uridine

#### B.1 Additional Analysis on Adenosine

##### B.1.1 Introduction

To supplement the research discussed in Chapter 2 of this thesis, additional steady state fluorescence spectroscopy and capillary electrophoresis-laser induced fluorescence (CE-LIF) experiments were carried out for analysis of adenosine (Ado), see Figure B1.1 for structure. All experiments were performed using a trinitrophenylated standard of Ado (TNP-Ado) that was synthesized using the procedure discussed in Chapter 2 and reported in Green et al.<sup>1</sup>.

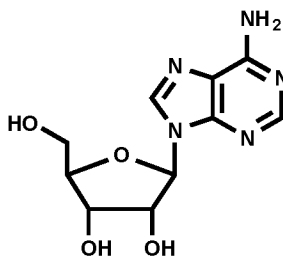


Figure B1.1. Structure of Adenosine (Ado).

##### B.1.2 Methods

For the steady state fluorescence spectroscopy experiments, 10  $\mu$ M samples of TNP-Ado were prepared in various aqueous and non-aqueous solvents: Milli-Q H<sub>2</sub>O, 20 mM sodium borate with 2 mM  $\gamma$ -cyclodextrin at pH 9.4, analytical-grade methanol, analytical-grade acetone, dimethylformamide (DMF) and N, N-dimethylformamide (NMF). Samples were analyzed at

ambient temperature and in replicate. A Perkin Elmer LS 50 B luminescence spectrometer with a 408 nm excitation wavelength was used.

An Agilent Technologies 7100 automated CE system coupled to a Picometrics Zetalif laser-induced fluorescence detector was used for CE-LIF analysis. A 405 nm Oxiuxx Laser Diode with the power adjusted to 25 mW was used for an excitation wavelength and separations were performed on a 75  $\mu\text{m}$  ID, 360  $\mu\text{m}$  OD fused silica capillary. Capillary were cut to a total length of 48 cm and an effective length of 20 cm (28 cm to the detection window). New capillaries were conditioned for a total of 45 min: 15 min 1 M NaOH, 15 min Milli-Q H<sub>2</sub>O and 15 min background electrolyte. (BGE). The BGE used for analysis was typically 20 mM sodium borate with 2 mM  $\gamma$ -cyclodextrin at pH 9.4, but other cyclodextrins and cyclodextrin concentrations were tested. Other cyclodextrins used were (2-hydroxypropyl)- $\gamma$ -cyclodextrin (2-HP- $\gamma$ -CD), 3A-amino-3A-deoxy-(2AS, 3AS)- $\gamma$ -cyclodextrin (Amino- $\gamma$ -CD), randomly methylated- $\gamma$ -cyclodextrin (Methyl- $\gamma$ -CD) and randomly carboxymethylated- $\gamma$ -cyclodextrin (Carboxymethylated- $\gamma$ -CD). BGE was filtered through a 0.2  $\mu\text{m}$  PTFE syringe filter prior to use. All experiments were performed at 25°C with normal polarity at +10 kV (anode at inlet) and hydrodynamic injections were typically 50 mbar for 1s.

For the comparison of Ado concentrations in rat brain tissue using different extraction techniques, various solvents and methods were used<sup>2-4</sup>. Brain tissue was kept frozen at -80°C and forebrain tissue ranging from 50 to 100 mg was removed from whole brain for analysis. For Ado extractions requiring the boiling of tissue samples, 5  $\mu\text{L}$  of either Milli-Q water (95-100°C), 20 mM sodium borate with 2 mM  $\gamma$ -cyclodextrin at pH 9.4 (95-100°C) or 0.1 M sodium carbonate buffer at pH 10 (95-100°C) was added for every 1 mg of tissue and samples were boiled at 95-100°C for 5 min. For extractions using cold techniques, 5  $\mu\text{L}$  of either 5% Perchloric acid (PCA), 50 mM Tris(hydroxymethyl)aminomethane (TRIS) containing 2 mM ethylenediaminetetraacetic acid (EDTA), 20 mM sodium borate with 2 mM  $\gamma$ -cyclodextrin at pH 9.4 or 0.1 M sodium carbonate buffer at pH 10 was added for every 1 mg of tissue. Samples were set on ice and

incubated for 5 min. After boiling or cold preparation, tissue was homogenized using a disposable pellet mixer and centrifuged at 13000 rmps at 4 °C for 5 min. Tissue supernatant was then transferred to a 0.22 µm nylon centrifuge tube filter centrifuged at 1300 rmps at 4 °C for 5 mins, and frozen at -80°C until reacted for analysis. For the trinitrophenylation reaction, 2.5 µL of TNBS (~1M in H<sub>2</sub>O), 2.5 µL of 1M NaOH and 30 uL of 0.1 M carbonate buffer (pH 10) was added to 5 µL of tissue supernatant. Samples were vortexed, placed in a heat block at 50 °C for 6 hr and diluted by 10x prior to CE-LIF analysis in Milli-Q H<sub>2</sub>O containing 0.02 µM of internal standard.

### **B.1.3 Results and Discussion**

It has been well reported that non-aqueous solvent systems can improve fluorescence emission of smaller aromatic molecules in capillary electrophoresis.<sup>5,6</sup> To investigate whether a non-aqueous BGE would be more beneficial for the analysis of TNP-Ado using CE-LIF, the steady state fluorescence emission of TNP-Ado in several common non-aqueous solvents was compared. Figure B1.2 shows this comparison for a 10 µM TNP-Ado standard. Overall, acetone resulted in a 76-fold fluorescence enhancement of TNP-Ado over water alone and a 1.5-fold fluorescence enhancement of TNP-Ado in 20 mM sodium borate with 2 mM γ-cyclodextrin at pH 9.4. DMF also resulted in a 58-fold fluorescence enhancement of TNP-Ado over water alone, but only a 1.1-fold fluorescence enhancement of TNP-Ado in 20 mM sodium borate with 2 mM γ-cyclodextrin at pH 9.4. Although acetone and DMF resulted in an increased fluorescence emission of TNP-Ado, we determined the additional enhancement of only 1.1-1.5-fold was not worth the cost of switching to a non-aqueous CE-LIF system for the analysis of Ado. Other factors also impacted this decision including the price of non-aqueous solvents and the evaporation risk of working with volatile of solvents.

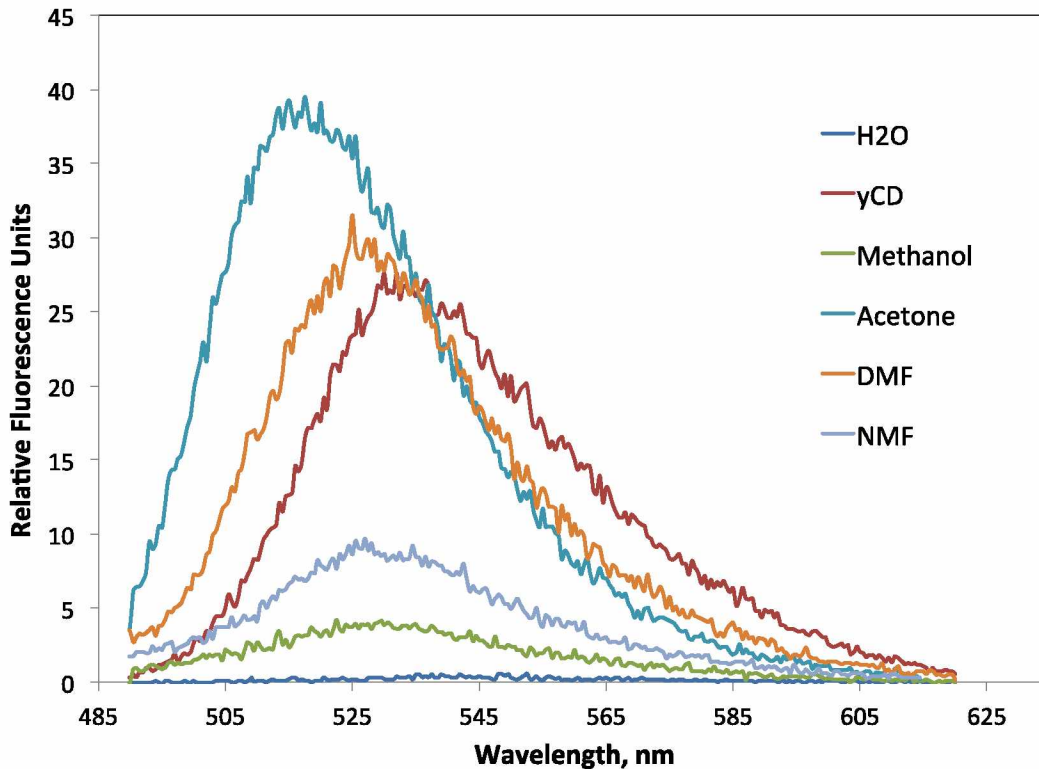


**Figure B1.2. Steady state fluorescence emission of 10  $\mu\text{M}$  TNP-Ado standard in various aqueous and non-aqueous solvents.** Abbreviations: Milli-Q  $\text{H}_2\text{O}$  ( $\text{H}_2\text{O}$ ), 20 mM sodium borate with 2 mM  $\gamma$ -cyclodextrin at pH 9.4 ( $\gamma$ -CD), dimethylformamide (DMF) and N, N-dimethylformamide (NMF).

Another parameter in the CE-LIF method that could be manipulated to increase the fluorescence emission of TNP-Ado is the addition of cyclodextrins to the BGE. Green et al. had shown an  $\sim 110$ -fold enhancement in the steady state fluorescence emission of a 4  $\mu\text{M}$  TNP-Ado sample in 10 mM of  $\gamma$ -CD compared to water alone.<sup>1</sup> Using this knowledge, we compared the relative fluorescence peak height of a 10  $\mu\text{M}$  TNP-Ado standard in  $\text{H}_2\text{O}$  using CE-LIF with several modified  $\gamma$ -CD at various concentrations in 20 mM sodium borate BGE at pH 9.4 (Figure B1.3). At 0.5 mM CD concentration, both the randomly methylated- $\gamma$ -CD and the 2-HP- $\gamma$ -CD increased the fluorescence emission by at least a factor of 3 for TNP-Ado compared to  $\gamma$ -CD in the BGE. As shown in Figure B1.3, it takes 10 times the concentration of  $\gamma$ -CD to achieve this same maximal increase in TNP-Ado fluorescence. This result is promising because it indicates that the maximal enhancement in TNP-Ado fluorescence can be achieved using less

cyclodextrin. However, if the price of cyclodextrin is also considered, ~\$170/gram for randomly methylated-  $\gamma$ -CD vs ~\$20 for 2-HP-  $\gamma$ -CD vs \$10/gram for  $\gamma$ -CD, these findings become negligible as it would not be cost effective to use a higher priced CD in this system.

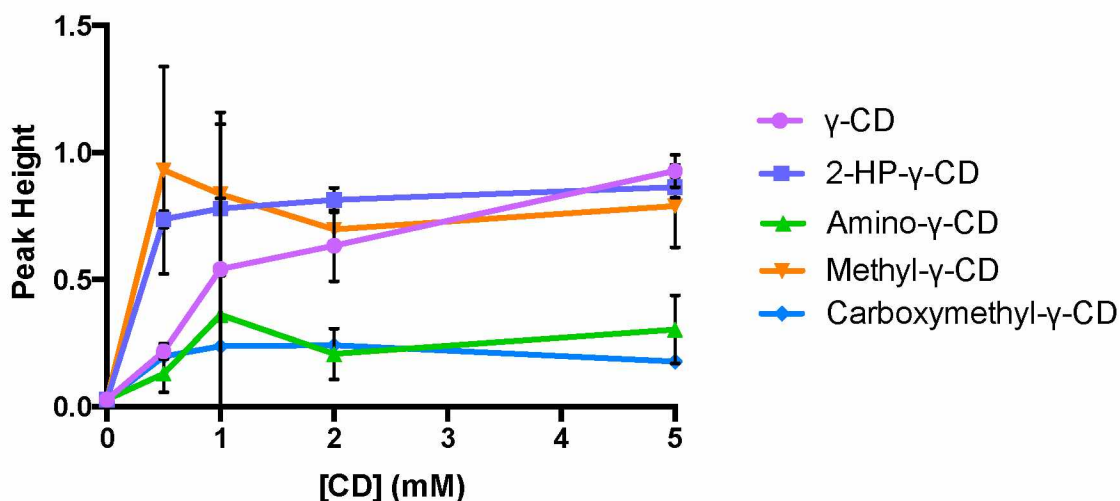


**Figure B1.3. Comparison of relative fluorescence peak height of 10  $\mu$ M TNP-Ado standard in H<sub>2</sub>O using CE-LIF with various types and concentrations of cyclodextrins in 20 mM sodium borate BGE at pH 9.4.** CE-LIF parameters: Inner capillary diameter 75  $\mu$ m; total length 48 cm, effective length 28 cm; injection pressure 50 mbar; injection time 1 s; applied voltage 20 kV; laser power 25 mW. Abbreviations:  $\gamma$ -cyclodextrin ( $\gamma$ -CD), 2-hydroxypropyl- $\gamma$ -cyclodextrin (2-HP- $\gamma$ -CD), 3A-amino-3A-deoxy-(2AS, 3AS)- $\gamma$ -cyclodextrin (Amino- $\gamma$ -CD), randomly methylated- $\gamma$ -cyclodextrin (Methyl- $\gamma$ -CD) and randomly carboxymethylated- $\gamma$ -cyclodextrin (Carboxymethylated- $\gamma$ -CD)

After all the parameters for the CE-LIF method were optimized as discussed in Chapter 2, biological validation was tested using tissue extracts from rat forebrain. Numerous extraction techniques are used in the literature instead of a single standard for the analysis of Ado.<sup>2-4</sup> This could be potentially problematic if reported Ado concentrations are directly compared from various sources using different extraction techniques. Chida et al. investigated this potential problem for ATP and found that different extraction techniques resulted in major discrepancies in final ATP concentrations.<sup>7</sup> To briefly investigate this potential dilemma while also searching

for the most user-friendly extraction technique for Ado, several extraction techniques were performed on tissue samples and then analyzed using CE-LIF

Figure B1.4 shows the comparison of Ado concentrations in rat forebrain tissue using different sample extraction techniques and solvents. No apparent differences were found between boiling tissue samples in either Milli-Q H<sub>2</sub>O or 0.1 M carbonate buffer and cold preparation in 0.1 M carbonate buffer. A 0.1 M carbonate buffer was chosen as a solvent because it is essential in the trinitrophenylation reaction step of the CE-LIF method. It is also apparent that the use of PCA, Tris and EDTA, and 20 mM Borate with 2 mM  $\gamma$ -CD resulted in different Ado concentrations compared to the other methods. It should be noted that because spike recovery experiments were not performed with these samples, we are unable to directly quantify and compare these values.

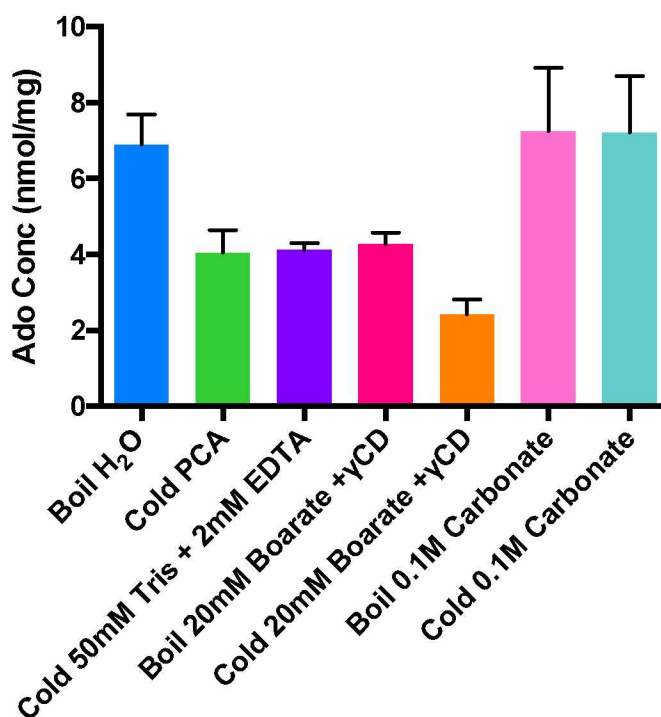


**Figure B1.4. Comparison of Ado concentrations in rat forebrain tissue using different sample extraction techniques.** CE-LIF parameters: Inner capillary diameter 75  $\mu\text{m}$ ; total length 48 cm, effective length 28 cm; injection pressure 50 mbar; injection time 1 s; applied voltage 20 kV; laser power 25 mW. Abbreviations: 5% perchloric acid (PCA), 50 mM tris(hydroxymethyl)aminomethane (TRIS) containing 2 mM ethylenediaminetetraacetic acid (EDTA), 20 mM sodium borate with 2 mM  $\gamma$ -cyclodextrin pH 9.4 (20 mM Borate +  $\gamma$ -CD) at or 0.1 M sodium carbonate buffer at pH 10 (0.1 M Carbonate).

#### B.1.4 Conclusions

The additional results presented for Ado broaden the scope and potential of the CE-LIF method presented in Chapter 2. Future studies should further investigate the use of non-aqueous solvent systems in the analysis of TNP-Ado and related compounds as well as determine if the use of other cyclodextrins in the BGE can enhance the selectivity of the CE-LIF system. Spike-recovery experiments should also be performed when comparing tissue extraction techniques so reported Ado concentrations can be quantifiable and directly compared in order to determine the most reliable extraction method.



## B.2 Adenine Ribonucleotides

### B.2.1 Introduction

As stated in Chapter 1, adenine ribonucleotides including adenosine 5'-monophosphate (AMP), adenosine 5'-diphosphate (ADP) and adenosine 5'-triphosphate are important in cell signaling and metabolism.<sup>8,9</sup> The structures of these molecules are shown in Figure B2.1 and contain diol functional groups, which can potentially undergo trinitrophenylation with 2,4,6-trinitrobenzenesulfonic acid (TNBS) to form a stable trinitrophenylated derivatives (TNP-AMP, TNP-ADP and TNP-ATP). Previous studies have successfully synthesized and characterized the spectroscopic properties of TNP-ATP.<sup>10-12</sup>

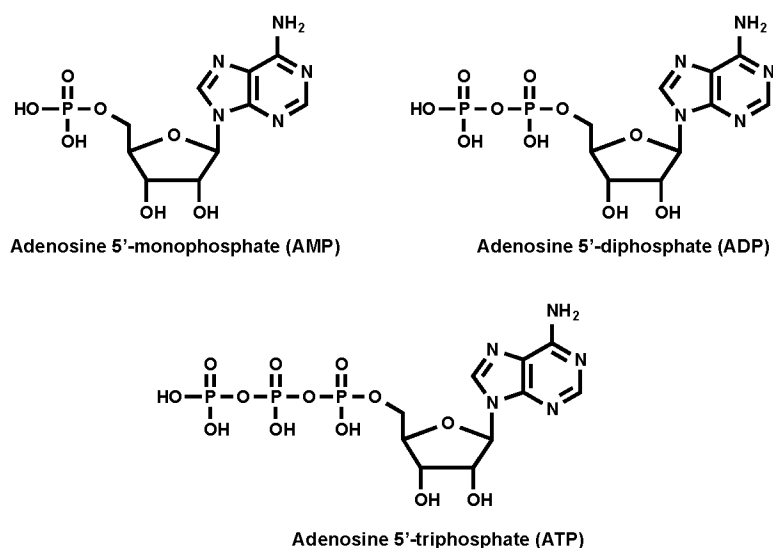


Figure B2.1. Structures of Adenine Ribonucleotides

In order to broaden the impact of the CE-LIF method described in Chapter 2, a secondary aim of this thesis was to expand the CE-LIF method for the analysis of adenine ribonucleotides in biological samples. The synthesis of pure TNP-AMP, TNP-ADP and TNP-ATP was attempted as well as preliminary CE-LIF analysis of TNP-AMP and TNP-ATP standards in H<sub>2</sub>O.

### B.2.2 Methods

A method similar to Green et al.<sup>1</sup> and Hiratsuka et al.<sup>12</sup> was followed for the trinitrophenylation of AMP, ADP and ATP. For the TNP-AMP standard, ~60 mg of AMP was dissolved in 1 mL of Milli-Q H<sub>2</sub>O and 1 mL 1M NaOH followed by the addition of 0.88 mL of TNBS (~1M in H<sub>2</sub>O). For TNP-ADP and TNP-ATP, ~60 mg of either ADP or ATP was dissolved in 2 mL of Milli-Q H<sub>2</sub>O and 0.88 mL of TNBS (~1M in H<sub>2</sub>O) was added. The pH of all reactions was continuously monitored for 3 hours, adding 1 M NaOH until the pH was stabilized at 10. Each reaction was left overnight and purified the next morning on a Sephadex LH-20 column, dimensions 2 cm x ~30 cm. Impurities of each reaction were eluted off the column with water, leaving the purified standard, which appeared as a bright reddish-orange band, retained at the top of the column. The standard was then eluted from the column with methanol, dried by rotary evaporation and ~10 mg of the final product was analyzed for purity by 600 MHz NMR spectroscopy in D<sub>2</sub>O.

For the CE-LIF analysis of TNP-AMP and TNP-ATP, the NMR samples of each standard was diluted 1:1000 in Milli-Q H<sub>2</sub>O. After initial analysis, each sample was spiked with 2  $\mu$ L TNBS (~1M in H<sub>2</sub>O) and run under the same conditions. Separations were performed on a 75  $\mu$ m inner diameter fused silica capillary cut to a total length of 48 cm and an effective length of 28 cm. The background electrolyte solution consisted of 20 mM sodium borate with 2 mM  $\gamma$ -cyclodextrin at pH 9.4 and was filtered through a 0.2  $\mu$ m syringe filter prior to use. Samples were hydrodynamically injected at 50 mbar for 2 seconds and 5 seconds for TNP-AMP and TNP-ATP, respectively, and run for a total 13 minutes at 10 kV.

### B.2.3 Results and Discussion

The trinitrophenylation of AMP yielded a pure standard. Figure B2.2 shows the <sup>1</sup>H NMR of TNP-AMP with correct hydrogen assignments. The large unassigned peaks with singlet multiplicities at ~4.6 ppm and ~8.8 ppm are D<sub>2</sub>O and residual TNBS, respectively. A <sup>31</sup>P NMR

spectrum was also collected to further confirm the purity of TNP-AMP (Figure B2.3). A pure TNP-AMP standard would result in a single phosphate resonance in the  $^{31}\text{P}$  NMR spectrum. This is confirmed in Figure B2.3.

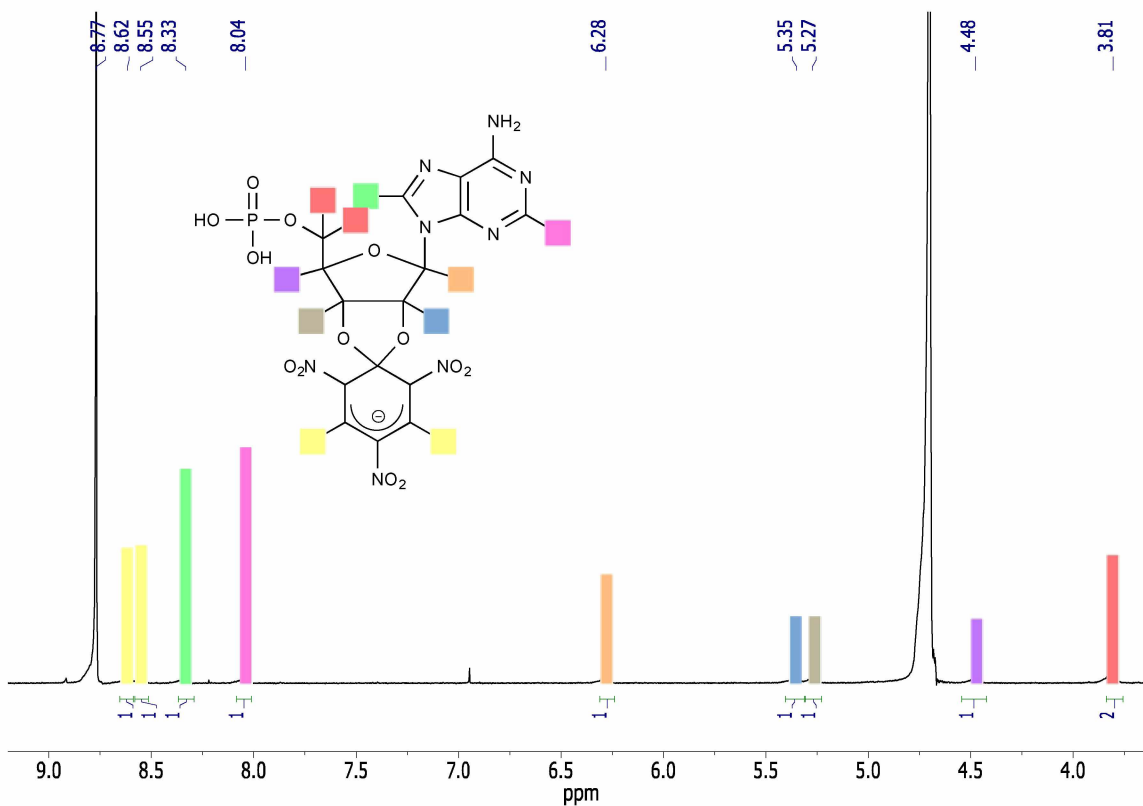
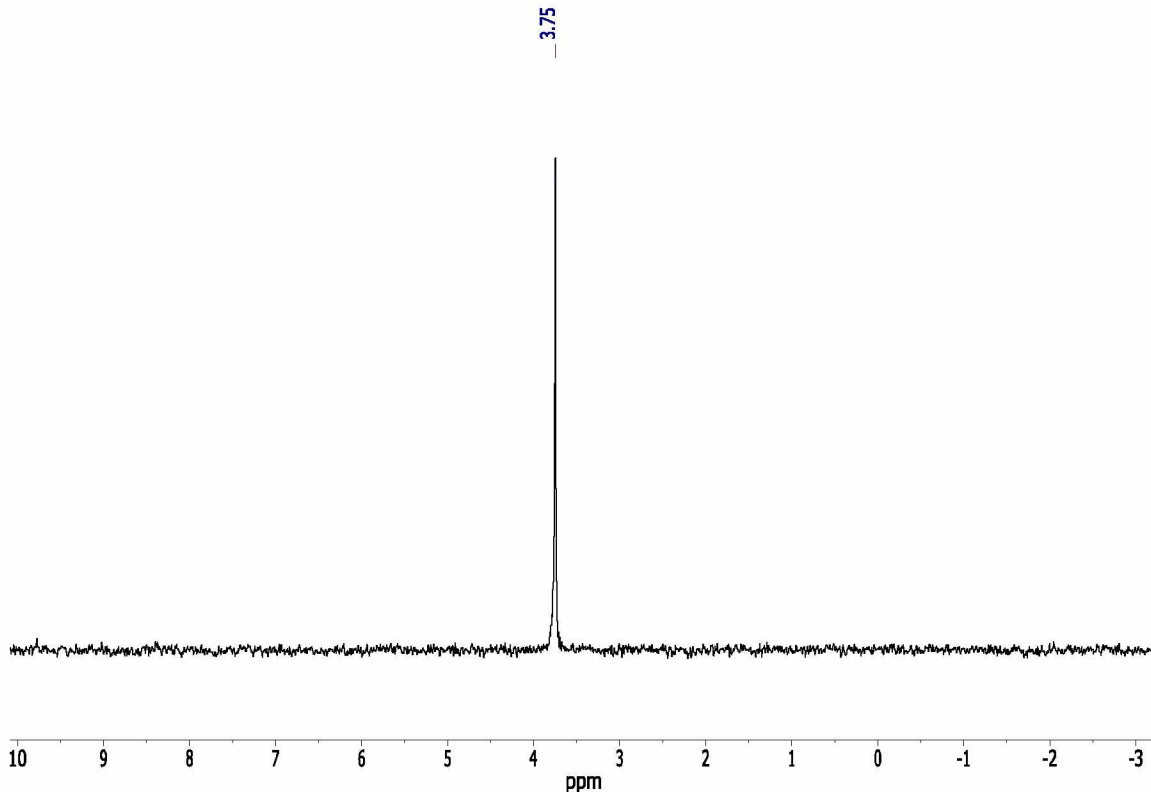
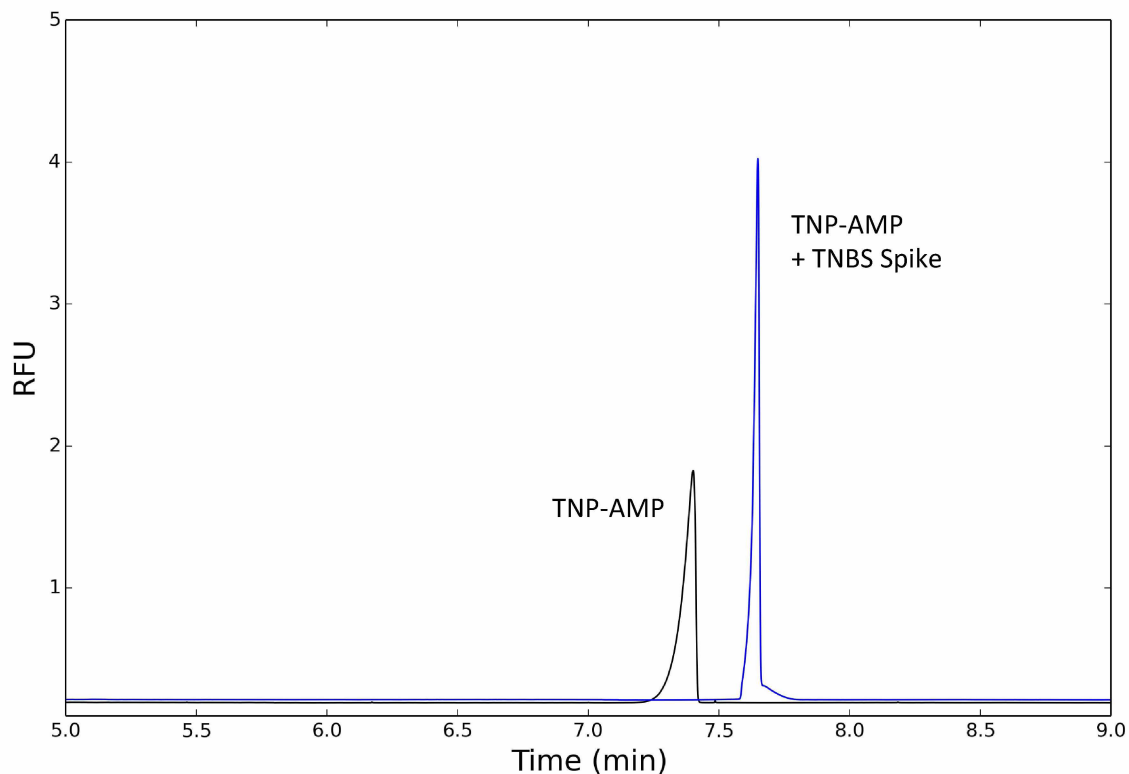


Figure B2.2.  $^1\text{H}$  NMR of TNP-AMP in  $\text{D}_2\text{O}$  (Bruker 600 MHz)



**Figure B2.3.  $^{31}\text{P}$  NMR of TNP-AMP in  $\text{D}_2\text{O}$  (Bruker 600 MHz)**

The next step in expanding the CE-LIF method for the analysis of adenine ribonucleotides was to analyze the TNP-AMP standard using the same conditions as for the analysis of TNP-Ado. This was also done to determine the potential of the method to separate TNP-AMP from TNP-Ado and TNBS. Figure B2.4 shows the electropherogram of a TNP-AMP standard in  $\text{H}_2\text{O}$  as well as the same sample with a TNBS spike. Unfortunately under these conditions, the CE-LIF method could not separate TNP-AMP from TNBS as shown by the doubling of the TNP-AMP signal after the addition of TNBS. However, it can be presumed that under this condition the CE-LIF method would have the potential to separate TNP-AMP from TNP-ADO since TNP-Ado is typically detected at ~ 6 min and TNP-AMP is detected after 7 min.



**Figure B2.4. CE-LIF electropherogram of TNP-AMP and TNP-AMP with TNBS spike.** CE Parameters: Inner capillary diameter 75  $\mu\text{m}$ ; total length 40 cm; effective length 28 cm; injection pressure 50 mbar; injection time 2 s; applied voltage 10 kV; laser power 25 mW; 25°C; BGE 20 mM sodium borate with various  $\gamma$ -CD concentrations at pH 9.4.

The trinitrophenylation of ADP also yielded a pure standard. Figure B2.5 shows the  $^1\text{H}$  NMR of TNP-ADP with correct hydrogen assignments. The large unassigned peak with multiplicity of a singlet at  $\sim 4.6$  ppm is  $\text{D}_2\text{O}$ . A  $^1\text{H}$  COSY NMR is shown in Figure B2.6 and used to confirm hydrogen peak assignment. A  $^{31}\text{P}$  NMR spectrum was also collected to further confirm the purity of TNP-ADP (Figure B2.7). A pure TNP-ADP standard would result in two doublets, corresponding to the two coupled phosphorus nuclei in TNP-ADP. This is confirmed in Figure B2.7.

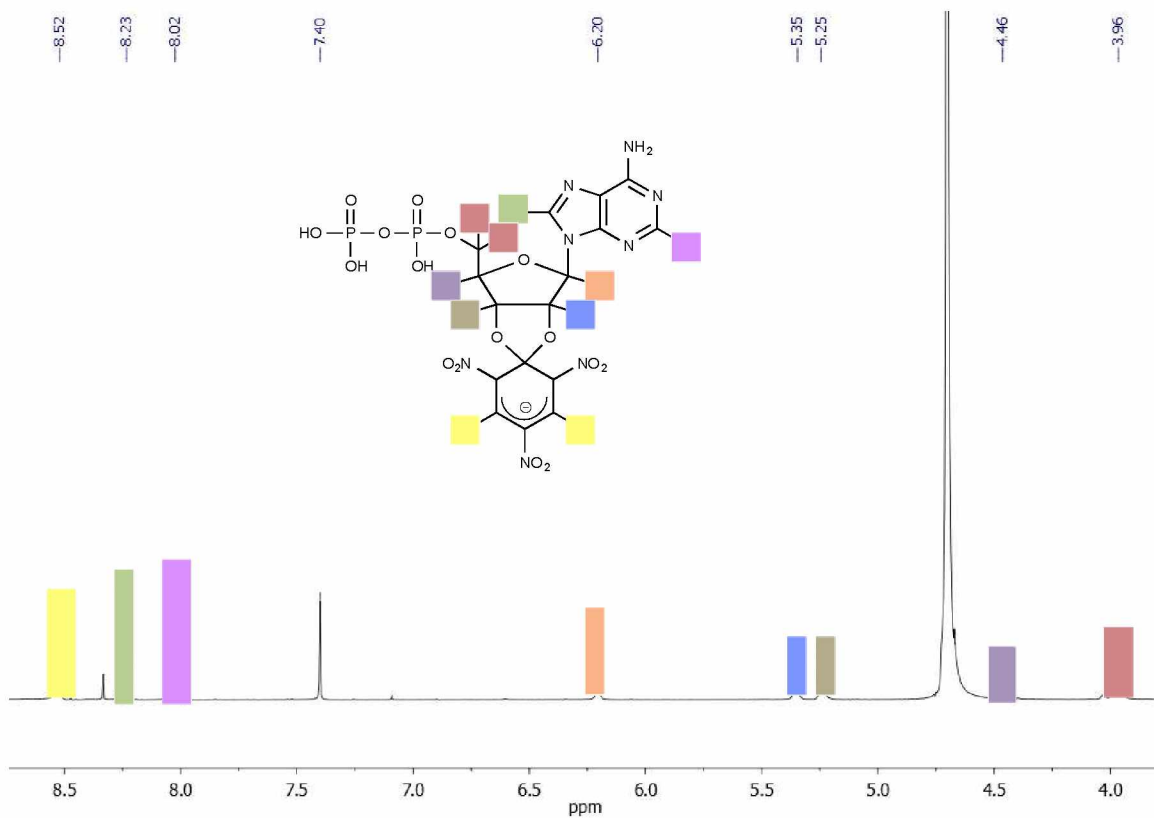


Figure B2.5.  $^1\text{H}$  NMR of TNP-ADP in  $\text{D}_2\text{O}$  (Bruker 600 MHz)

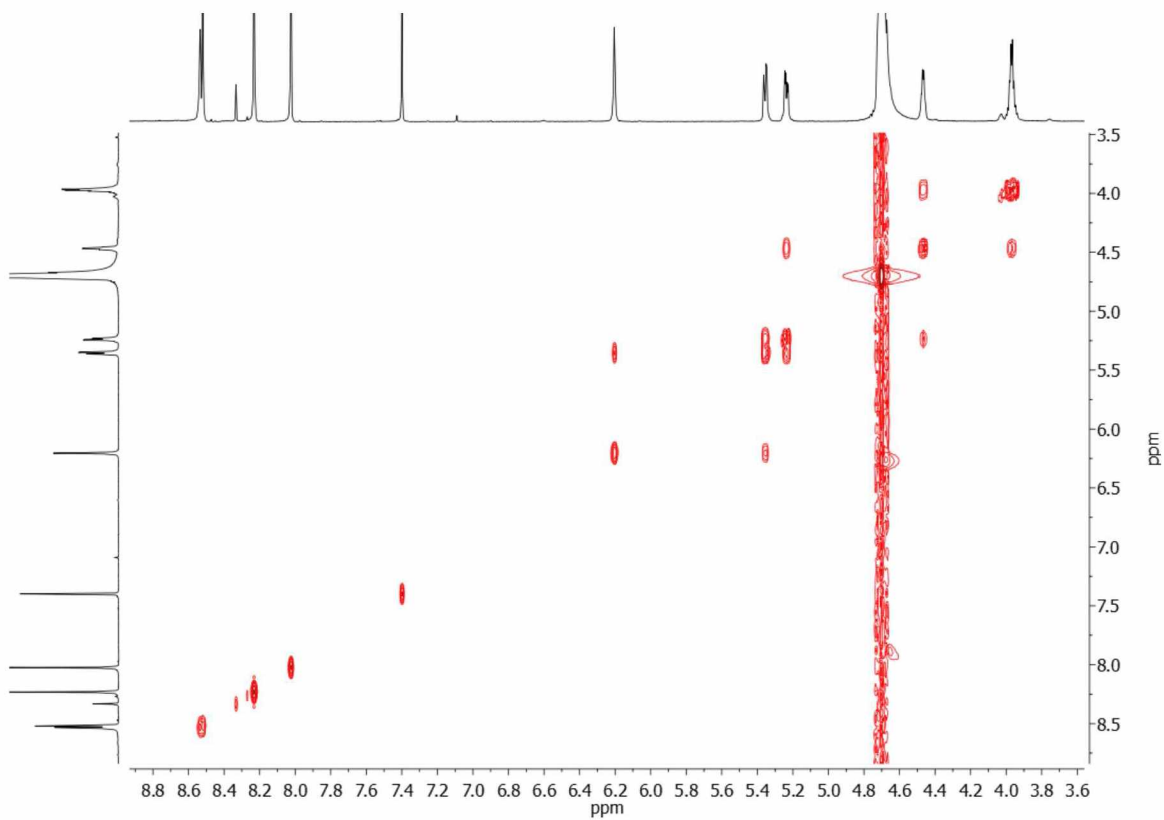
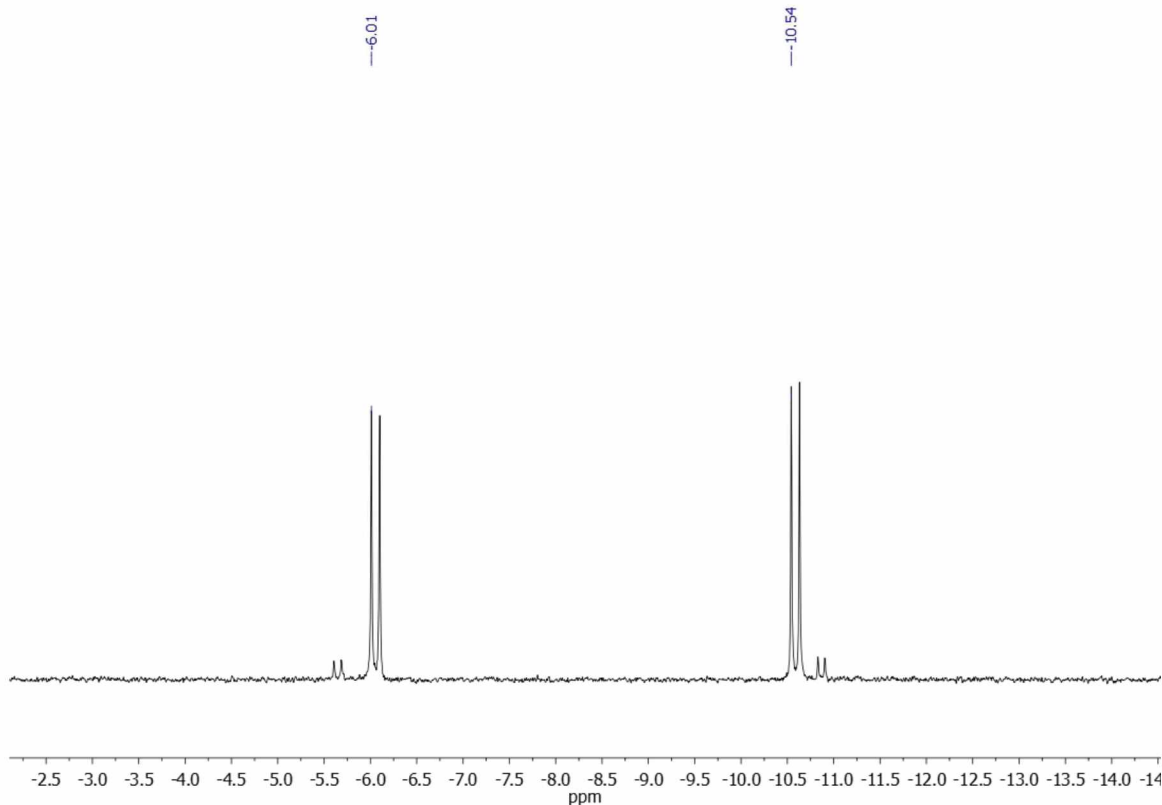


Figure B2.6. <sup>1</sup>H COSY NMR of TNP-ADP in D<sub>2</sub>O (Bruker 600 MHz)



**Figure B2.7.  $^{31}\text{P}$  NMR of TNP-ADP in  $\text{D}_2\text{O}$  (Bruker 600 MHz)**

The trinitrophenylation of ATP did not yield a pure standard. Figure B2.8 shows the  $^1\text{H}$  NMR of TNP-ATP with most of the hydrogens correctly assigned. A  $^1\text{H}$  COSY NMR is shown in Figure B2.9 and used for determining correct peak assignments. However, the two hydrogens located on the adenine base, which can be typically assigned for other TNP compounds, cannot be correctly identified in Figure B2.8. A  $^{31}\text{P}$  (Figure B2.10) and  $^{31}\text{P}$  COSY NMR (Figure B2.11) was also acquired to determine the degree of purity of the TNP-ATP standard. A pure TNP-ATP standard would result in three resonances with multiplicities of a triplet and two doublets that correspond to the three phosphates in TNP-ATP. As shown in Figure B2.10, multiple chemical shifts appear for the TNP-ATP standard. One potential explanation for this result is that TNP-ATP is hydrolyzing while in solution into its metabolites TNP-ADP and TNP-AMP.



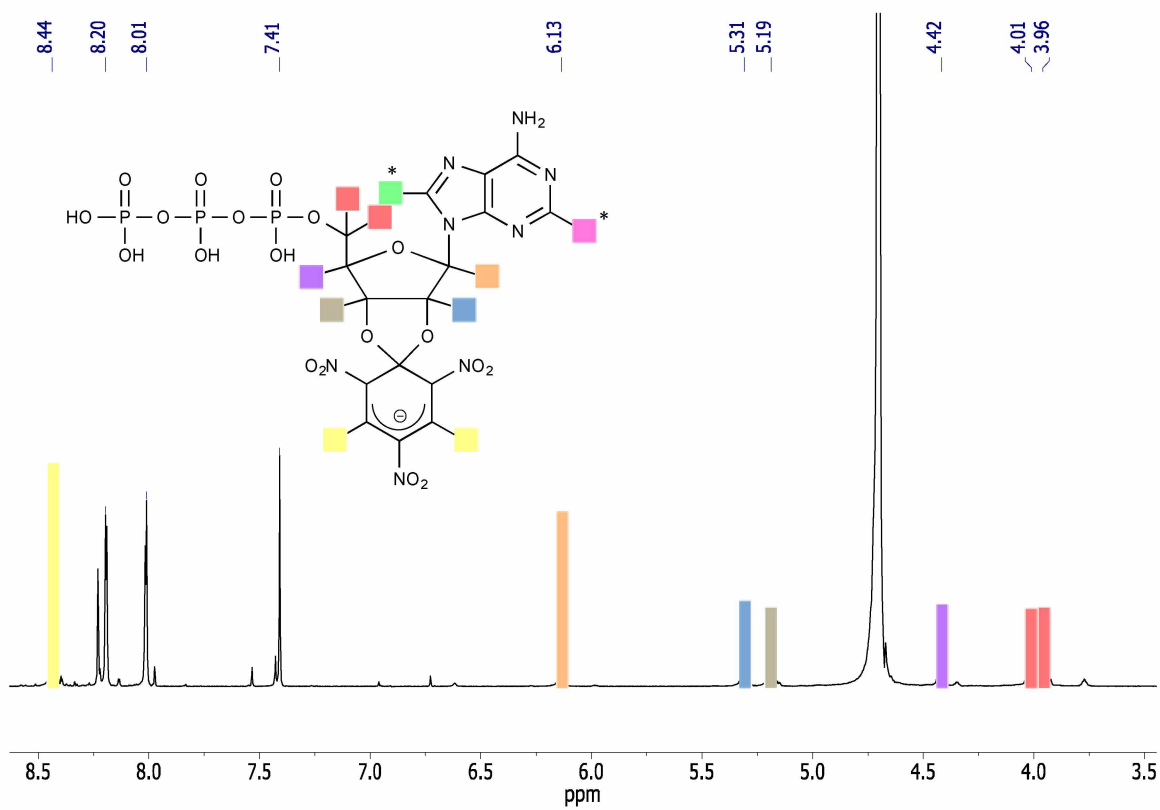


**Figure B2.8.** <sup>1</sup>H NMR of TNP-ATP in D<sub>2</sub>O (Bruker 600 MHz). Hydrogens on the adenine base could not be correctly assigned.

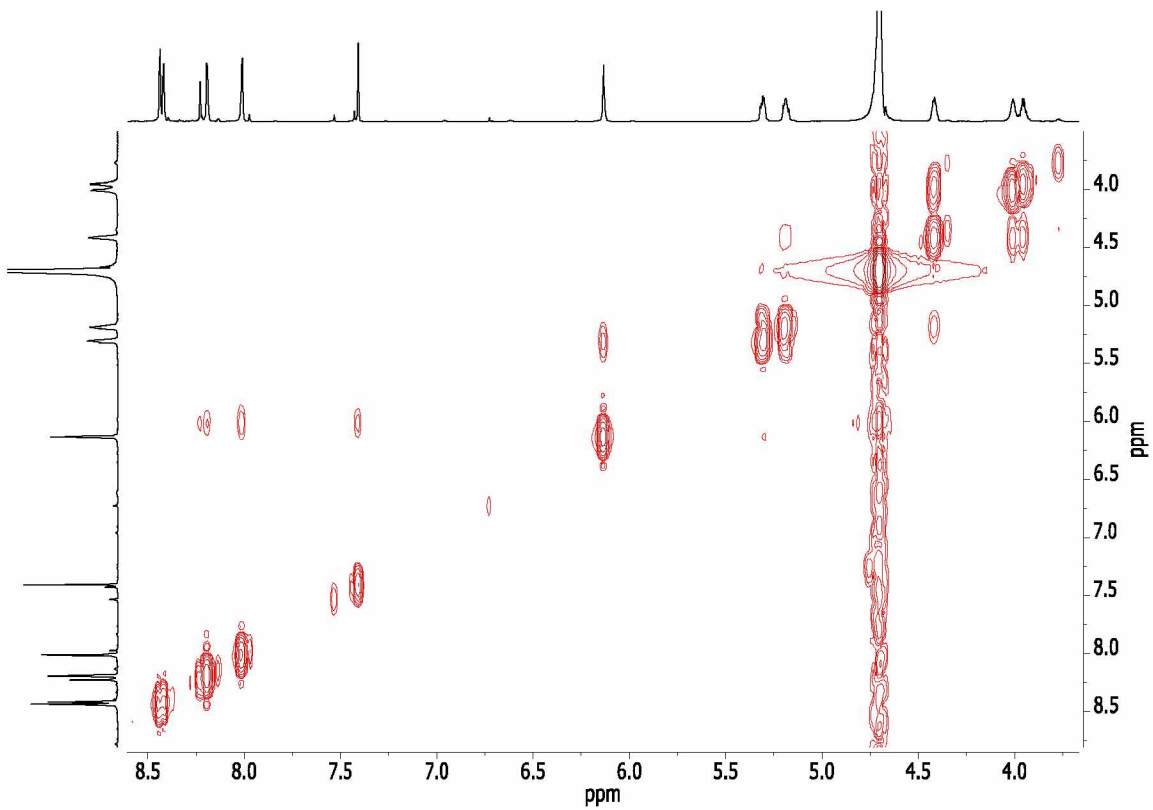


Figure B2.9.  $^1\text{H}$  COSY NMR of TNP-ATP in  $\text{D}_2\text{O}$  (Bruker 600 MHz)

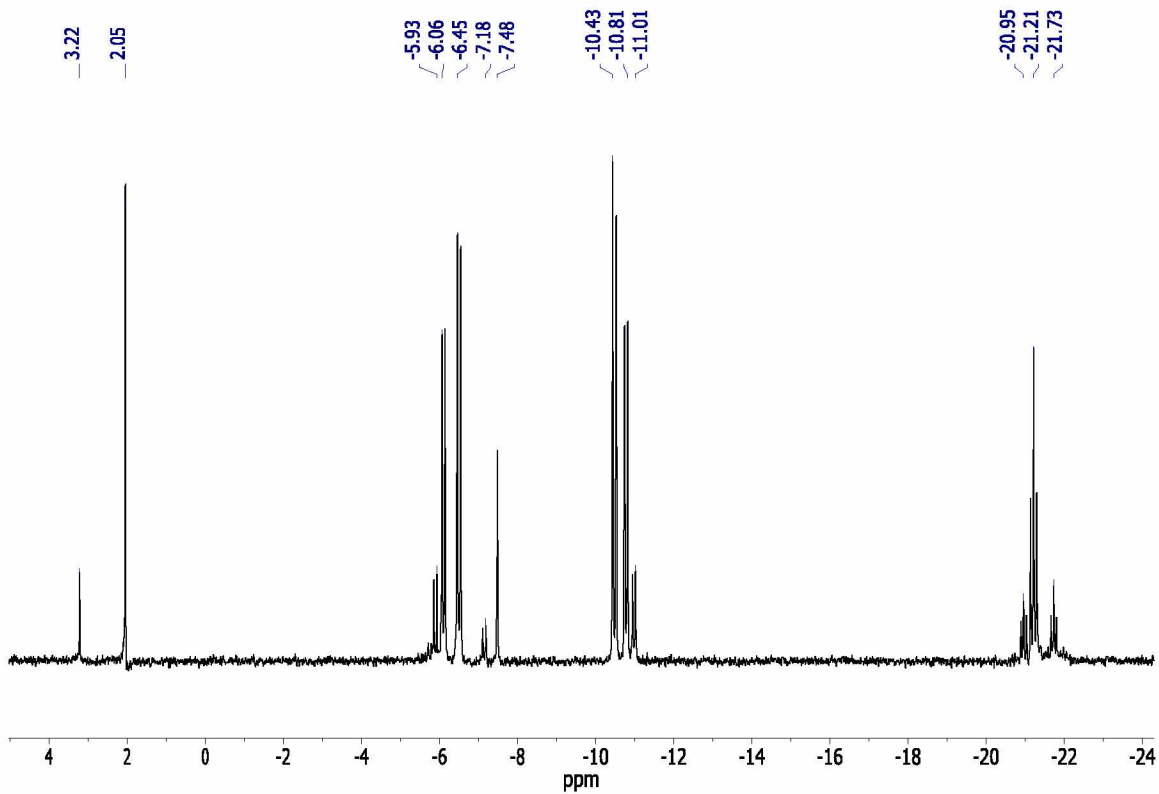
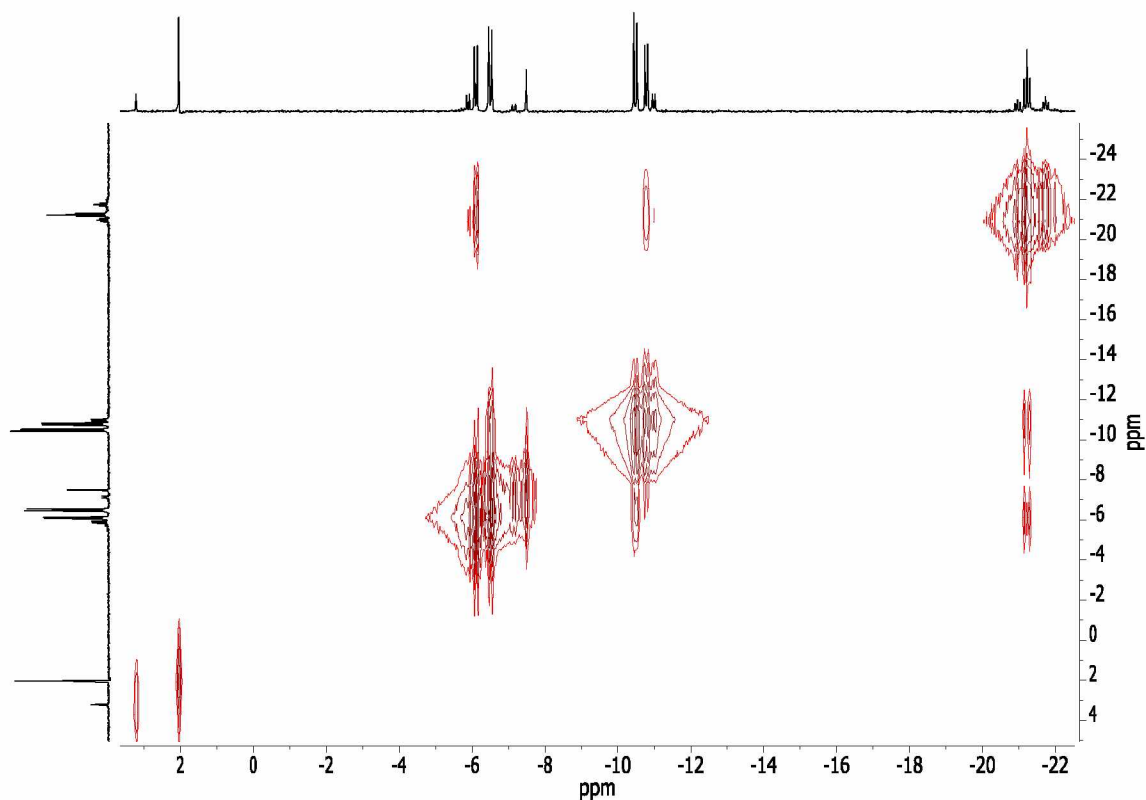
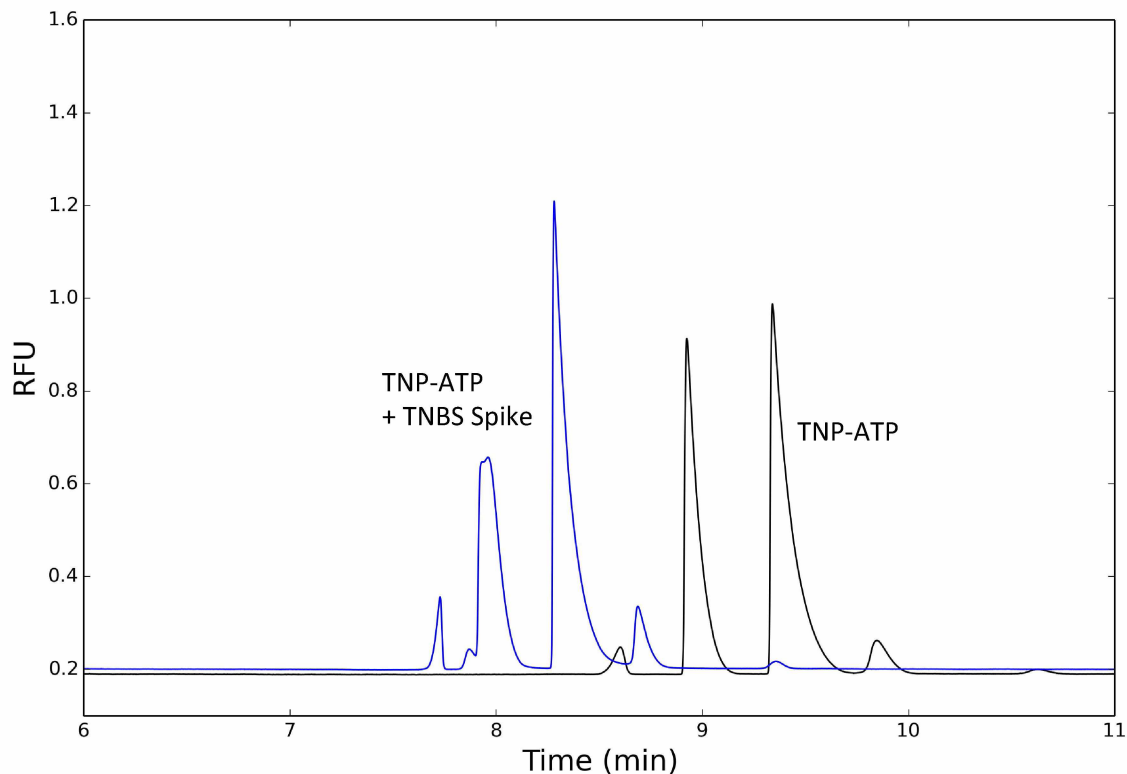


Figure B2.10.  $^{31}\text{P}$  NMR of TNP-ATP in  $\text{D}_2\text{O}$  (Bruker 600 MHz)



**Figure B2.11.  $^{31}\text{P}$  COSY NMR of TNP-ATP in  $\text{D}_2\text{O}$  (Bruker 600 MHz)**

Although it was determined that the synthesis of TNP-ATP did not yield a pure standard, CE-LIF analysis was performed using the same conditions as for the analysis of TNP-Ado. Figure B2.12 shows the electropherogram of the synthesized TNP-ATP standard in  $\text{H}_2\text{O}$  as well as the same sample with a TNBS spike. As predicted from the NMR, the electropherogram of the standard resulted in multiple signals. This result also highlights that the CE-LIF method could not separate TNBS from the TNP-ATP signals as shown by the increase in peak height of one of the TNP-ATP signals.



**Figure B2.12. CE-LIF electropherogram of TNP-ATP and TNP-ATP with TNBS spike.** CE Parameters: Inner capillary diameter 75  $\mu\text{m}$ ; total length 40 cm; effective length 28 cm; injection pressure 50 mbar; injection time 2 s; applied voltage 10 kV; laser power 25 mW; 25°C; BGE 20 mM sodium borate with various  $\gamma$ -CD concentrations at pH 9.4.

## B.2.4 Conclusions

Pure standards of TNP-AMP and TNP-ADP were successfully synthesized. Future studies should work towards optimizing the purification step of the trinitrophenylation reaction for TNP-ATP to minimize impurities and possible hydrolysis. Experiments should be performed with pure standards of TNP-Ado, TNP-AMP, TNP-ADP and TNP-ATP in order to determine optimal CE-LIF conditions for successful analytical separation and quantification. Once these studies are complete, the trinitrophenylation reaction kinetics of each of these molecules at biologically relevant concentrations and volumes should be investigated to determine a standard reaction procedure. Lastly, once an optimized CE-LIF method and trinitrophenylation reaction procedure is developed for TNP-AMP, TNP-ADP and TNP-ATP, the expansion of the CE-LIF method for

the detection of adenine ribonucleotides can be validated in real biological samples like brain tissue or microdialysis samples.

### B.3 N<sup>6</sup>-Cyclohexyladenosine

#### B.3.1 Introduction

Due to the significance of Ado and adenine ribonucleotides in cellular signaling, several structurally similar analogs have been developed for potential use as pharmaceutical interventions in a variety of pathological conditions and disease.<sup>13-15</sup> One of these analogs is N<sup>6</sup>-Cyclohexyladenosine (CHA), structure shown in Figure B3.1. CHA is a selective A1 adenosine receptor agonist and is of great interest to Dr. Kelly Drew's research group at UAF because of its role in inducing entrance into torpor<sup>16</sup> and a hypothermic, torpor-like state<sup>17</sup> in hibernators and non-hibernators, respectively. Because of this interest, we were asked if the CE-LIF method could be also used to analyze CHA in rat brain tissue. Similarly to Ado, which is discussed in Chapter 2 of the thesis, a standard of trinitrophenylated CHA (TNP-CHA) was synthesized in addition to CE-LIF optimization studies for potential detection of CHA in biological tissue.

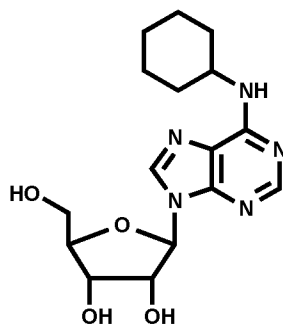


Figure B3.1. Structure of N<sup>6</sup>-Cyclohexyladenosine (CHA)

### B.3.2 Methods

A method similar to Green et al.<sup>1</sup> and Hiratsuka et al.<sup>12</sup> was followed for the trinitrophenylation of CHA. ~60 mg of CHA was dissolved in 1 mL of Milli-Q H<sub>2</sub>O and 1 mL 1M NaOH followed by the addition of 0.88 mL of TNBS (~1M in H<sub>2</sub>O). The pH of the reaction was continuously monitored for 3 hours, adding 1 M NaOH until the pH was stabilized at 10. The reaction was left overnight and purified the next morning on a Sephadex LH-20 column, dimensions 2 cm x ~30 cm. Impurities were eluted off the column with water, leaving the purified standard, which appeared as a bright reddish-orange band, retained at the top of the column. The standard was then eluted from the column with methanol, dried by rotary evaporation and analyzed for purity by 600 MHz NMR spectroscopy in DMSO-d<sub>6</sub>.

For binding studies using CE-LIF, a 10  $\mu$ M sample of the TNP-CHA standard was diluted in H<sub>2</sub>O and the background electrolyte (BGE) solution consisted of 20 mM sodium borate with various  $\gamma$ -cyclodextrin concentrations at pH 9.4. The BGE was filtered through a 0.2  $\mu$ m syringe filter prior to use. Separations were performed on a 50  $\mu$ m inner diameter fused silica capillary cut to a total length of 48 cm, effective length 28 cm. Samples were hydrodynamically injection at 50 mbar for 1 s. Applied voltage was 20 kV and laser power was 25 mW.

A stock solution of CHA was diluted to 0.1 mM in aCSF for monitoring of the trinitrophenylation reaction by CE-LIF. Reactions were performed in triplicates and 20  $\mu$ L of 0.1 mM of the standard solution in aCSF was reacted with 10  $\mu$ L of TNBS (~1 M in H<sub>2</sub>O), 10  $\mu$ L of 1 M NaOH and 120  $\mu$ L of 0.1 M carbonate buffer at pH 10. The reactions were vortexed and then placed in a heat block set at 50°C. To determine the percentage of product conversion by CE-LIF analysis, 10  $\mu$ L of the reaction mixture was diluted by 10x in Milli-Q H<sub>2</sub>O containing 0.02  $\mu$ M of sodium fluorescein (internal standard) and monitored every 2 hours for 10 hr, then at 20 and 24 hr. Calibration curves were made using standards of 8, 40, 80, 400 and 800  $\mu$ M TNP-CHA containing the same ratios volumes of TNBS, NaOH and carbonate buffer as the trinitrophenylation reactions (1  $\mu$ L sample to 0.5  $\mu$ L ~1M TNBS, 0.5  $\mu$ L 1M NaOH and 6  $\mu$ L 0.1M

carbonate buffer). These calibration standards were diluted by 10x prior to CE-LIF analysis in Milli-Q H<sub>2</sub>O containing 0.02 μM of internal standard. CE-LIF conditions were similar to the binding studies, however, a 75 μm inner diameter fused silica capillary cut to a total length of 48 cm, effective length 28 cm, was used and applied voltage was set at 10 kV.

For comparing a CHA standard before and after 24 hr storage at -80°F, a 1 mM sample was prepared in aCSF. The sample was then analyzed before and after storage by <sup>1</sup>H NMR spectroscopy using the same parameters like the number of scan etc.

### **B.3.3 Results and Discussion**

The trinitrophenylation of CHA yielded a pure standard. Figure B3.2 shows the <sup>1</sup>H NMR of TNP-CHA with correct hydrogen assignments. The large unassigned peaks at ~2.5 ppm and ~3.4 ppm are residual H<sub>2</sub>O and DMSO, respectively. A <sup>1</sup>H COSY NMR is shown in Figure B3.3 and aided in determining correct peak assignments.



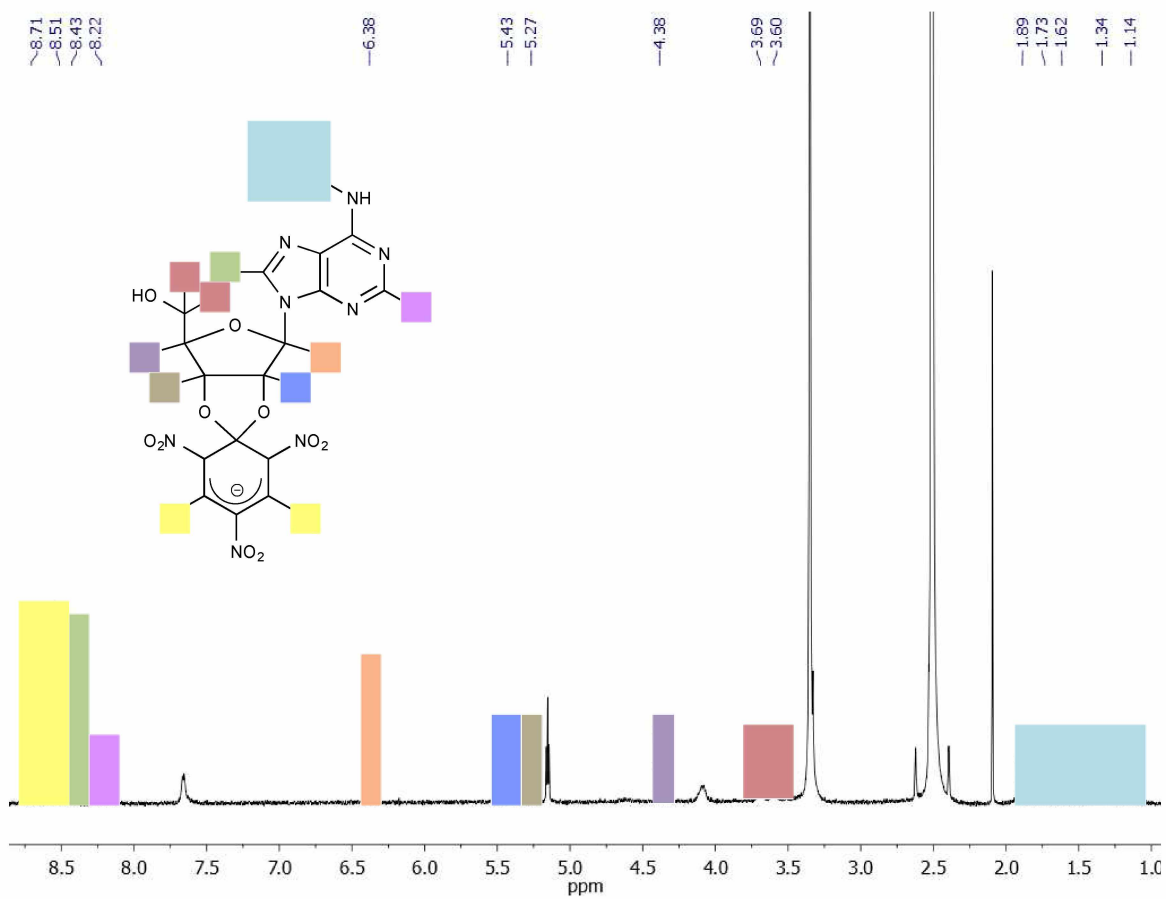
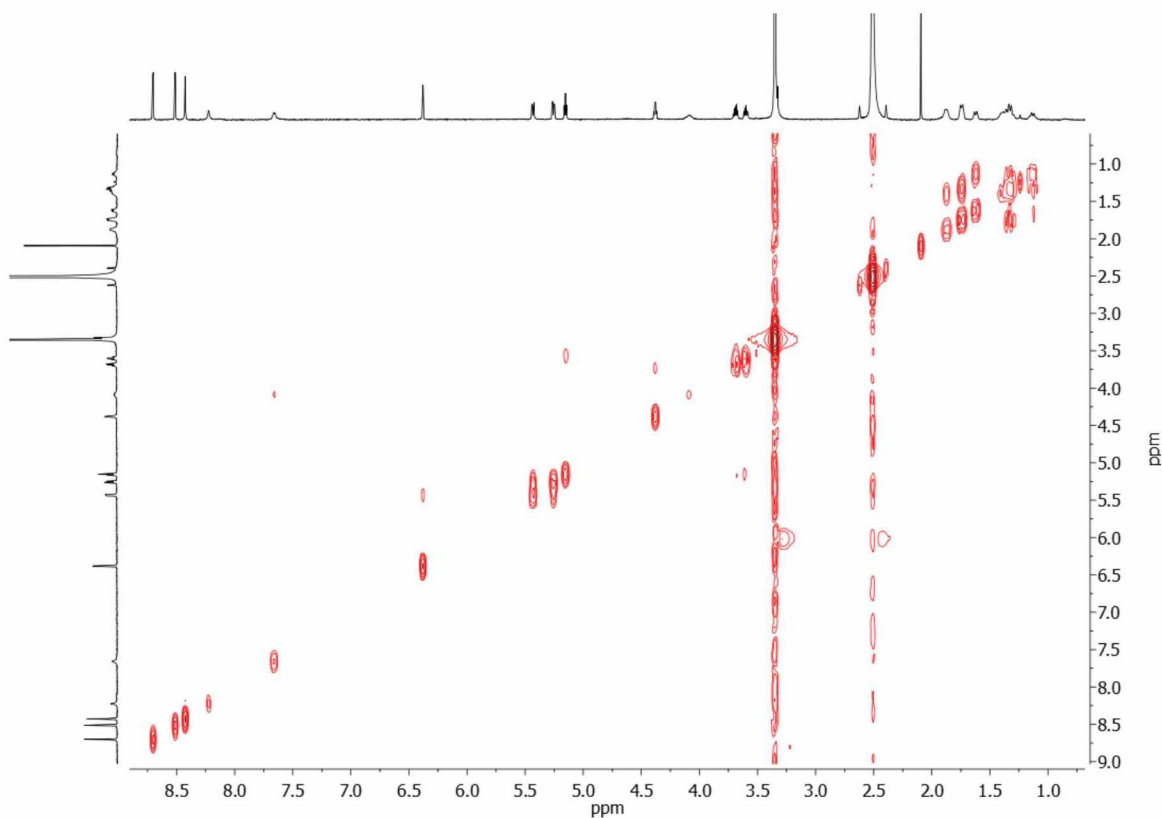
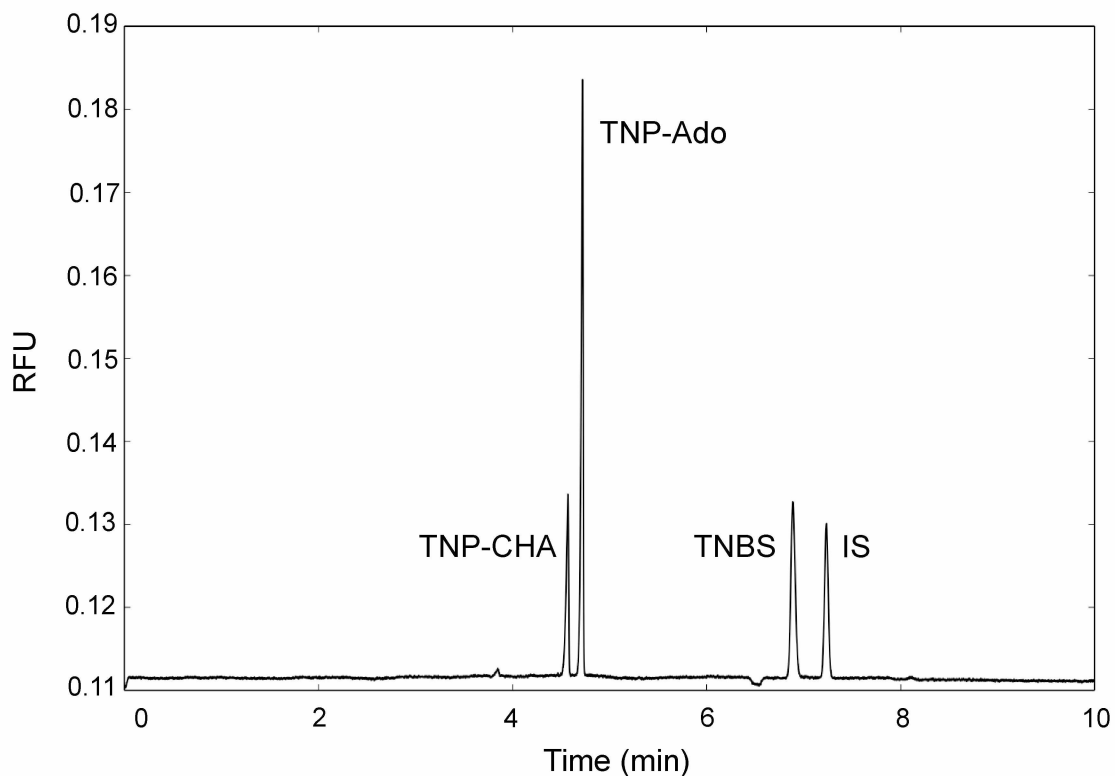


Figure B3.2.  $^1\text{H}$  NMR of TNP-CHA in  $\text{DMSO-d}_6$  (Bruker 600 MHz)



**Figure B3.3.  $^1\text{H}$  COSY NMR of TNP-CHA in  $\text{DMSO-d}_6$  (Bruker 600 MHz)**

A sample of the TNP-CHA, TNP-Ado, TNBS and the internal standard fluorescein in aCSF was analyzed by CE-LIF under the same conditions typically used for Ado detection. Figure B3.4 shows the electropherogram of this sample and resulted in the successful separation of TNP-CHA from TNP-Ado, TNBS and the internal standard. This result demonstrates the potential of the CE-LIF method to analyze not only endogenous molecules, but also structurally similar analogs.



**Figure B3.4. CE-LIF electropherogram of TNP-Ado, TNP-CHA, TNBS and IS in aCSF.** CE Parameters: Inner capillary diameter 75  $\mu\text{m}$ ; total length 48 cm; effective length 28 cm; injection pressure 50 mbar; injection time 1 s; applied voltage 10 kV; laser power 25 mW; 25°C; BGE 20 mM sodium borate with various  $\gamma$ -CD concentrations at pH 9.4.

In order to quantify the analysis of CHA by CE-LIF,  $\gamma$ -CD association constants and trinitrophenylation reaction kinetics studies were completed. Figure B3.5 shows the relationship between the electrophoretic mobility of TNP-CHA and concentration of  $\gamma$ -CD. Similarly to the research discussed in Chapter 2, 2-parameter non-linear curve fitting was performed. The association constant for TNP-CHA was calculated to be  $2700 \pm 320 \text{ M}^{-1}$ . This result was significantly lower than the association constant calculated for TNP-Ado,  $4600 \pm 460 \text{ M}^{-1}$ , suggesting that TNP-CHA has a weaker association with  $\gamma$ -CD compared to TNP-Ado.

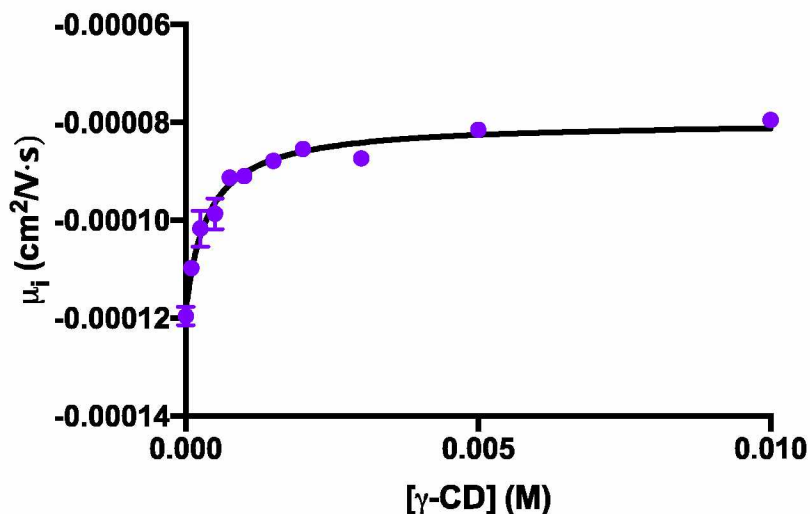


**Figure B3.5.** The relationship between the electrophoretic mobility  $\mu_i$  ( $\text{cm}^2/\text{V}\cdot\text{s}$ ) of  $10 \mu\text{M}$  standard of TNP-CHA and concentration of  $\gamma\text{-CD}$  (M) at  $25^\circ\text{C}$ . CE-LIF parameters: Inner capillary diameter  $50 \mu\text{m}$ ; effective length  $28 \text{ cm}$ ; injection pressure  $50 \text{ mbar}$ ; injection time  $1 \text{ s}$ ; applied voltage  $20 \text{ kV}$ ; laser power  $25 \text{ mW}$ ; BGE  $20 \text{ mM}$  sodium borate with various  $\gamma\text{-CD}$  concentrations at pH  $9.4$ .

Figure B3.6 shows a comparison of the percent conversion of CHA to TNP-CHA as a function of reaction time and at  $50^\circ\text{C}$ . The same reaction conditions were used as the Ado trinitrophenylation studies in Chapter 2 (For every  $1 \mu\text{L}$  of sample:  $0.5 \mu\text{L}$  of TNBS ( $\sim 1\text{M}$  in  $\text{H}_2\text{O}$ ),  $0.5 \mu\text{L}$  of  $1\text{M}$  NaOH and  $6 \mu\text{L}$  of  $0.1\text{M}$  carbonate buffer at pH  $10$  are added). The trinitrophenylation of CHA at  $50^\circ\text{C}$  resulted in  $\sim 100\%$  conversion to TNP-CHA after  $2 \text{ hr}$ . There were no signs of TNP-CHA degradation at  $50^\circ\text{C}$  since the CHA conversion rate was stable after  $24 \text{ hr}$ .

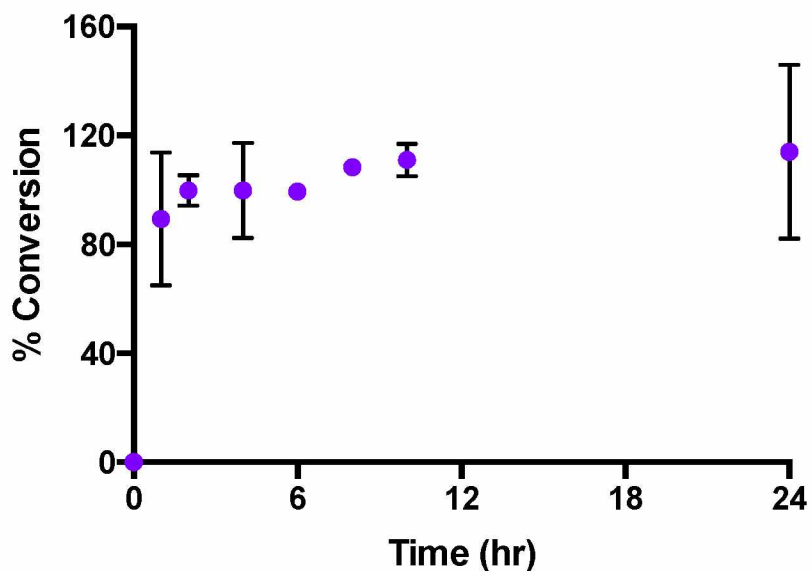


**Figure B3.6. Rate of the trinitrophenylation of CHA (100  $\mu\text{M}$ ) at 50°C.** CE Parameters: Inner capillary diameter 75  $\mu\text{m}$ ; total length 48 cm; effective length 28 cm; injection pressure 50 mbar; injection time 1 s; applied voltage 10 kV; laser power 25 mW; 25°C; BGE 20 mM sodium borate with various  $\gamma$ -CD concentrations at pH 9.4.

After determining an optimal trinitrophenylation reaction procedure for CHA, the next step in expanding the CE-LIF method for the analysis of CHA was to validate the method in biological tissue. Several attempts to analyze CHA in homogenized rat brain tissue were made, but eventually determined unsuccessful. In order to ensure the reaction procedure was valid, standards containing CHA in aCSF were reacted and analyzed simultaneously with tissue samples spiked with CHA after the homogenization/extraction processing but prior to storage at  $-80^{\circ}\text{F}$  and trinitrophenylation. However, it became apparent that the tissue samples spiked with CHA resulted in limited or no detection of CHA by CE-LIF whereas CHA was detectable in the control reactions. This result suggested that CHA could be potentially degrading prior to analysis.

To further investigate if CHA was degrading prior to analysis, a preliminary NMR study was performed on a solution of CHA in aCSF before and after 24 hr storage at  $-80^{\circ}\text{F}$ . The  $^1\text{H}$  NMR spectra of the solution before and after storage are shown in Figure B3.7. The same sample

and NMR parameters were used for each spectrum acquisition. Only one hydrogen signal was used for comparison. These results suggested that after 24 hr storage at  $-80^{\circ}\text{F}$ , there is some evidence that CHA is starting to degrade. This is determined by comparing the peak heights and areas of the two spectra, which are not the same before and after storage at  $-80^{\circ}\text{F}$ .

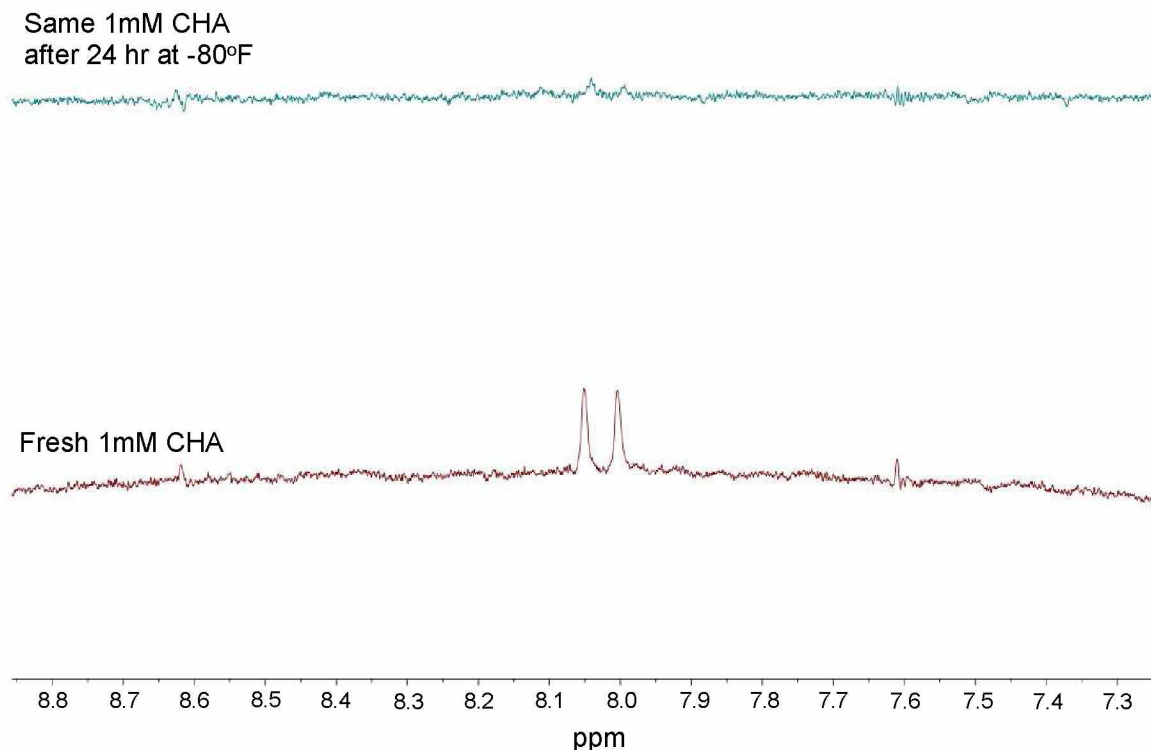


**Figure B3.7. Comparison of  $^1\text{H}$  NMR of 1mM CHA standard in aCSF diluted in  $\text{D}_2\text{O}$  before and after 24 hr storage at  $-80^{\circ}\text{F}$  (Bruker 600 MHz).**

### B.3.4 Conclusions

A pure standard of TNP-CHA was successfully synthesized and separated from a TNP-Ado standard. From the reaction kinetic experiments, a standard procedure was established for the trinitrophenylation CHA. More research is needed to determine the cause of CHA degradation and the inability of the CE-LIF method to successfully detect CHA in biological samples. Experiments should be designed to minimize storage of tissue homogenate prior of analysis and

incorporate additional controls to ensure successful trinitrophenylation and analysis of CHA in addition to other endogenous molecules like Ado and ATP.

## B.4 Guanosine, Cytidine and Uridine

### B.4.1 Introduction

Other ribonucleosides including Guanosine (Gua), Cytidine (Cyt) and Uridine (Uri) exist in nature and play a number of key roles cell signaling, RNA synthesis and metabolism.<sup>18</sup> Similarly to Ado, these molecules contain a 5-carbon ribose sugar ring joined by a  $\beta$ -N<sub>9</sub>-glycosidic bond to a nitrogenous base. Figure B4.1 shows the molecular structures of Gua, Cyt and Uri. Due to the presence of the diol functional groups, there is potential that these molecules can also undergo trinitrophenylation with 2,4,6-trinitrobenzenesulfonic acid (TNBS) to form stable trinitrophenylated derivatives (TNP-Gua, TNP-Cyt and TNP-Uri). If the trinitrophenylation is successful, the selectivity and impact of the CE-LIF method could be further expanded for the analysis of these molecules in biological samples. The synthesis of TNP-Gua, TNP-Cyt and TNP-Uri standards is the first step in expanding the CE-LIF method. Results from these experiments are discussed.

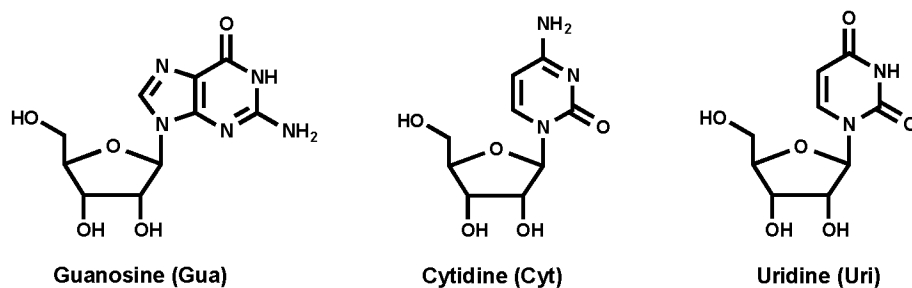


Figure B4.1. Structure of Guanosine (Gua), Cytidine (Cyt) and Uridine (Uri).

### B.3.2 Methods

A method similar to Green et al.<sup>1</sup> and Hiratsuka et al.<sup>12</sup> was followed for the trinitrophenylation of Gua, Cyt and Uri. ~60 mg of each compound was dissolved in 2 mL of Milli-Q H<sub>2</sub>O and 0.88 mL of TNBS (~1M in H<sub>2</sub>O) was added. The pH of all reactions was continuously monitored for 3 hours, adding 1 M NaOH until the pH was stabilized at 10. Each reaction was left overnight and purified the next morning on a Sephadex LH-20 column, dimensions 2 cm x ~30 cm. Impurities of each reaction were eluted off the column with water, leaving the purified standard, which appeared as a bright reddish-orange band, retained at the top of the column. The standards were then eluted from the column with methanol, dried by rotary evaporation and were analyzed for purity by 600 MHz NMR spectroscopy in D<sub>2</sub>O.

### B.4.3 Results and Discussion

A pure standard of TNP-Gua was synthesized. Figure B4.2 shows the <sup>1</sup>H NMR of TNP-Gua with correct hydrogen assignments. The large peak at ~4.8 ppm is D<sub>2</sub>O. A <sup>1</sup>H NMR COSY was also acquired to further confirm the purity of TNP-Gua (Figure B4.3). It should be noted that during purification by column chromatography, the TNP-Gua standard took much longer to elute from the column (~2 days) compared to Ado and other molecules (~8 hr). During this time, the band corresponding to TNP-Gua also started to change color from a bright reddish-orange to a dark maroon-purple color.



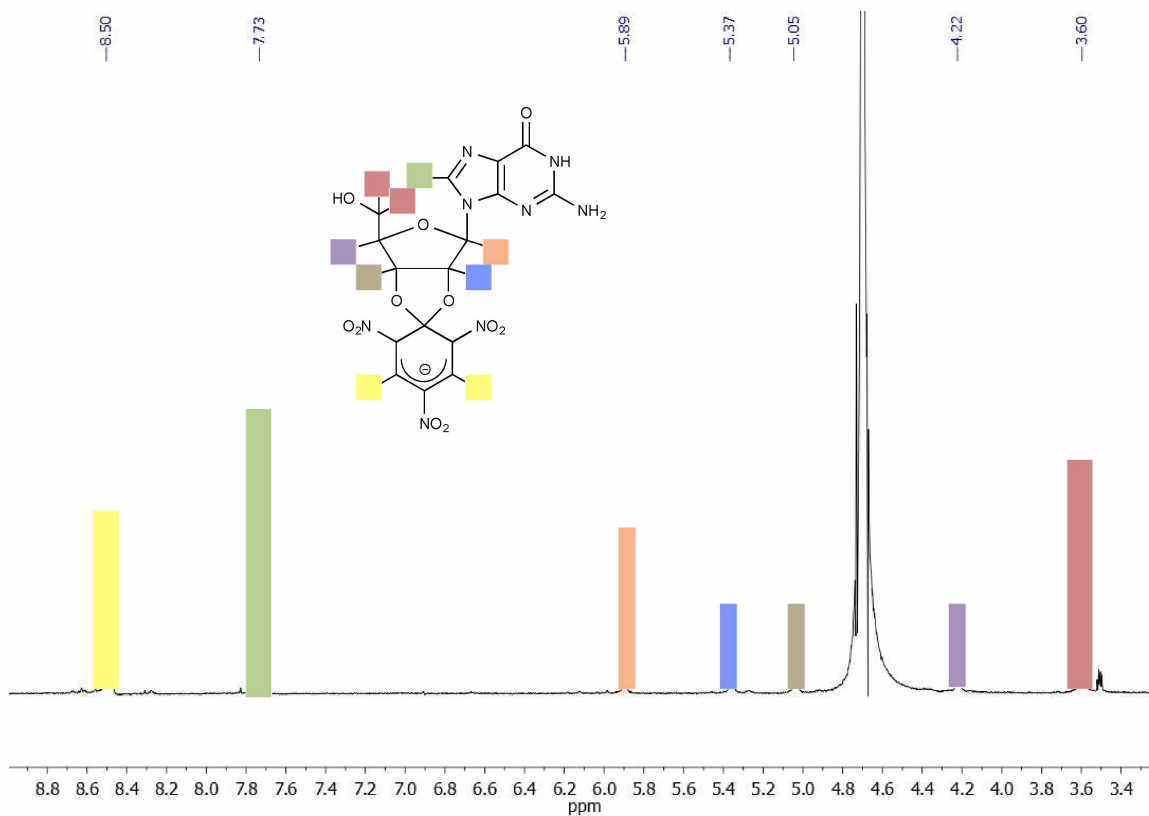


Figure B4.2. <sup>1</sup>H NMR of TNP-Gua in D<sub>2</sub>O (Bruker 600 MHz).

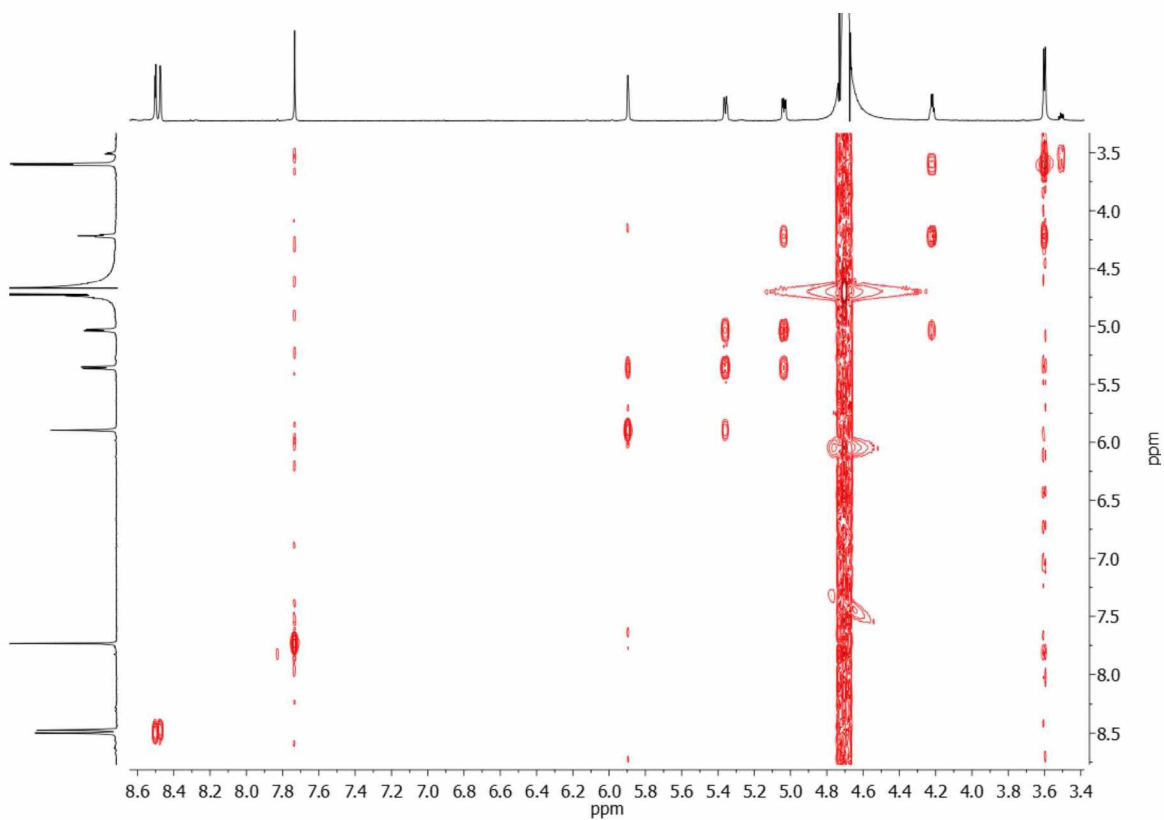


Figure B4.3  $^1\text{H}$  COSY NMR of TNP-Gua in  $\text{D}_2\text{O}$  (Bruker 600 MHz).

A pure standard of TNP-Cyt was synthesized. Figure B4.4 shows the  $^1\text{H}$  NMR of TNP-Cyt with correct hydrogen assignments. The large unassigned peak at  $\sim 4.8$  ppm is  $\text{D}_2\text{O}$ . A  $^1\text{H}$  NMR COSY was also acquired to further confirm the purity of TNP-Cyt (Figure B4.5).

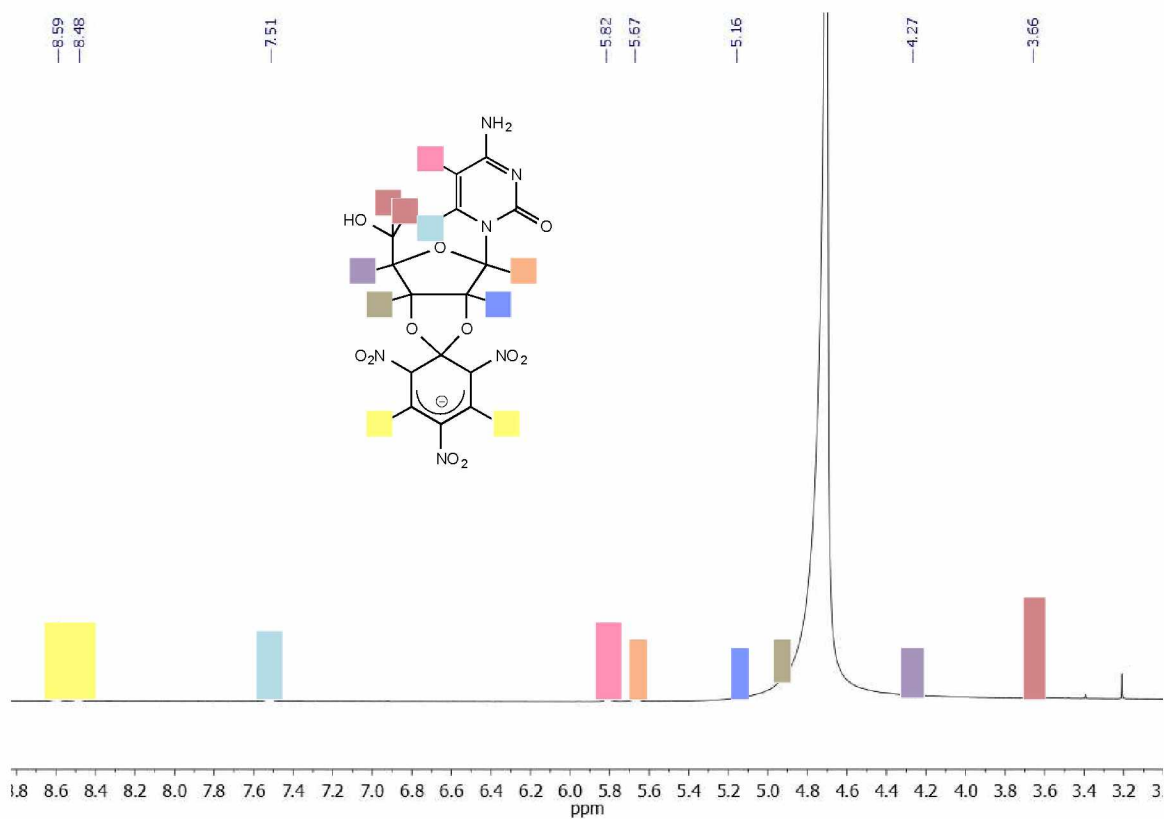


Figure B4.4.  $^1\text{H}$  NMR of TNP-Cyt in  $\text{D}_2\text{O}$  (Bruker 600 MHz).

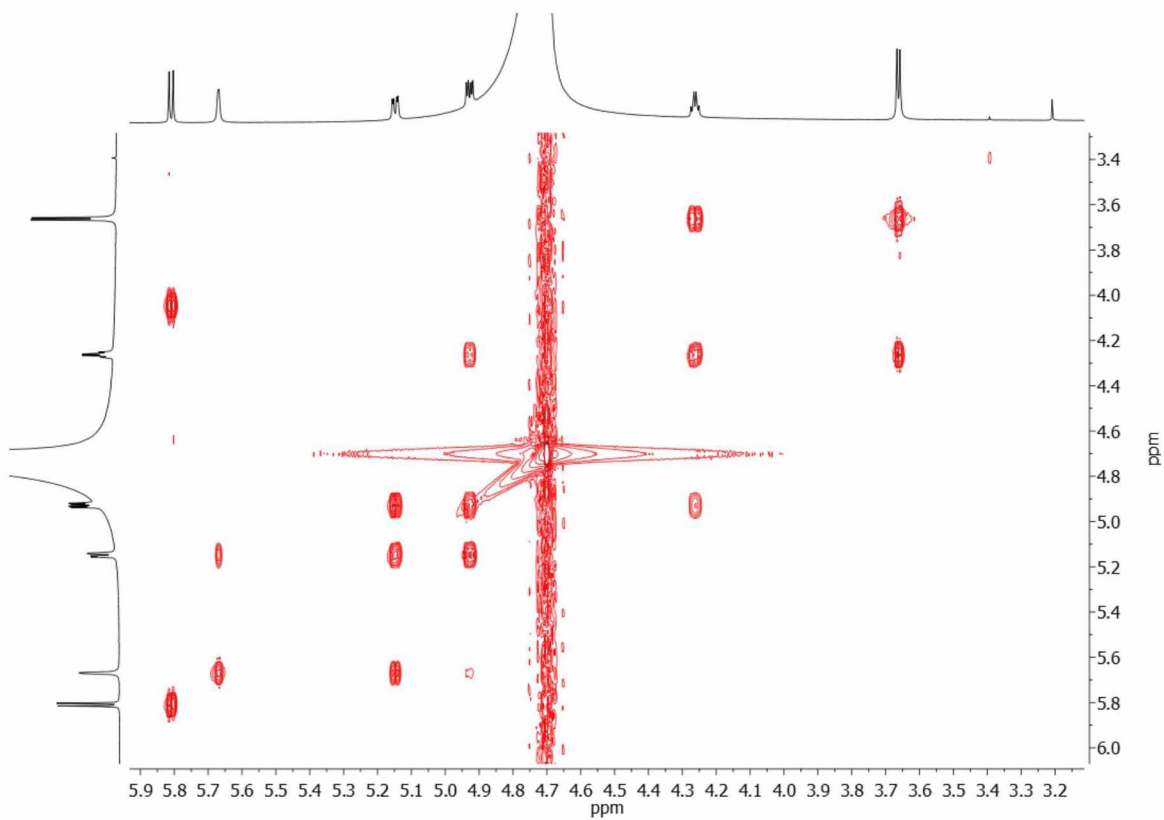


Figure B4.5.  $^1\text{H}$  COSY NMR of TNP-Cyt in  $\text{D}_2\text{O}$  (Bruker 600 MHz).

A pure standard of TNP-Uri was also synthesized. Figure B4.6 shows the  $^1\text{H}$  NMR of TNP-Uri with correct hydrogen assignments. The large unassigned peak at  $\sim 4.8$  ppm is  $\text{D}_2\text{O}$ . A  $^1\text{H}$  NMR COSY was also acquired to further confirm the purity of TNP-Uri (Figure B4.7).

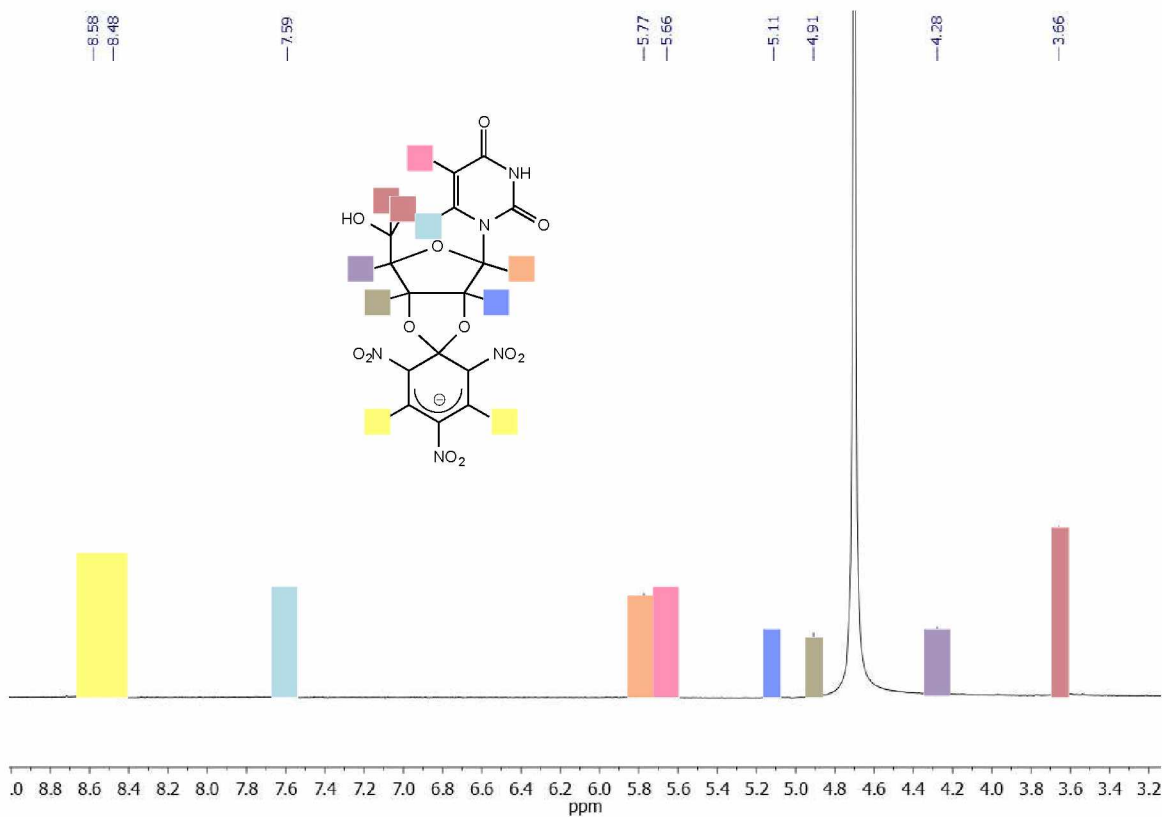


Figure B4.6.  $^1\text{H}$  NMR of TNP-Uri in  $\text{D}_2\text{O}$  (Bruker 600 MHz).

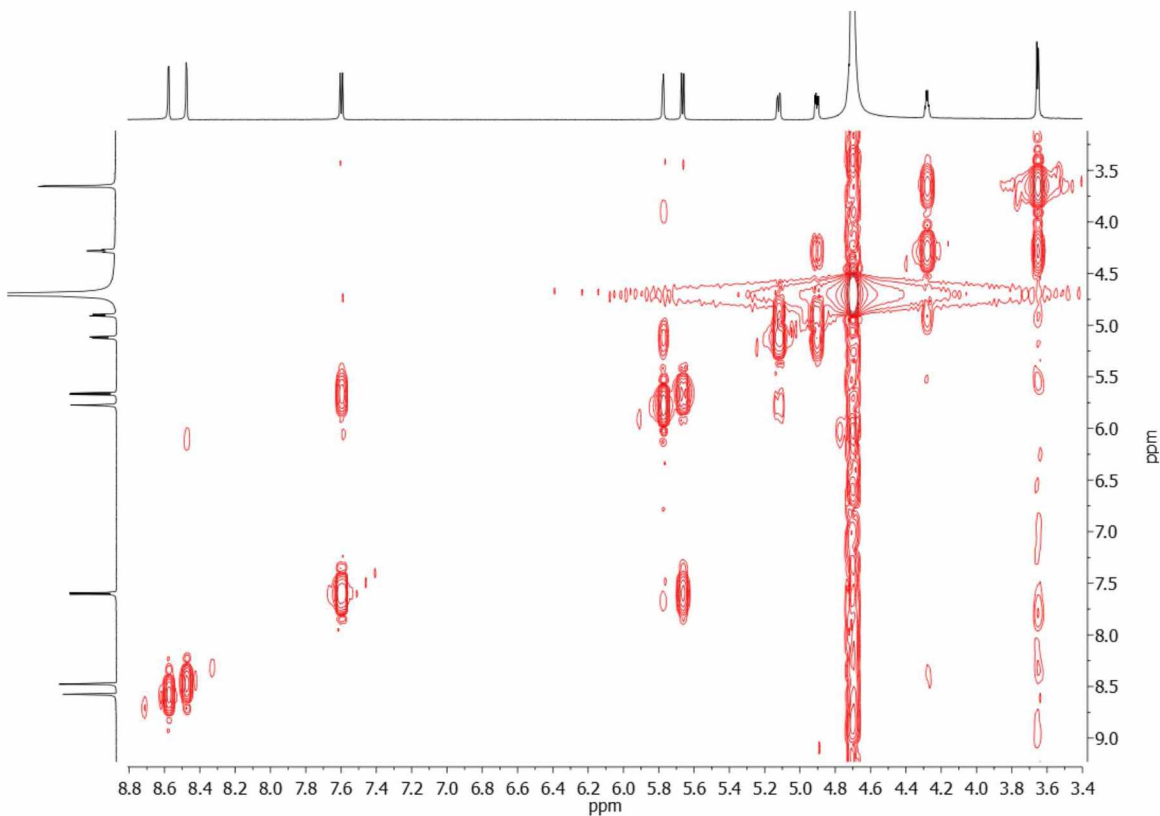


Figure B4.7.  $^1\text{H}$  COSY NMR of TNP-Uri in  $\text{D}_2\text{O}$  (Bruker 600 MHz).

#### B.4.4 Conclusion

Pure standards of TNP-Gua, TNP-Cyt and TNP-Uri were successfully synthesized. Future experiments should be performed with these standards in addition to TNP-Ado, TNP-AMP, TNP-ADP and TNP-ATP to determine optimal CE-LIF conditions for successful analytical separation and quantification. Once these studies are complete, the trinitrophenylation reaction kinetics of each of these molecules at biologically relevant concentrations and volumes should be investigated to determine a standard reaction procedure for real biological samples. Lastly, once an optimized CE-LIF method and trinitrophenylation reaction procedure is established for TNP-Gua, TNP-Cyt and TNP-Uri, the expansion of the CE-LIF method for the detection of these molecules can be validated in real biological samples like brain tissue or microdialysis samples.



## B.5 References

- (1) Green, T. K.; Denoroy, L.; Parrot, S. *The Journal of Organic Chemistry* **2010**, *75*, 4048-4055.
- (2) Özer, N.; Aksoy, Y.; Ögüs, I. H. *Journal of biochemical and biophysical methods* **2000**, *45*, 141-146.
- (3) Fang, H.; Pajski, M. L.; Ross, A. E.; Venton, B. J. *Analytical Methods* **2013**, *5*, 2704-2711.
- (4) Serkova, N. J.; Rose, J. C.; Epperson, L. E.; Carey, H. V.; Martin, S. L. *Physiological genomics* **2007**, *31*, 15-24.
- (5) Ward, V. L.; Khaledi, M. G. *Journal of Chromatography B: Biomedical Sciences and Applications* **1998**, *718*, 15-22.
- (6) Tjørnelund, J.; Hansen, S. H. *Journal of Chromatography A* **1997**, *779*, 235-243.
- (7) Chida, J.; Yamane, K.; Takei, T.; Kido, H. *Analytica chimica acta* **2012**, *727*, 8-12.
- (8) Koupenova, M.; Ravid, K. *Journal of cellular physiology* **2013**.
- (9) Fields, R. D.; Burnstock, G. *Nature Reviews Neuroscience* **2006**, *7*, 423-436.
- (10) Hiratsuka, T. *Biochimica et Biophysica Acta (BBA)-Protein Structure* **1976**, *453*, 293-297.
- (11) Ye, J. Y.; Yamauchi, M.; Yogi, O.; Ishikawa, M. *The Journal of Physical Chemistry B* **1999**, *103*, 2812-2817.
- (12) Hiratsuka, T.; Sakata, I.; Uchida, K. *Journal of biochemistry* **1973**, *74*, 649-659.
- (13) Liu, P.; Zhao, L.; Xu, X.; Liu, F.; Zhang, W.; Zhou, C.; Chen, J.; Pan, Y.; Du, Y.; Yang, J. *Cancer letters* **2014**, *354*, 43-57.
- (14) Tsutsui, S.; Schnermann, J.; Noorbakhsh, F.; Henry, S.; Yong, V. W.; Winston, B. W.; Warren, K.; Power, C. *The Journal of neuroscience* **2004**, *24*, 1521-1529.
- (15) Gungor, T.; Malabre, P.; Teulon, J.-M.; Camborde, F.; Meignen, J.; Hertz, F.; Virone-Oddos, A.; Caussade, F.; Cloarec, A. *Journal of medicinal chemistry* **1994**, *37*, 4307-4316.
- (16) Jinka, T. R.; Tøien, Ø.; Drew, K. L. *The Journal of Neuroscience* **2011**, *31*, 10752-10758.
- (17) Tupone, D.; Madden, C. J.; Morrison, S. F. *The Journal of Neuroscience* **2013**, *33*, 14512-14525.
- (18) Nelson, D. L.; Lehninger, A. L.; Cox, M. M. *Lehninger principles of biochemistry*; Macmillan, 2008.